

**A THESIS
FOR THE DEGREE OF DOCTOR OF PHILOSOPHY**

**Zebrafish as an alternative animal model for
functional bioactive material screening**

Seon-Heui Cha

**Department of Aquatic Life Medicine
GRADUATE SCHOOL
JEJU NATIONAL UNIVERSITY**

2010. 02

CONTENTS

국문초록	vii
LEGEND OF FIGURES	xi
LEGEND OF TABLES	xxii
GENERAL INTRODUCTION	1
Part I . Toxicity evaluation using a zebrafish embryo	
ABSTRACT	8
INTRODUCTION	9
MATERIALS AND METHODSD	11
Chemicals	11
Origin and maintenance of parental zebrafish	11
Chemical administration and embryos observance	11
Heart rate and hatching time	12
Estimation of intracellular ROS generation and image analysis	13
Statistical analysis	13
RESULTLTS	14
Embryotoxicity of H ₂ O ₂	14
Embryotoxicity of AAPH	18
DISCUSSION	27

Part II. Zebrafish embryo as an alternative animal model to evaluate
antioxidant of functional food materials

Part II-1. Protective effects of phlorotannins against H₂O₂-induced oxidative stress
in zebrafish embryo

ABSTRACT	31
INTRODUCTION	32
MATERIALS AND METHODSD	37
Materials	37
Preparation of phlorotannins from <i>Ecklonia cava</i>	37
Origin and maintenance of parental zebrafish	38
Waterborne exposure of embryos to phlorotannins and H ₂ O ₂	38
Measurement of heart-beat rate	38
Estimation of intracellular ROS generation and image analysis	40
Lipid peroxidation inhibitory activity and image analysis	40
Measurement of oxidative stress cell death in zebrafish embryo	41
Western blotting	42
Statistical analysis	42
RESULTTS	43
Toxicity of phlorotannins or H ₂ O ₂ in zebrafish embryo	43
Inhibitory effect of ROS generated by H ₂ O ₂ -induced in zebrafish	47
Lipid peroxidation inhibitory activity	51
Protective effects of phlorotannins on H ₂ O ₂ -induced cell death in live zebrafish ..	54

DISCUSSION	58
Part II-2. Protective effects of phlorotannins against 2,2'-Azobis (2-amidopropane) dihydrochloride (AAPH)-induced oxidative stress in zebrafish embryo	
ABSTRACT	62
MATERIALS AND METHODSD	64
Materials	64
Preparation of phlorotannins from <i>Ecklonia cava</i>	64
Origin and maintenance of parental zebrafish	65
Waterborne exposure of embryos to phlorotannins and H ₂ O ₂	65
Measurement of heart-beat rate	65
Estimation of intracellular ROS generation and image analysis	66
Lipid peroxidation inhibitory activity and image analysis	66
Measurement of oxidative stress cell death in zebrafish embryo	67
Statistical analysis	68
RESUTLTS	69
Toxicity of phlorotannins or AAPH in zebrafish embryo	69
Inhibitory effect of ROS generation by AAPH-induced in zebrafish	72
Lipid peroxidation inhibitory activity	75
Protective effects of phlorotannins on AAPH-induced cell death in live zebrafish	78
DISCUSSION	81

Part III. Evaluate the efficacy of cosmetic materials using a zebrafish

Part III-1. Whitening effects of phlorotannins using zebrafish as an alternative *in vivo* model

ABSTRACT	86
INTRODUCTION	87
MATERIALS AND METHODSD	91
Materials	91
Preparation of phlorotannins from <i>Ecklonia cava</i>	91
Origin and maintenance of parental zebrafish	92
Zebrafish pigmentation evaluating	92
Melanin synthesis inhibitory activity of phlorotannins in zebrafish embryos	94
Tyrosinase inhibitory activity of phlorotannins in zebrafish embryos	94
Measurement of heart-beating rate	95
Statistical analysis	95
RESUTLTS	96
Melanin synthesis inhibitory activity of phlorotannins in zebrafish embryo	96
Tyrosinase inhibitory activity of phlorotannins in zebrafish embryo	99
Toxicity of melanogenic inhibitors in zebrafish embryo	99
DISCUSSION	103

Part III-2. UV-B protective effects of phlorotannins using zebrafish as an alternative
in vivo model

ABSTRACT	107
MATERIALS AND METHODSD	108
Materials	108
Preparation of phlorotannins from <i>Ecklonia cava</i>	108
Origin and maintenance of parental zebrafish	109
UV-B irradiation	109
Waterborne exposure of embryos to phlorotannins	109
Measurement of heart-beat rate	110
Zebrafish pigmentation evaluating	110
Determination of UV-B induced melanin contents in zebrafish	110
Estimation of UV-B induced intracellular ROS generation and image analysis	110
Estimation of UV-B induced NO generation and image analysis	111
Measurement of UV-B induced cell death in zebrafish embryo	112
Statistical analysis	112
RESULTLTS	114
Toxicity of phlorotannins in zebrafish after UV-B radiation	114
Inhibitory effect of phlorotannins on melanogenesis after UV-B radiation in zebrafish	114
Inhibitory effect of ROS generation by UV-B radiation in zebrafish embryos	118
Inhibitory effect of NO generation by UV-B radiation in zebrafish	121
Protective effects of phlorotannins on UV-B radiation-induced cell death in live	

zebrafish	124
DISCUSSION	127
REFERENCES	131
ACKNOWLEDGEMENT	141



국문초록

최근에 마우스, 쥐 및 토끼 등은 실험동물로 사용되는 동물학대로 인한 윤리적인 문제가 대두되면서 이들의 이용과 관리를 제도적으로 보완하는 법적인 제도 장치가 생겨났다. 2007 년 1 월에 동물 보호법이 개정되어 2008 년 8 월 28 일부터 시행이 되는데, 이에 따라 일반 실험실의 실험동물을 이용한 연구가 부자연스러워질 것으로 예측된다. 이러한 사회적인 동향은 향후 연구논문의 학술저널에 투고에 대한 제한을 시사하며, 무엇보다도 실험실에서 규제에 자유로운 실험 대체 동물의 필요성이 절실하게 되었다.

이에 따라 2000 년 중반에 들어 새로운 실험동물 모델로서 생명과학 전 분야에 폭넓게 도입되고 있는 제브라피쉬(zebrafish; *Danio rerio*)는 생물학, 유전학 및 독성학 연구에 훌륭한 모델로 사용되고 있다. 제브라피쉬는 마우스와 비슷하게 수명은 2 년 정도이고 생후 3 개월이면 번식이 가능하다. 계절에 관계없이 암컷은 일주일 간격으로 200-300 개의 알을 낳을 수 있고, 체외수정을 하고 발생배가 투명하기 때문에 일반 해부현미경 하에서 쉽게 발생의 모든 과정을 관찰할 수 있다. 이들은 발생이 매우 빨라 초기 세포분열이 대장균(20 분)보다도 빠른 15 분 간격으로 진행되며, 발생 6 시간째에 gastrulation 이 시작되어 4 시간 만에 마치며, 12 시간이 지나면 눈의 형태형성이 이미 시작된다. 수정 후 24 시간이 지나면 심장의 박동과 혈액순환을 관찰할 수 있다. 제브라피쉬는 허파를 제외하고는 간과 췌장 그리고 지라와 흉선 등 면역계를 포함한 대부분의 기관을 가지며, 특히 돌연변이 연구에서 밝혀지는 여러 결과들이 인간의 유전질환과 매우 유사한 것으로 밝혀졌고, 인간과의 유전적 상동성도 현재 약 90%까지 일치하는 것으로 밝혀졌다. 대량으로 쉽게 구할 수 있는 수정란를 이용하여 마이크로 인젝션을 통한 expression cloning, antisense oligonucleotide morpholino 를

이용한 gene knock out/down 과 생체기능조절물질 탐색을 위한 chemical genomics 등 다양한 분야에 이용되고 있다.

일반적으로 현재 시중에서 판매되고 있는 특정 발현 단백질을 측정하는 항원 항체의 경우도 대부분이 포유동물 유래의 것으로 어류를 동물 모델로 생리학적 신호 기전을 연구하는데 있어서는 제한적이다. 그러나 제브라피쉬는 마우스, 랫, 인간 등의 포유동물 유래 항체에 반응을 하기 때문에 실험동물모델로서 대체하기에 적합한 실험 어종이다.

수컷 한 마리로부터 평균 500 종류 이상의 돌연변이체를 얻을 수가 있으나, 특정 돌연변이주의 분리와 유지에 많은 인력과 공간이 필요하다. 현재 세계적인 연구 분야 중 하나는 대량의 돌연변이를 이용한 positional cloning 방법으로 원인유전자를 밝혀 새로운 기능성 유전자를 확보하고 (gene hunting), 나아가 관련 질환연구와 신약개발의 타겟 발굴에 집중적인 노력을 기울이고 있다. 더욱이, 국내 연구진에 의하여 positional cloning 방법으로 유전자를 밝혀낸 headless 와 mind bomb mutant 및 관련된 Wnt, Notch 신호전달 등이 알려져 있다. 뿐만 아니라, 현재 세계적으로 positional cloning 을 통하여 돌연 변이체의 원인 유전자를 밝힘으로써 새로운 기능성 유전자를 확보하고 나아가 관련 질환연구와 신약 개발의 타겟발굴에 집중적인 노력을 기울여 인간 질환 모델로서의 제브라피쉬의 연구 현황이 상당히 많이 보고되고 있다. 그러나 국내에서 제브라피쉬를 이용한 실험동물 모델로서의 연구는 일부 연구실에만 집중되어 있을 뿐만 아니라 유전체를 중심으로 연구는 되었지만, 유전체를 조작하지 않고 기능성 소재를 탐색하는 연구는 수행은 되어 있지 않다. 따라서 다양한 분야 연구자들의 관심이 집중되어야 더 다양한 연구 분야의 개척이 가능할 것이다.

1) 제브라피쉬 연구모델의 문제점

- ▶ 제브라피쉬 동물모델은 국내에서는 아직도 초기 보급 단계임

제브라피쉬는 유전적인 기능이 완전히 밝혀지진 않았으나 수 많은 연구를 통하여 생리나 발생학적인 기능조작을 위한 저서들도 많이 출간되었다. 그럼에도 불구하고 국내에서는 기능성 생리활성 물질을 탐색하기 위한 제브라피쉬를 이용하는 사례가 아주 미약하다.

2) 제브라피쉬 모델의 장점

- ▶ 제브라피쉬의 수정란을 대량으로 쉽게 확보할 수 있음
- ▶ 발생이 매우 빨라 대부분의 조직 및 장기가 하루 만에 형성
- ▶ 투명한 난-현미경으로 발생단계, 혈류 흐름 및 형태적 관찰이 용이
- ▶ 척추동물로서 유전체 구성이 인간과 비슷함.

마우스와 인간과 아주 유사한 게놈 구조를 가지면서도 선충이나 초파리에서나 가능한 유전학적, 세포생물학적인 실험실이나 대규모 연구가 가능하다. 제브라피쉬의 발생배는 직경 0.7mm 정도로 작기 때문에 96-well microplate 에 3-5 embryo 정도씩 분주가 가능하며 소량의 화합물에 대해서도 형태 형성, 혈관형성 등 생체를 이용한 생리활성물질 검출이 가능하다. 따라서 이 연구에서 제브라피쉬를 실험 대체 동물 모델로 사용하기 위하여 1) 독상학적 검증, 2) 기능성 식품 및 3) 화장품 개발을 위한 평가 시스템 구축을 위해 제브라피쉬를 통하여 기능성물질의 항산화 활성, 미백 및 자외선 보호효과를 검증하였다. 앞서 여러연구자들에 의하여 제브라피쉬 발생배를 이용한 환경 독성학적 평가는 활발하게 진행되어 왔다. 이 연구에서는 독성물질로 사람의 질병의 근원이라 할 수 있는 활성산소종을 generation 하는 전구체인 과산화수소와 AAPH 를 사용하였다. 이 연구 결과는 다른 연구결과와 유사하여, 사용한 독성물질들이 제브라피쉬 발생에 관여하여 비정상적인 성장과 부종 그리고 혈관 침착 등의 다양한 외형적인 변형을 보여 주었다.

이미 항산화 활성이 우수하다고 연구가 진행되고 있는 해조류인 감태 유래의 폴리페놀 물질인 플로로탄닌은 동물 세포 수준에서도 우수한 항산화 효과를 보여주었다. 이에 이 천연 항산화 물질이 제브라피쉬에서도 작용

하는지를 독성물질로 사용한 과산화수소와 AAPH 와 co-treatment 하여 이에 대한 보호효과를 측정하였다. 이 연구에서 제브라피쉬 발생배가 투명하다는 점을 이용하여 형광 탐침자를 이용한 결과는 제브라피쉬 체내에서 발생하는 활성산소종의 생성을 감태의 플로로탄닌이 유의적으로 억제시킴을 관찰하였다. 뿐만 아니라 제브라피쉬 체내에서의 지질과산화 및 세포 사멸도 감소함을 확인 하였다. 마지막으로, 기본적으로 항산화 효과를 가지는 물질은 세포 보호 기능이 우수하여 화장품 소재로도 응용이 되고 있다. 이 연구에서 사용한 감태 플로로탄닌은 동물 세포 수준에서 우수한 화장품 소재로의 가치가 확인된 바 있다. 따라서 이 연구에서는 이 천연 화장품 소재 후보 물질인 감태의 플로로탄닌이 제브라피쉬 발생배를 통하여 확인한 결과 우수한 미백 및 자외선 보호효과를 보이는 것을 확인 할 수 있었다.

종합적으로, 제브라피쉬는 독성물질 스크리닝 동물모델로 사용이 가능할 뿐만 아니라, 기능성 소재 탐색을 위한 실험 대체 동물 모델로 사용이 가능할 것으로 예상된다. 이에 가장 큰 문제가 되고 있는 실험 동물 사용의 윤리적인 문제를 포함하여, 기능성 물질 탐색을 위한 실험동물 연구 시간 및 비용을 절감할 수 있고, 좀 더 폭 넓은 분야에서도 실험동물 모델 연구를 할 수 있는 장을 기대 할 수 있을 것이다.

Legend of Figures

Fig. I . Development stage of zebrafish embryo.

Fig. 1-1. Dose- or time- response curve between H₂O₂ exposed concentration or time and survival rates of zebrafish embryos. Zebrafish embryos were exposed from 3 hpf for 1, 3, 6, and 12 h with various H₂O₂ concentrations (2, 5 and 10 mM). The results are expressed as percentage of the survival rate of controls and survivals were scored at 48 hpf. N=500-525.

Fig. 1-2. Dose- or time- response curve between H₂O₂ exposed concentration or time and (A) yolk sac edema, (B) yolk swelling, (C) pericardial edema, and (D) total malformation rates of zebrafish embryos. Zebrafish embryos were exposed from 3 hpf with various H₂O₂ concentrations (2, 5 and 10 mM) for 1, 3, 6, and 12 h and the effect on malformations were scored at 48 hpf. Line graphs represent mean percentage embryonic yolk sac edema, yolk swelling, pericardial edema, and total malformation. N=500-525.

Fig. 1-3. Hydrogen peroxide induced dysmorphogenesis in developing zebrafish. Bent tail (yellow arrows), pericardial edema (red arrows), curving trunk (blue arrows), red blood cell accumulation (white arrows), short body length, swollen yolk sac and trunk abnormalities were characterized by H₂O₂ toxicity.

Fig. 1-4. Dose- or time- response curve between AAPH exposed concentration or time and survival rates of zebrafish embryos. Zebrafish embryos were exposed from 3 hpf for 1, 3, 6, 12, 24, 48, and 72 h with various AAPH concentrations (2, 5, 10 and 25 mM). The results are expressed as percentage of the survival rate of controls and survivals were scored at 48 hpf. N=505-

537.

Fig. 1-5. Dose- or time- response curve between AAPH exposed concentration or time and (A) yolk swelling, (B) pericardial edema, and (C) total malformation rates of zebrafish embryos. Zebrafish embryos were exposed from 3 hpf with various AAPH concentrations (2, 5, 10 and 25 mM) for 1, 3, 6, and 12 h and the effect on malformations were scored at 48 hpf. Line graphs represent mean percentage embryonic yolk swelling, pericardial edema, and total malformation. N=505-537.

Fig. 1-6. AAPH induced dysmorphogenesis in developing zebrafish. Pericardial edema (red arrows), curving trunk (blue arrows), red blood cell accumulation (white arrows), tissue malformation (yellow arrows), swollen yolk sac, and losing eye (purple arrows) were characterized by AAPH toxicity. Also, AAPH-exposed zebrafish exhibited contorted tail and other tail malformations.

Fig. 1-7. Photographs of H₂O₂- or AAPH-induced ROS level in zebrafish embryo. The ROS levels were measured by image analysis using fluorescence microscope.

Fig. 1-8. Effects of H₂O₂ and AAPH on the heart-beat rate for measurement of the toxicity. The embryos were exposed to various concentration of H₂O₂ for 6 h. The heart-beat was measured at 48 hpf, under the microscopy. The number of heart beat in 3 min was counted, and the results are expressed as the beats/min. Experiments were performed in triplicate and the data are expressed as mean± SE. **p*<0.05, ***p*<0.01.

Fig. 2-1. Several human diseases caused by oxidative stress.

Fig. 2-2. The chemical structures of the phlorotannins.

Fig. 2-3. Survival rate after treated with H₂O₂ or co-treated with phlorotannins.

The embryos were exposed to 5 mM H₂O₂ and phlorotannins treated. Dieckol (DK), Eckstolonol (ES), Eckol (EK), Triphlorethol A (TA), and Phloroglicinol (PG). Experiments were performed in triplicate and the data are expressed as mean± SE. ***p*<0.01.

Fig. 2-4. Effects of phlorotannins on the heart-beat rate for measurement of the toxicity of the tested samples. The embryos were exposed to 5 mM H₂O₂ and phlorotannins treated. The heart-beat was measured at 48 hpf, under the microscopy. The number of heartbeat in 3 min was counted, and the results are expressed as the beats/min. Dieckol (DK), Eckstolonol (ES), Eckol (EK), Triphlorethol A (TA), and Phloroglicinol (PG). Experiments were performed in triplicate and the data are expressed as mean± SE. **p*<0.05, ***p*<0.01.

Fig. 2-5. Effects of the phlorotannins on the H₂O₂-mediated toxicity in zebrafish embryos. The embryos were treated to 5 mM H₂O₂ and co-treated phlorotannins. Images are representative of the morphological change in embryos exposure to vehicle, H₂O₂, phlorotannins + H₂O₂ (1). Incompletely differentiated tail ends, and spinal column curving (2). Dieckol (DK), Eckstolonol (ES), Eckol (EK), Triphlorethol A (TA), and Phloroglicinol (PG).

Fig. 2-6. Effect of phlorotannins isolated from *E. cava* on H₂O₂-induced ROS level in zebrafish embryos. The embryos were treated to 5 mM H₂O₂ and co-treated phlorotannins. After incubation, the intracellular ROS detected by

fluorescence spectrophotometer after DCFH-DA staining. Dieckol (DK), Eckstolonol (ES), Eckol (EK), Triphlorethol A (TA), and Phloroglicinol (PG). Experiments were performed in triplicate and the data are expressed as mean± SE. * p <0.05.

Fig. 2-7. Photographs of H₂O₂-induced ROS level in zebrafish embryo. The embryos were treated to 5 mM H₂O₂ and co-treated phlorotannins. The ROS levels were measured by image analysis and fluorescence microscope. Dieckol (DK), Eckstolonol (ES), Eckol (EK), Triphlorethol A (TA), and Phloroglicinol (PG).

Fig. 2-8. Expression of phosphor-JNK and b-actin in zebrafish embryo. The embryos were treated to 5 mM H₂O₂ and co-treated 50 uM phlorotannins. Dieckol (DK), Eckstolonol (ES), Eckol (EK), Triphlorethol A (TA), and Phloroglicinol (PG).

Fig. 2-9. Effect of phlorotannins isolated from *E. cava* on H₂O₂-induced lipid peroxidation level in zebrafish embryos. The embryos were treated to 5 mM H₂O₂ and co-treated phlorotannins. After incubation, the lipid peroxidation was detected by fluorescence spectrophotometer after DPPP staining. Dieckol (DK), Eckstolonol (ES), Eckol (EK), Triphlorethol A (TA), and Phloroglicinol (PG). Experiments were performed in triplicate and the data are expressed as mean± SE.

Fig. 2-10. Photographs of H₂O₂-induced lipid peroxidation level in zebrafish embryo. The embryos were treated to 5 mM H₂O₂ and co-treated

phlorotannins. The lipid peroxidation levels were measured by image analysis and fluorescence microscope. Dieckol (DK), Eckstolonol (ES), Eckol (EK), Triphlorethol A (TA), and Phloroglicinol (PG).

Fig. 2-11. Protective effect of phlorotannins isolated from *E. cava* on H₂O₂-induced cell death in live zebrafish embryo. The embryos were treated to 5 mM H₂O₂ and co-treated phlorotannins. After incubation, the cell death was detected by fluorescence spectrophotometer after acridine orange staining. Dieckol (DK), Eckstolonol (ES), Eckol (EK), Triphlorethol A (TA), and Phloroglicinol (PG). Experiments were performed in triplicate and the data are expressed as mean± SE. **p*<0.05.

Fig. 2-12. Photographs of H₂O₂-induced cell death in live zebrafish embryo. The embryos were treated to 5 mM H₂O₂ and co-treated phlorotannins. The cell death levels were measured by image analysis and fluorescence microscope. Dieckol (DK), Eckstolonol (ES), Eckol (EK), Triphlorethol A (TA), and Phloroglicinol (PG).

Fig. 2-13. Expression of Bcl-xL, PARP and b-actin in zebrafish embryo. The embryos were treated to 5 mM H₂O₂ and co-treated 50 uM phlorotannins. Dieckol (DK), Eckstolonol (ES), Eckol (EK), Triphlorethol A (TA), and Phloroglicinol (PG).

Fig. 2-14. Survival rate after treated with AAPH or co-treatment with phlorotannins. The embryos were treated to 25 mM AAPH and co-treated phlorotannins. Dieckol (DK), Eckstolonol (ES), Eckol (EK), Triphlorethol A

(TA), and Phloroglicinol (PG). Experiments were performed in triplicate and the data are expressed as mean± SE. ** p <0.01.

Fig. 2-15. Effects of phlorotannins on the heart-beat rate for measurement of the toxicity of the tested samples. The embryos were treated to 25 mM AAPH and co-treated phlorotannins. The heart-beat was measured at 48 hpf, under the microscopy. The number of heartbeat in 3 min was counted, and the results are expressed as the beats/min. Dieckol (DK), Eckstolonol (ES), Eckol (EK), Triphlorethol A (TA), and Phloroglicinol (PG). Experiments were performed in triplicate and the data are expressed as mean± SE. * p <0.05.

Fig. 2-16. Effect of phlorotannins isolated from *E. cava* on AAPH-induced ROS level in zebrafish embryos. The embryos were treated to 25 mM AAPH and co-treated phlorotannins. After incubation, the intracellular ROS detected by fluorescence spectrophotometer after DCFH-DA staining. Dieckol (DK), Eckstolonol (ES), Eckol (EK), Triphlorethol A (TA), and Phloroglicinol (PG). Experiments were performed in triplicate and the data are expressed as mean± SE. ** p <0.01.

Fig. 2-17. Photographs of AAPH-induced ROS level in zebrafish embryo. The embryos were treated to 25 mM AAPH and co-treated phlorotannins. The ROS levels were measured by image analysis and fluorescence microscope. (A) Control, (B) AAPH (positive control), (C) Dieckol (DK), (D) Eckstolonol (ES), (E) Eckol (EK), (F) Triphlorethol A (TA), and (G) Phloroglicinol (PG).

Fig. 2-18. Effect of phlorotannins isolated from *E. cava* on AAPH-induced lipid peroxidation level in zebrafish embryos. The embryos were treated to 25 mM AAPH and co-treated phlorotannins. After incubation, the lipid peroxidation was detected by fluorescence spectrophotometer after DPPP staining. The embryos were exposed to 25 mM AAPH and phlorotannins treated. Dieckol (DK), Eckstolonol (ES), Eckol (EK), Triphlorethol A (TA), and Phloroglicinol (PG). Experiments were performed in triplicate and the data are expressed as mean± SE. ** $p < 0.01$.

Fig. 2-19. Photographs of AAPH-induced lipid peroxidation level in zebrafish embryo. The embryos were treated to 25 mM AAPH and co-treated phlorotannins. The lipid peroxidation levels were measured by image analysis and fluorescence microscope. (A) Control, (B) AAPH (positive control), (C) Dieckol (DK), (D) Eckstolonol (ES), (E) Eckol (EK), (F) Triphlorethol A (TA), and (G) Phloroglicinol (PG).

Fig. 2-20. Protective effect of phlorotannins isolated from *E. cava* on AAPH-induced cell death in live zebrafish embryo. The embryos were treated to 25 mM AAPH and co-treated phlorotannins. After incubation, the cell death was detected by fluorescence spectrophotometer after acridine orange staining. Dieckol (DK), Eckstolonol (ES), Eckol (EK), Triphlorethol A (TA), and Phloroglicinol (PG). Experiments were performed in triplicate and the data are expressed as mean± SE.

Fig. 2-21. Photographs of AAPH-induced cell death in live zebrafish embryo. The embryos were treated to 25 mM AAPH and co-treated phlorotannins. The cell

death levels were measured by image analysis and fluorescence microscope.

(A) Control, (B) AAPH (positive control), (C) Dieckol (DK), (D) Eckstolonol (ES), (E) Eckol (EK), (F) Triphlorethol A (TA), and (G) Phloroglicinol (PG).

Fig. 3-1. Chemical structure of phlorotannins isolated from *Ecklonia cava*.

Fig. 3-2. Melanin synthesis inhibitory activity of phlorotannins in zebrafish embryos. 1-phenyl-2-thiourea (PTU) and arbutin utilized as positive controls. Dieckol (DK), Eckstolonol (ES), Eckol (EK), Triphlorethol A (TA), and Phloroglicinol (PG). Experiments were performed in triplicate and the data are expressed as mean \pm SE.

Fig. 3-3. Effects of melanogenic inhibitors on the pigmentation of zebrafish. The effects of the pigmentation of zebrafish were observed at 35 hpf (hour post-fertilization) under microscope. (A) Untreated zebrafish embryos as a control, (B, C) 1-phenyl-2-thiourea (PTU), arbutin as positive controls, (D) dieckol (DK), (E) eckstolonol (ES), (F) eckol (EK), (G) triphlorethol A (TA), and (H) phloroglicinol (PG).

Fig. 3-4. Tyrosinase inhibitory activity of phlorotannins in zebrafish embryos. 1-phenyl-2-thiourea (PTU) and arbutin utilized as positive controls. Dieckol (DK), Eckstolonol (ES), Eckol (EK), Triphlorethol A (TA), and Phloroglicinol (PG). Experiments were performed in triplicate and the data are expressed as mean \pm SE. * p <0.05, ** p <0.01.

Fig. 3-5. Effects of melanogenic inhibitors on the heart-beating rate. The heart-beating rate was measured under the microscope. The number of heart-

beating for 3 min was counted, and the result represented as the beat/min. 1-phenyl-2-thiourea (PTU) and arbutin utilized as positive controls. Dieckol (DK), Eckstolonol (ES), Eckol (EK), Triphlorethol A (TA), and Phloroglicinol (PG). Experiments were performed in triplicate and the data are expressed as mean± SE. * p <0.05, ** p <0.01.

Fig. 3-6. Protective effect of phlorotannins isolated from *E. cava* on UV-B radiation-induced heart-beat disturbance in zebrafish. The embryos were exposed to UV-B (50 mJ/cm²) and phlorotannins treated. The heart-beat was measured at 48 hpf, under the microscopy. The number of heartbeat in 3 min was counted, and the results are expressed as the beats/min. Dieckol (DK), Eckstolonol (ES), Eckol (EK), Triphlorethol A (TA), and Phloroglicinol (PG). Experiments were performed in triplicate and the data are expressed as mean± SE. ** p <0.01.

Fig. 3-7. Inhibitory effect of phlorotannins on melanogenesis after UV-B radiation in zebrafish embryos. The embryos were exposed to UV-B (50 mJ/cm²) and phlorotannins treated. After incubation, melanin contents were detected by spectrophotometer after dissolved in 1N NaOH. Dieckol (DK), Eckstolonol (ES), Eckol (EK), Triphlorethol A (TA), and Phloroglicinol (PG). Experiments were performed in triplicate and the data are expressed as mean± SE. ** p <0.01.

Fig. 3-8. Inhibitory effect of phlorotannins on melanogenesis after UV-B radiation in zebrafish embryos. The embryos were exposed to UV-B (50 mJ/cm²) and phlorotannins treated. Dieckol (DK), Eckstolonol (ES), Eckol (EK), Triphlorethol A (TA), and Phloroglicinol (PG).

Fig. 3-9. Effect of phlorotannins isolated from *E. cava* on UV-B radiation-induced ROS level in zebrafish. The embryos were exposed to UV-B (50 mJ/cm²) and phlorotannins treated. After incubation, the intracellular ROS detected by fluorescence spectrophotometer after DCFH-DA staining. Dieckol (DK), Eckstolonol (ES), Eckol (EK), Triphlorethol A (TA), and Phloroglicinol (PG). Experiments were performed in triplicate and the data are expressed as mean± SE. **p*<0.05.

Fig. 3-10. Photographs of UV-B radiation-induced ROS level in zebrafish. The embryos were exposed to UV-B (50 mJ/cm²) and phlorotannins treated. The ROS levels were measured by image analysis and fluorescence microscope.

Fig. 3-11. Effect of phlorotannins isolated from *E. cava* on UV-B radiation-induced NO level in zebrafish. The embryos were exposed to UV-B (50 mJ/cm²) and phlorotannins treated. After incubation, the intracellular ROS detected by fluorescence spectrophotometer after DAF-FM DA staining. Dieckol (DK), Eckstolonol (ES), Eckol (EK), Triphlorethol A (TA), and Phloroglicinol (PG). Experiments were performed in triplicate and the data are expressed as mean± SE. **p*<0.05, ***p*<0.01.

Fig. 3-12. Photographs of UV-B radiation-induced NO level in zebrafish. The embryos were exposed to UV-B (50 mJ/cm²) and phlorotannins treated. The ROS levels were measured by image analysis and fluorescence microscope. Dieckol (DK), Eckstolonol (ES), Eckol (EK), Triphlorethol A (TA), and Phloroglicinol (PG).

Fig. 3-13. Protective effect of phlorotannins isolated from *E. cava* on UV-B radiation-induced cell death in live zebrafish. The embryos were exposed to UV-B (50 mJ/cm²) and phlorotannins treated. After incubation, the cell death was detected by fluorescence spectrophotometer after acridine orange staining. Dieckol (DK), Eckstolonol (ES), Eckol (EK), Triphlorethol A (TA), and Phloroglicinol (PG). Experiments were performed in triplicate and the data are expressed as mean± SE. ***p*<0.01.

Fig. 3-14. Photographs of UV-B radiation-induced cell death in live zebrafish. The embryos were exposed to UV-B (50 mJ/cm²) and phlorotannins treated. The cell death levels were measured by image analysis and fluorescence microscope. Dieckol (DK), Eckstolonol (ES), Eckol (EK), Triphlorethol A (TA), and Phloroglicinol (PG).

Legend of Table

Table 1. Hatching time for measurement of the toxicity of the tested chemical

Table 2. Lethal concentration (LC₅₀) of the toxicity of the tested chemical



GENERAL INTRODUCTION

Fish are the most widely used non-mammalian vertebrates in risk assessment and regulation (**Schirmer, 2006**). Several fish species are recommended for standard testing of chemicals or environmental sample. Among them, zebrafish has special characteristics, which expedite its use as a model organism.

The zebrafish (*Danio rerio*) is a small tropical freshwater fish which lives in rivers of northern India, northern Pakistan, Nepal, and Bhutan in South Asia. The characteristic stripes running along the body and the fins give its name to this species, zebrafish adults are only approximately 3-5 cm long, so that they can be easily managed in large numbers in the laboratory. Zebrafish have short generation times of approximately three to five months. The development of the zebrafish is very similar to the embryogenesis in higher vertebrates, including humans, but, unlike mammals, zebrafish develop from a fertilized egg to adults outside the female in a transparent egg. Moreover, the embryos themselves are transparent during the first few days of their lives (**Wixon, 2000**).

The embryonic development of zebrafish is very rapid: in the first 24 hours after fertilization, all major organs are developed and within three days the fish hatch. At 5 dpf - at the time of complete yolk consumption and start of external feeding - organogenesis of major organs is completed (**Rubinstein 2003, Fig. I**). The transparent chorion enables the easy observation of development (**Kimmel et al. 1995**). After three to four months, zebrafish are sexually mature and can generate new offspring. A single female can lay up to 200 eggs per week (**Stern and Zon, 2003**).

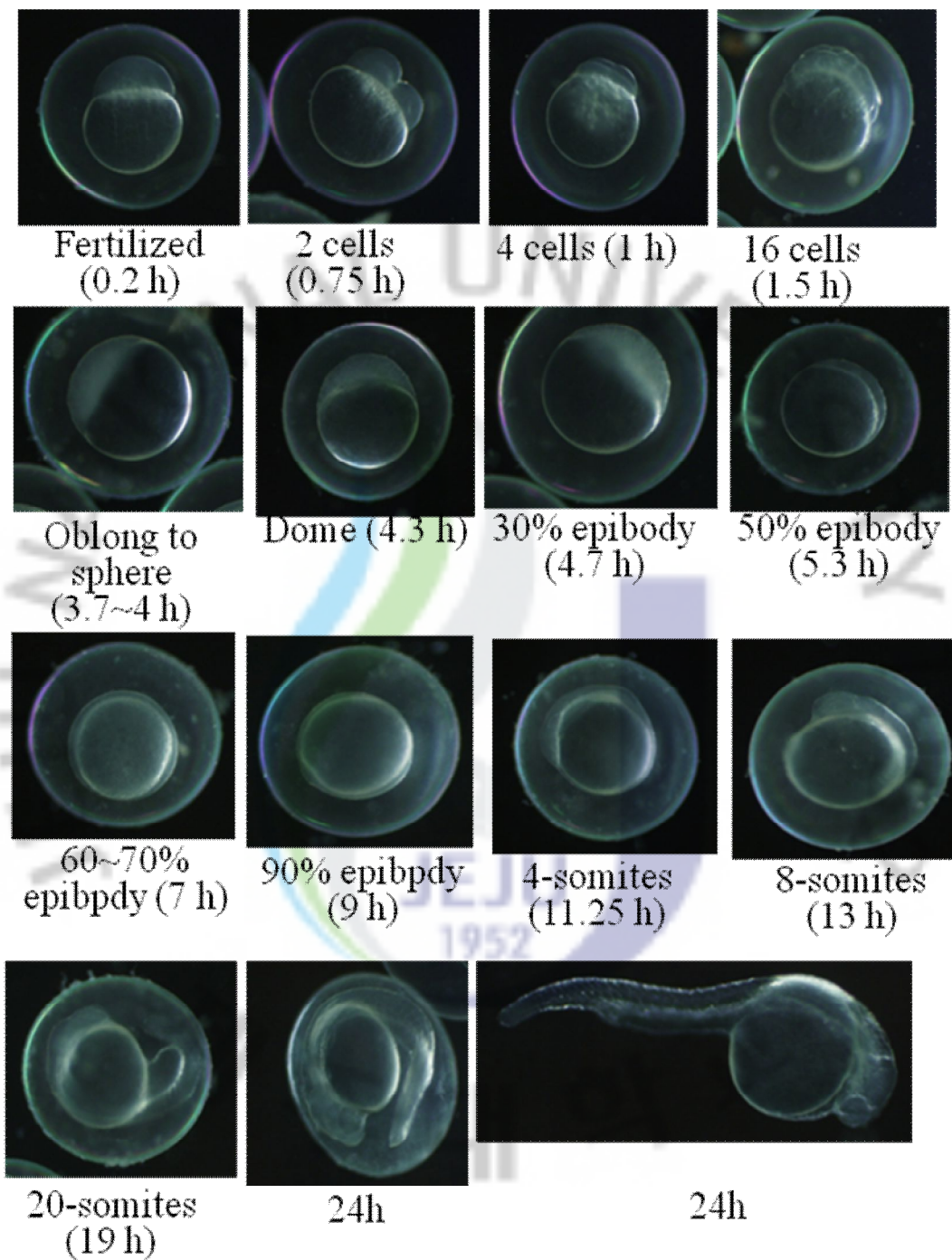


Fig. I . Development stage of zebrafish embryo.

Under laboratory conditions several thousand embryos can easily be produced daily and used for parallel experimental treatments. The genomic sequencing of the zebrafish is highly advanced and, at the time of this review, about 32,000 transcript sequences have been identified (www.ensembl.org, *D. rerio* genome release **Zv7**, **April 2007**). Due to the principal similarities of vertebrates, the zebrafish is used as a model for human disease and development and has attracted large-scale funding, e.g. by the European Union (ZF-MODELS, **Bradbury 2004**).

Recently the whole genome of zebrafish has been sequenced (Sanger Institute, http://www.sanger.ac.uk/Projects/D_retio). It is even more complex than the human genome, as zebrafish have two more pairs of chromosomes than humans. This difference arose during evolution in teleosts, when the whole genome was duplicated, which did not occur in mammals. Many of these duplicated genes were lost again and only a small proportion remains today. Functions of these duplicated genes changed in several cases (**Hill et al, 2005**).

The principal physiological characteristics of zebrafish mentioned above, were initially the most important advantages that made this species a popular model to study the development of vertebrates. The tiny size of the larval and adult zebrafish greatly reduces costs as it enables the reduction of housing space and husbandry costs. Furthermore, in toxicological and pharmacological studies (i.e. investigating drugs, potentially toxic compounds, environmental samples, etc.), testing can be performed in miniaturized format, which minimizes the quantities of chemicals to deploy and reduces the volumes of potentially hazardous waste (**Hill et al., 2005; Spitsbergen and Kent, 2003**). In addition, the small size of eggs and juveniles allows the operation of tests in high-throughput screenings, i.e. in multi-well plates,

and thus a sufficient database from many replicate samples can be gained for statistical evaluation and validation of results.

Another advantage of this species is its high fecundity. One pair of adult fish is capable of laying 300 eggs a day, and depending on the conditions of maintenance, this yield can be expected every 5~7 days. In addition, the rapid maturation of zebrafish also enables the performance of transgenerational studies. Thus, with sexual maturation after around 100 days, zebrafish can be utilized in mutagenesis analyses (Hill et al, 2005).

Zebrafish embryonic development has been well characterized (Kimmel et al., 1995). As already mentioned above, zebrafish eggs are transparent as well as the embryos themselves during their first days of life. Pigmentation in the embryos starts only about 30~72 hours post fertilization (Hill et al, 2005). Therefore, changes in the morphology within their early-stage development can be easily observed the microscope.

Pigmentation can further be prevented *in vivo* by treatment with 0.003% phenylthiourea or removed by bleaching after fixation, in order to extend the period of unhindered observation (Hill et al, 2005). Obviously, due to the fact that zebrafish develop outside the mothers body, developmental stages can be followed easily *in vivo*, unlike in mammals, where embryos have to be harvested.

Another important characteristic of zebrafish is that mutant zebrafish embryos, even having strong morphological malformations of displaying organ dysfunction, are still able to survive substantially past the time in which the particular organs normally start to function in healthy individuals. In contrast, malformed embryos of rodents mostly die *in utero* (Hill et al, 2005). Because mutants are useful for many kinds of

studies, such as human diseases, due to the high homology with humans, hundreds of zebrafish phenotypic mutants were produced and applied to unravel molecular regulations of ontogeny (**Stern and Zon, 2003**). As already reported above, the zebrafish underwent a whole-genome duplication event during teleost evolution. Some of these duplicated genes have new functions, and others no longer expressed in the same tissues as the original genes. Therefore, in comparison to mutations causing embryonic lethality in mammals, mutations in zebrafish paralogs many show a less severe phenotype with the embryo remaining viable (**Hill et al, 2005**). This may permit analyses of gene function in mutant zebrafish that would be difficult to achieve in mutant mammals due to the associated embryo mortality (**Spitsbergen and Kent, 2003**). The obvious disadvantage of the gene duplication, however, is that certain changes in gene expression caused by toxic agents or a mutation may be hard to extrapolate to other vertebrates including mammals.

The availability of the complete genome sequence of zebrafish allowed the production of commercially available microarrays (Agilent, Affymetrix, Compugen/Sigma-Aldrich, MWGBiotech and Qiagen/Operon) that offer a standardized tool set for zebrafish transcriptional profiling studies.

The availability of different new technologies as well as the spreading of their application in different fields, greatly supported the prevalence of zebrafish as a model, so that it is no longer limited to the field of vertebrate developmental research. Zebrafish is a widely used model organism in many different fields of research. In the past, it was a major vertebrate model especially in the developmental and genetic research (**Hill et al, 2005**), whereas now, the zebrafish gains also growing importance in other fields.

Zebrafish has become a popular model in pharmacological studies for screening of chemical libraries, mode-of-action studies, analysis of gene function, predictive toxicology, teratogenicity, and pharmaco- and toxico-genomics. It was shown that zebrafish can be used as a suitable model in cancerogenesis studies, anti-cancer drug investigations, inflammatory processes, as well as for lipid metabolism, since the response to cholesterol blockers is similar to those in mammals (**Langenheinrich, 2003**). The replacement of mammalian test systems by zebrafish, as less cost-intensive alternative in late-phase toxicity screening of drugs, was proposed by **Rubinstein (2006)**, because of the many similar biological processes. Furthermore, *Danio rerio* is an excellent system for chemical toxicity testing. The number of chemicals that need to be tested in the field of chemical toxicity and drug discovery is steadily increasing. Therefore, also the need for high-throughput screening methods arises, where the use of zebrafish embryos was proposed (**Hill et al 2005**), because of their small size and thus suitability for studies in multi well plates. Not only toxicity screening applications are imaginable; also applications for the clarification of mechanisms of toxicity have been reported (**Spitsbergen and Kent, 2003**). According to current European Union legislation for the protection of animals used for experimental and other scientific purposes, the use of embryonic stages of vertebrates is not regulated (Commission of the European Communities 1986). Hence, experiments with embryos are considered as alternative to animal experiments (**Fleming 2007**). In contrast to cellular replacement methods, such as fish cell lines (**Schirmer 2006**), the embryo model offers a complex, multicellular system integrating the interaction of various tissues and differentiation processes.



Part I

Toxicity evaluation using a zebrafish embryo

Part I .

Toxicity evaluation using a zebrafish embryo

ABSTRACT

Although rodents have previously been used in toxicological studies, they are expensive, time-consuming, and are limited by strict legal restrictions. Zebrafish are becoming an important model system for evaluation of chemical and drug toxicity. Here we treated embryos of the naive-type, for comparing toxicity levels with the well-known hydrogen peroxide (H_2O_2) and 2,2'-azobid (2-amideinopropane) dihydrochloride (AAPH). Embryos were exposed to waterborne H_2O_2 and AAPH concentrations for various lengths of time. The waterborne H_2O_2 concentrations that cause 50% mortality (LC_{50}) following a 1, 3, 6 and 12 h exposure were 8.10, 7.25, 5.03, and 3.69 mM, respectively. The waterborne AAPH concentration that causes 50% mortality (LC_{50}) following a 1, 3, 6, 12, 24 and 48 h exposure were >25, >25, 24.11, 10, 9.1 and 2 mM, respectively. These toxicants induced an increase in morphological disruption, indicating toxicity at early life-stages. The transient zebrafish embryo was sensitive enough to this toxicant to express the ROS regulated enhanced green fluorescent. The findings of this study demonstrated that the zebrafish *in vivo* model might allow for extremely rapid and reproducible toxicological profiling of early life-stage embryo development.

INTRODUCTION

There is a great public demand for the replacement of animal tests for ethical reasons, but industry is also interested in alternative testing methods that are less cost intensive and less time- and space-consuming. Various alternative approaches for predicting environmental risks of chemicals are available, including analyses of structure– activity relationships or toxicity tests with cell-based systems and fish embryos. The use of fish embryos is not regulated by current legislations on animal welfare and is therefore considered as a refinement, if not replacement of animal experiments. Fish embryos represent an attractive model for environmental risk assessment of chemicals since they offer the possibility to perform small-scale, high-throughput analyses.

The early life stages of fish are potentially useful as an alternative experimental model (Frayse et al., 2006) because embryonic stages are the most sensitive in the life cycle of the teleost (Lele and Krone, 1996; McKim, 1985). In addition, fish have been used for animal welfare reasons. The main benefits of using zebrafish as a toxicological model over other vertebrate species are with regards to their small size, husbandry, and early morphology (Hill et al., 2005). Furthermore, zebrafish embryos that are malformed can usually survive substantially past the time in which those organs start to function in healthy individuals (Hill et al., 2005). For example, mutant zebrafish such as still heart, and slow mo (Chen et al., 1996), and toxicant-exposed embryos with heart abnormalities (Antkiewicz et al., 2005) survive well beyond 24 h when the heart normally begins to beat (Kimmel et al., 1995). Because of the advantages of this *in vivo* system, we studied the developmental toxicities of

some well-known oxidative stress, hydrogen peroxide (H_2O_2) and 2,2'-azobid (2-amideinopropane) dihydrochloride (AAPH), on zebrafish embryos. The early life stages of fish are potentially useful as an alternative experimental model (**Fraysse et al., 2006**) because embryonic stages are the most sensitive in the life cycle of the teleost (**Lele and Krone 1996**). In addition, fish have been used for animal welfare reasons. The main benefits of using zebrafish as a toxicological model over other vertebrate species are with regards to their small size, husbandry, and early morphology (**Hill et al., 2003**). Furthermore, zebrafish embryos that are malformed can usually survive substantially past the time in which those organs start to function in healthy individuals (**Hill et al., 2003**). For example, mutant zebrafish such as still heart, and slow mo (**Chen et al., 1996**) and toxicant-exposed embryos with heart abnormalities (**Antkiewicz et al., 2005; Incardona et al., 2004**) survive well beyond 24 h when the heart normally begins to beat (**Kimmel et al., 1995**). Because of the advantages of this *in vivo* system, we studied the developmental toxicities of some well-known ROS generator toxicant, H_2O_2 and AAPH, on zebrafish embryos.

The main objective of this study was to demonstrate the potential for obtaining valuable and novel insights in chemical toxicology using the zebrafish as an alternative model vertebrate.

MATERIALS AND METHODS

Chemicals

Hydrogen peroxide of 30% purity was purchased from Daejung (Korea), and 2,2'-azobid (2-amideinopropane) dihydrochloride (AAPH) was purchased from Sigma (USA).

Origin and maintenance of parental zebrafish

Adult zebrafishes were obtained from a commercial dealer (Seoul aquarium, Korea) and 10 fishes were kept in 3 l acrylic tank with the following conditions; 28.5°C, with a 14/10 h light/dark cycle. Zebrafishes were fed three times a day, 6 d/week, with Tetramin flake food supplemented with live brine shrimps (*Artemia salina*). Embryos were obtained from natural spawning that was induced at the morning by turning on the light. Collection of embryos was completed within 30 min and staged as described by **Kimmel et al (1995)**.

Chemical administration and embryos observance

In order to determine the chemical exposure does for the estimation of hydrogen peroxide (H₂O₂) and 2,2'-azobid (2-amideinopropane) dihydrochloride (AAPH) toxicity using a zebrafish embryo, we performed toxicity tests. As part of toxicity tests, at 3-to 4-hpf (hour post fertilization) embryos were exposed to H₂O₂ (2 mM, 5 mM 10 mM and 25 mM) for 1, 3, 6, and 12 h. For AAPH studies, embryos exposed to AAPH (2 mM, 5 mM 10 mM and 25 mM) for 1, 3, 6, 12, 24, 48 and 72 h. Chemicals were administrated into embryo media. Control embryo were exposed to vehicle

(0.1% DMSO) only and used as negative control to compare effects on chemical-treated embryo. Approximately fifty embryos were used for each treatment and examined. Three replicate treatment groups were exposed to each dose in 6 well polystyrene multi-well plates (50 embryos per well). After the incubation period, the media was removed and added fresh embryo media. At 2-dpf (day post fertilization) zebrafish embryos were observed for signs of malformations and mortalities. Dead embryos were counted and removed. The average of proportion of embryo corresponding to a given end point was calculated for each time or concentration. To reduce variation among the batches, randomized embryos from 4 or 5 independent pair-wise mating were utilized. Each individual embryo was scored for morphological malformations, mortality, behavioral abnormalities and developmental delays daily.

Heart rate and hatching time

The heart-beating rate of both atrium and ventricle was measured at 48 hpf to determine the toxicity. Counting and recording of atrial and ventricular contraction were performed for 3 min under the microscope, and results were presented as the average heart-beating rate per min. At 48 hpf, the embryos are able to hatch. The number of hatched embryos were recorded every 2 h until 80 hpf. A embryo is considered - was calculated for each multi-well plate as the percentage of hatched larvae per plate. Then the number of hatched embryos in each replicate was pooled to calculate the mean hatching time (HT₅₀) by **Fraiese's (2006)** method.

Estimation of intracellular ROS generation and image analysis

Generation of reactive oxygen species (ROS) production of zebrafish embryos was analyzed using an oxidation-sensitive fluorescent probe dye, 2,7-dichlorofluorescein diacetate (DCF-DA). DCF-DA was deacetylated intracellularly by nonspecific esterase, which was further oxidized to the highly fluorescent compound dichlorofluorescein (DCF) in the presence of cellular peroxides (**Rosenkranz et al, 1992**). At 3 hpf, the embryos were treated 5 mM H₂O₂ and 25 mM AAPH to the plate. After treating embryos with H₂O₂ and AAPH the embryo media was changed. The embryos were transferred in to 96 well plate and treated with DCF-DA solution (20 µg/ml), and the plates were incubated for 1 h in the dark at 28.5°C. After incubation, the embryos were rinsed in embryo media and anesthetized before visualization. The images of stained embryos were observed using a fluorescent microscope, which was equipped with a CoolSNAP-Pro color digital camera (Olympus, Japan).

Statistical analysis

All the measurements were made in triplicate and all values were represented as mean±S.E. The results were subjected to an analysis of the variance using the Tukey test to analyze the difference. $P < 0.05$, $P < 0.01$ were considered significantly.

RESULTS

Embryotoxicity of H₂O₂

It was administered to naive zebrafish to determine the toxicity of H₂O₂ in the early larval stage of zebrafish. Initially, zebrafish embryos were exposed to various waterborne H₂O₂ concentrations from 3 to 4, 6, 9, and 15 hpf (1, 3, 6 and 12 h exposure). As shown in **Fig. 1-1**, survival rates were decreased in a concentration-dependant manner after exposure with H₂O₂. In addition, a time-dependant decrease in the survival was observed. Embryo survival was severely impacted at exposure time greater than 6 h with 95% mortality occurring at exposure time greater than 12 h. The H₂O₂ calculated lethal concentration to cause 50% mortality (LC₅₀) in embryo was 8.10, 7.25, 5.03, and 3.69 mM for 1, 3, 6 and 12 h. The H₂O₂ calculated lethal concentration to cause 50% mortality (LC₅₀) in embryo was 8.10, 7.25, 5.03, and 3.69 mM 1, 3, 6 and 12 h (**Table 1**). The predominant effects observed after H₂O₂ exposure were pericardial edema, swollen yolk sac, trunk abnormalities and contorted tail (**Figs. 1-2, 1-3**). As shown in **Fig. 1-2**, vascular impairment was detected, such as irregular arrangement of the caudal artery and vein. Moreover, intracellular ROS dramatically increased by H₂O₂ as shown in **Fig. 1-7**. These data suggested that H₂O₂ might cause gross morphological differences. Apart from gross morphological differences, sub-lethal effects (heart rate and hatching time disturbance) were observed following exposure to H₂O₂. At 48 hpf, the heart consists chambers and presents a regular heart rate. This sub-lethal end point was calculated by direct observation of the heart beat for 1 min. The heart rate is described by discrete values. The mean values of heart rates for H₂O₂ are reported in **Fig. 1-8**.

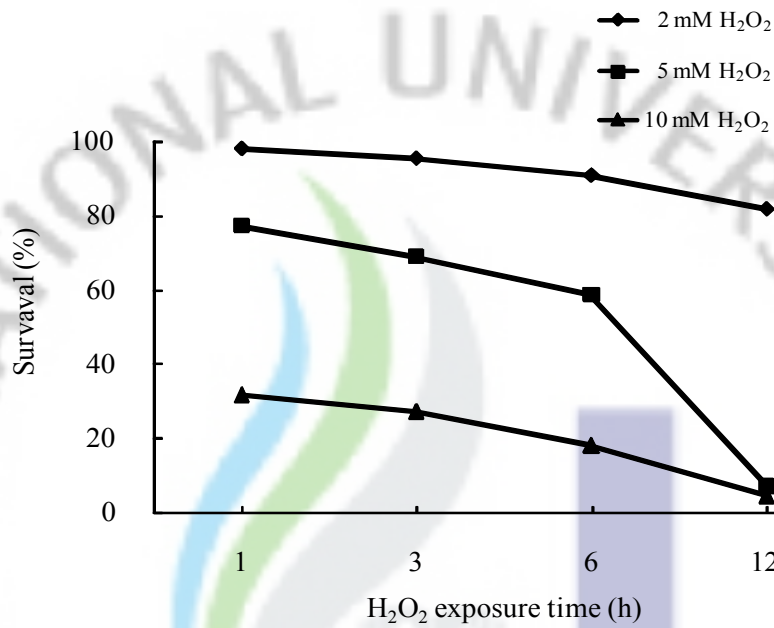


Fig. 1-1. Dose- or time- response curve between H₂O₂ exposed concentration or time and survival rates of zebrafish embryos. Zebrafish embryos were exposed from 3 hpf for 1, 3, 6, and 12 h with various H₂O₂ concentrations (2, 5 and 10 mM). The results are expressed as percentage of the survival rate of controls and survivals were scored at 48 hpf. N=500-525.

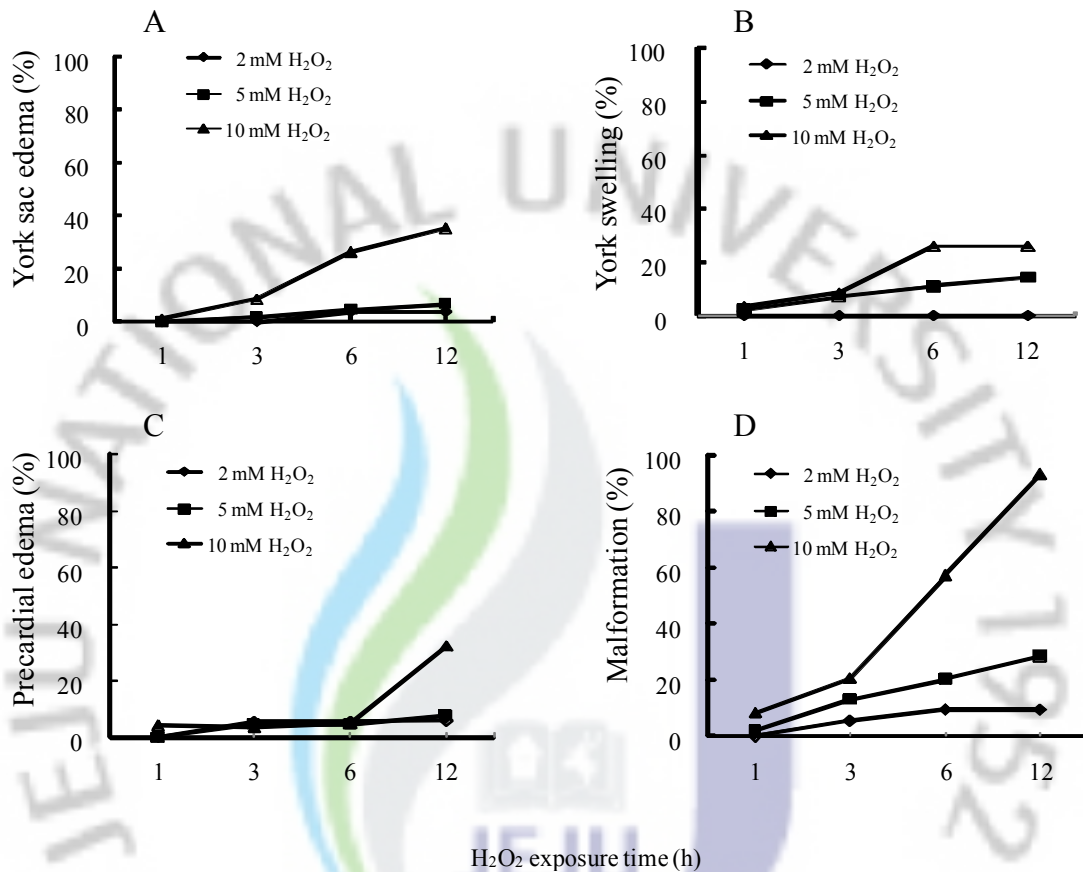


Fig. 1-2. Dose- or time- response curve between H_2O_2 exposed concentration or time and (A) york sac edema, (B) york swelling, (C) pericardial edema, and (D) total malformation rates of zebrafish embryos. Zebrafish embryos were exposed from 3 hpf with various H_2O_2 concentrations (2, 5 and 10 mM) for 1, 3, 6, and 12 h and the effect on malformations were scored at 48 hpf. Line graphs represent mean percentage embryonic york sac edema, york swelling, pericardial edema, and total malformation. N=500-525.

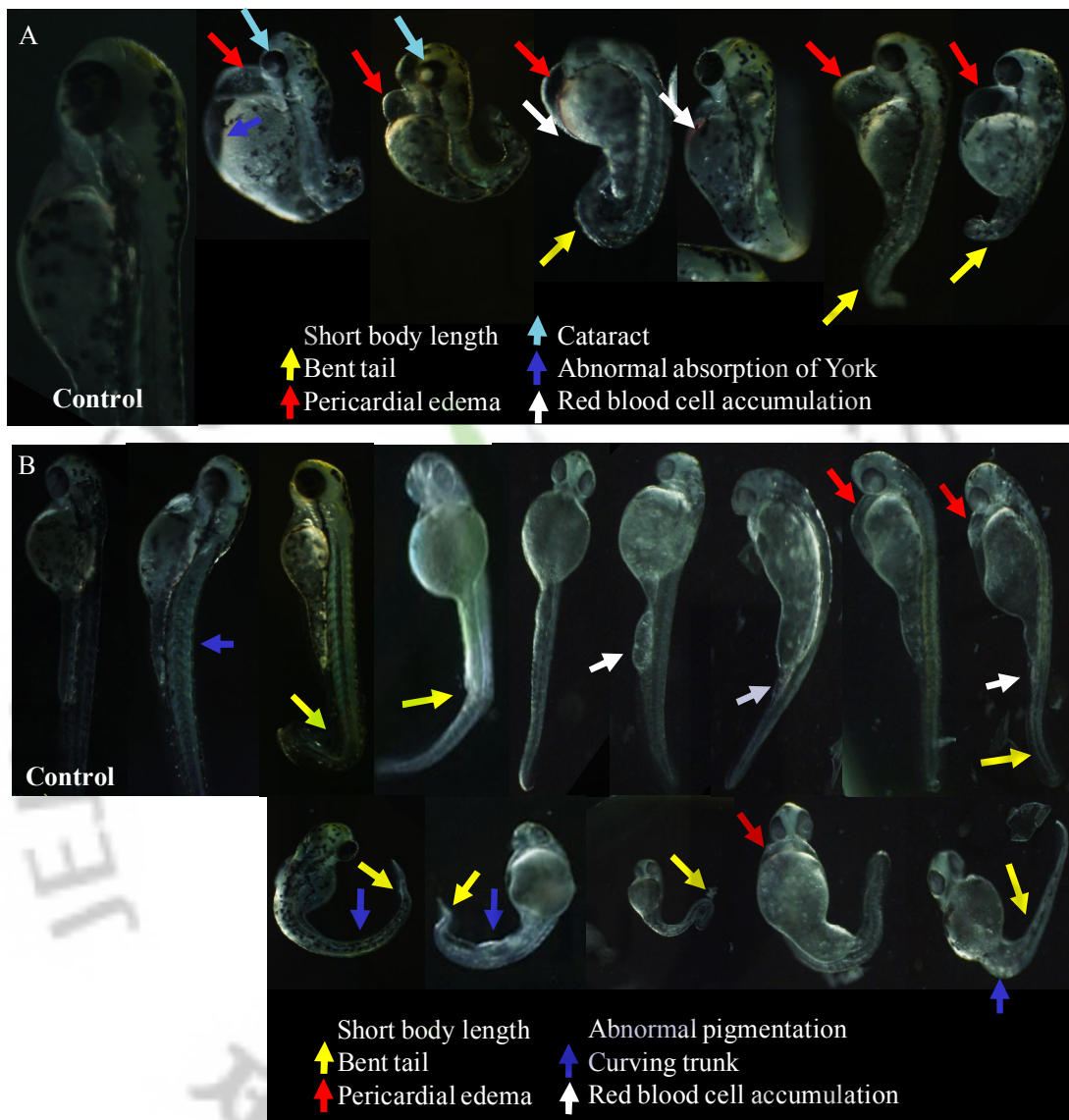


Fig. 1-3. Hydrogen peroxide induced dysmorphogenesis in developing zebrafish. Bent tail (yellow arrows), pericardial edema (red arrows), curving trunk (blue arrows), red blood cell accumulation (white arrows), short body length, swollen yolk sac and trunk abnormalities were characterized by H_2O_2 toxicity.

The recorded values ranged from 161 to 215 beats/min. The heart rate of each concentrations of H₂O₂ indicated statistically significant differences ($p < 0.05$) at 48 hpf zebrafish. For all groups, 100% of the embryos hatched at 72 hpf and there was no time lag between the first and the last hatching. Chemical exposure delayed hatching, as measured by HT₅₀ estimation, compared to the negative control.

Embryotoxicity of AAPH

It was administered to naive zebrafish to determine the toxicity of AAPH in the early larval stage of zebrafish. Initially, zebrafish embryos were exposed to various waterborne AAPH concentrations from 3 to 4, 6, 9, 15, 27, 51, and 75 hpf (1, 3, 6, 12, 24, 48, and 72 h exposure) and were monitored each time for survival rate until 3 dpf. The AAPH calculated lethal concentration to cause 50% mortality (LC₅₀) in embryo was 8.10, 7.25, 5.03, and 3.69 mM for 1, 3, 6 and 12 h. The AAPH calculated lethal concentration to cause 50% mortality (LC₅₀) in embryo was >25, >25, 24.11, 10, 9.1, and 2 mM for 1, 3, 6, 12, 24 and 48 h (**Table 1**). As shown **Fig. 1-4**, survival rates were decreased in a concentration-dependant manner after exposure with AAPH. In addition, a time-dependant decrease in the survival was observed. Embryo survival was severely impacted at exposure time greater than 12 h with 80% mortality occurring at exposure time greater than 50 h. The toxic manifestations of the well-known AAPH reported in our toxicity tests included pericardial edema, no swim bladder inflation, swollen yolk sac and lower jaw shortening (**Fig. 1-5**). AAPH predominantly caused elongated and pericardial edema, no swim bladder inflation, swollen yolk sac, and lower jaw shortening. These data suggested that AAPH might cause gross morphological differences. Apart from gross morphological differences,

sub-lethal effects (heart rate and hatching time disturbance) were observed following exposure to AAPH. At 48 hpf, the heart consists of chambers and presents a regular heart rate. This sub-lethal end point was calculated by direct observation of the heart beat for 1 min. The heart rate is described by discrete values. The mean values of heart rates for AAPH are reported in **Fig. 1-8**. The recorded values ranged from 175 to 198 beats/min. The heart rate of each concentrations of AAPH toxicants indicated statistically significant differences ($p < 0.05$) at 48 hpf zebrafish. Moreover, intracellular ROS dramatically increased by H_2O_2 as shown in **Fig. 1-7**. For all groups, 100% of the embryos hatched at 72 hpf and there was no time lag between the first and the last hatching. Chemical exposure delayed hatching, as measured by HT_{50} estimation, compared to the negative control.

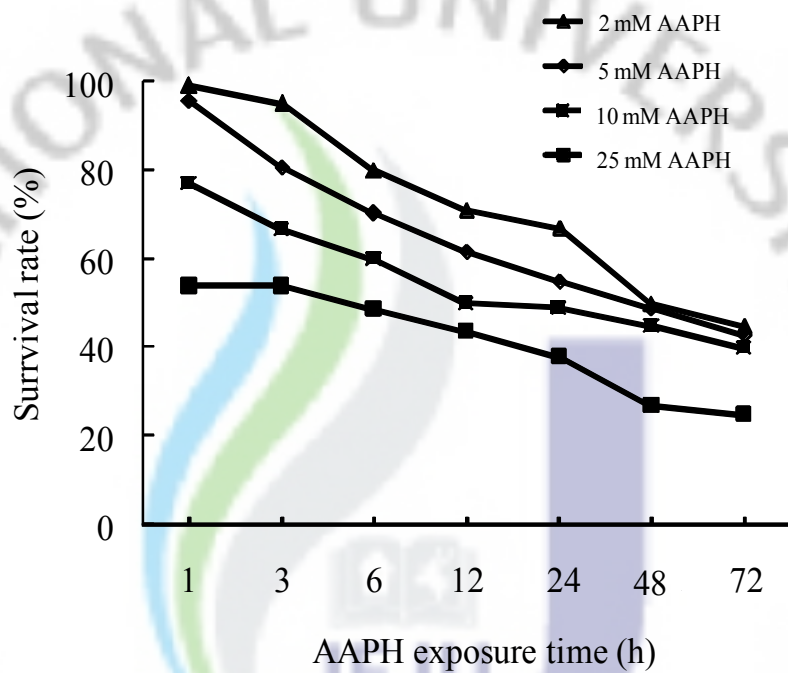


Fig. 1-4. Dose- or time- response curve between AAPH exposed concentration or time and survival rates of zebrafish embryos. Zebrafish embryos were exposed from 3 hpf for 1, 3, 6, 12, 24, 48, and 72 h with various AAPH concentrations (2, 5, 10 and 25 mM). The results are expressed as percentage of the survival rate of controls and survivals were scored at 48 hpf. N=505-537.

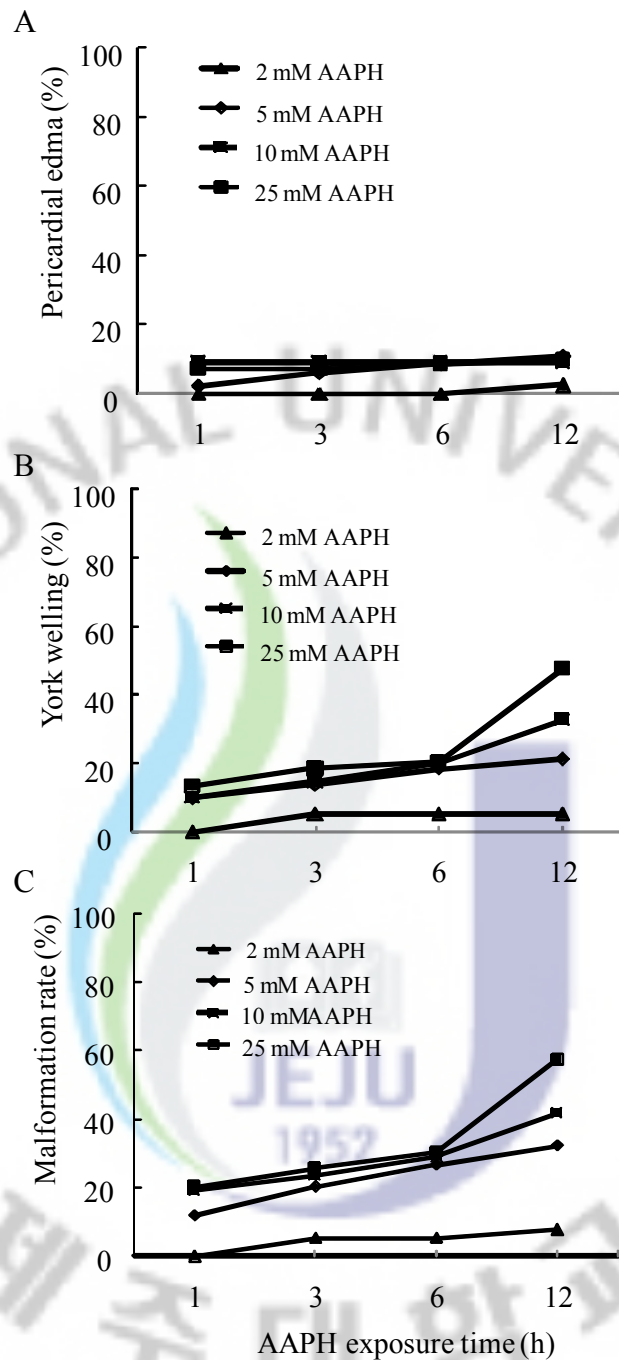


Fig. 1-5. Dose- or time- response curve between AAPH exposed concentration or time and (A) yolk swelling, (B) pericardial edema, and (C) total malformation rates of zebrafish embryos. Zebrafish embryos were exposed from 3 hpf with various AAPH concentrations (2, 5, 10 and 25 mM) for 1, 3, 6, and 12 h and the effect on malformations were scored at 48 hpf. Line graphs represent mean percentage embryonic yolk swelling, pericardial edema, and total malformation. N=505-537.

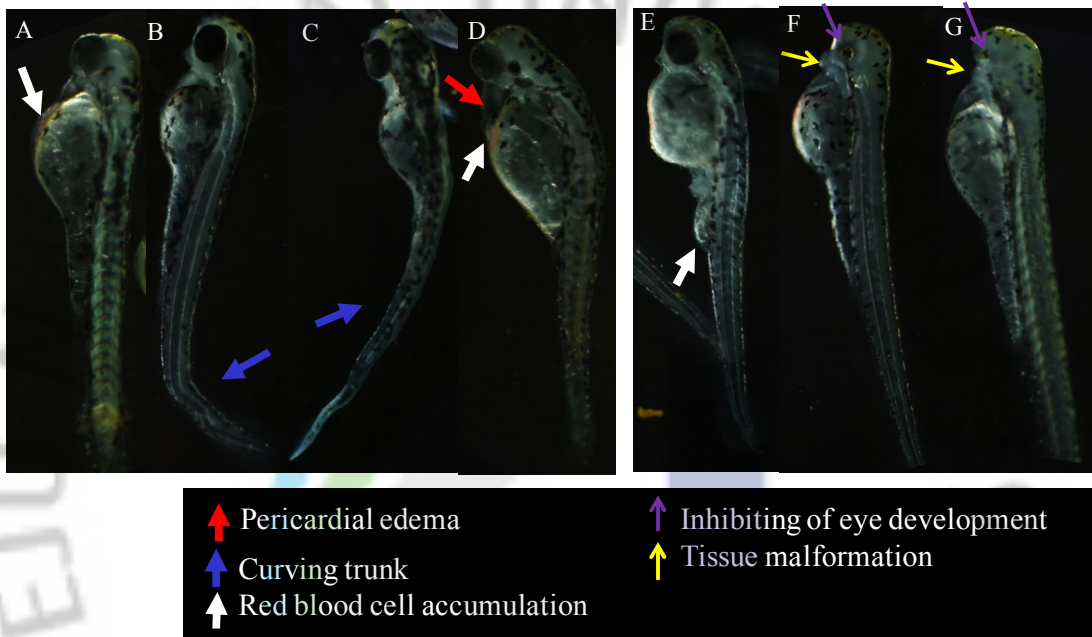


Fig. 1-6. AAPH induced dysmorphogenesis in developing zebrafish. Pericardial edema (red arrows), curving trunk (blue arrows), red blood cell accumulation (white arrows), tissue malformation (yellow arrows), swollen yolk sac, and losing eye (purple arrows) were characterized by AAPH toxicity. Also, AAPH-exposed zebrafish exhibited contorted tail and other tail malformations.

Table 1. Hatching time (HT₅₀) for measurement of the toxicity of the tested chemical

Hatching time (HT ₅₀)* (lower/upper)	Vehicle	H ₂ O ₂ (mM)			AAPH (mM)			
		2	5	10	2	5	10	25
	58.20*	59.01*	60.70*	62.77*	60.30*	63.06**	67.77*	60.02**
	(56.30/67.00)	(60.00/72.01)	(54.73/75.11)	(58.00/70.30)	(55.97/63.02)		(57.00/79.07)	

*95% confidence limits (lower/upper)

Table 2. Lethal concentration (LC₅₀) of the toxicity of the tested chemical

	H ₂ O ₂ (exposure time, h)				AAPH (exposure time, h)					
Lethal concentration (LC ₅₀)*	1	3	6	12	1	3	6	12	24	48
	8.10 mM	7.25 mM	5.03 mM	3.69 mM	>25 mM	>25 mM	24.11 mM	10 mM	9.1 mM	2 mM

*95% confidence limits (lower/upper).

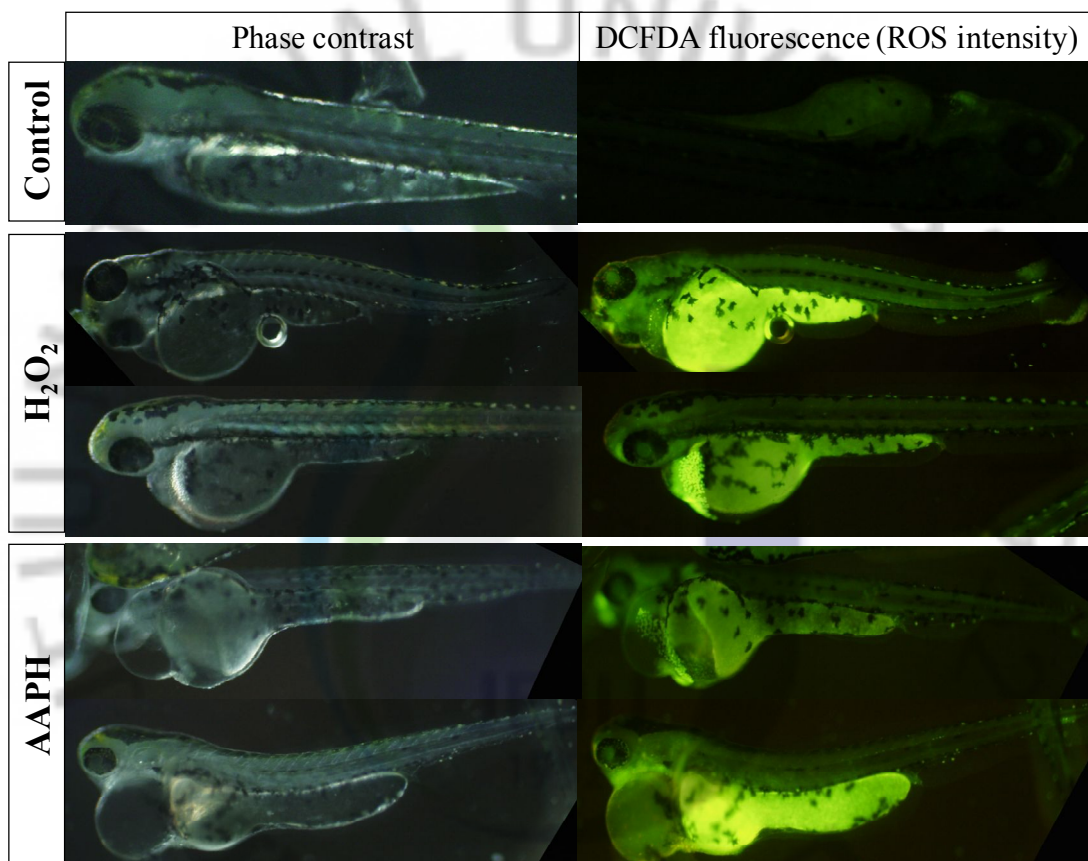


Fig. 1-7. Photographs of H₂O₂- or AAPH-induced ROS level in zebrafish embryo. The ROS levels were measured by image analysis using fluorescence microscope.

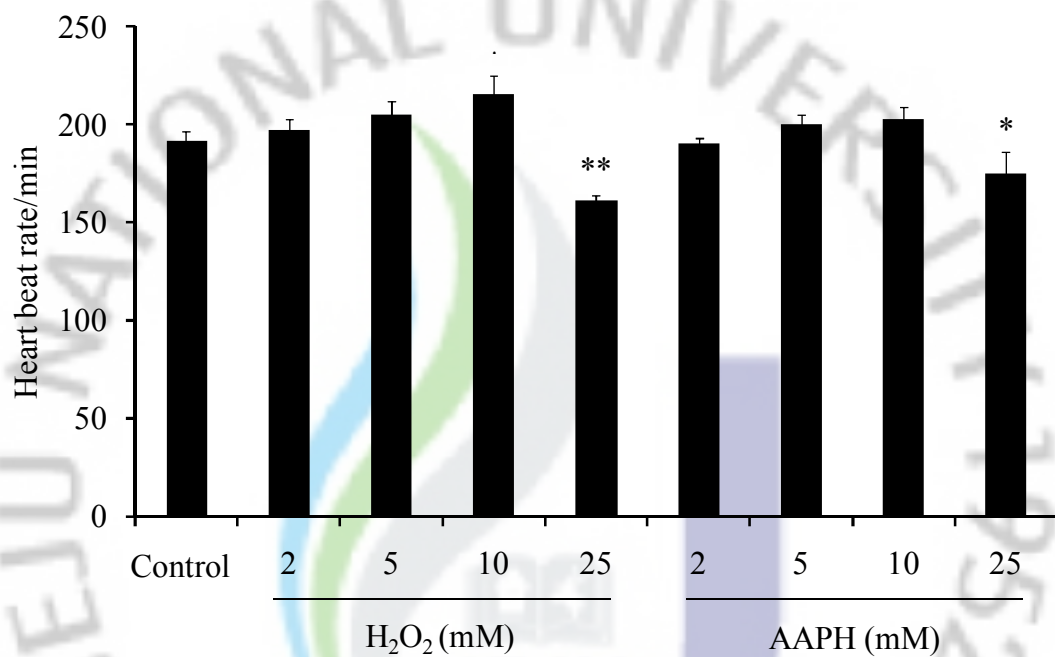


Fig. 1-8. Effects of H₂O₂ and AAPH on the heart-beat rate for measurement of the toxicity. The embryos were exposed to various concentration of H₂O₂ for 6 h. The heart-beat was measured at 48 hpf, under the microscopy. The number of heart beat in 3 min was counted, and the results are expressed as the beats/min. Experiments were performed in triplicate and the data are expressed as mean± SE. **p*<0.05, ***p*<0.01.

DISCUSSION

The toxicological effects of H₂O₂ and AAPH were assessed *in vivo* using the zebrafish embryo as an alternative animal model. Research presented herein clearly demonstrates the usefulness of this model as an effective platform to rapidly assess their toxicity. The embryos develop rapidly with most body organs formed within 48 hours; thus, thorough toxicological evaluations can be completed within just a few days. Due to the transparent nature of the embryos, numerous effects can be assessed non-invasively over the course of the experiment. Females produce hundreds of eggs weekly so large sample sizes are easily achieved for statically powerful dose-response studies. This abundant supply of embryos also makes it possible to simultaneously assess the toxicity of a large number of materials in a short period of time (Usenko et al., 2007).

There are additional advantages to using zebrafish as part of a comprehensive approach to toxicants risk assessment. Although beyond the scope of this paper, many routes of exposure (i.e. ingestion, injection and dermal) could also be assessed individually or in combination. Since zebrafish are amenable to genetic manipulations, biological targets and modes of action can be determined. Because embryos are transparent, tissue dose and distribution could potentially be determined using fluorescently labeled materials and laser scanning confocal microscopy. In addition, zebrafish attain sexual maturity by 90 days post-fertilization (dpf) making chronic studies feasible. Because zebrafish adults grow to an average size of 3-4 cm and are easy to maintain at high densities, the infrastructure and maintenance costs required for housing the large numbers of animals required for screening are

relatively low. Such features are favorable for adapting this model system to high-throughput assays for toxicant or drug toxicity evaluations (Usenko et al., 2007).

The use of the zebrafish as an alternative model vertebrate for toxicology and pharmacology has only recently been initiated in Korea (Seok et al., 2008). The zebrafish model may provide useful information for recognizing and understanding the effects of *in utero* exposure to H₂O₂ and AAPH in humans. In our studies, we determined developmental toxicities in early stages of developmental vertebrates with oxidative stress related toxicants. One of the most striking responses to H₂O₂ and AAPH in zebrafish embryos was the accumulation of edematous fluid in the pericardium and the yolk sac. Edema was first observed in the pericardial region and yolk sac. Elongation and failure of the heart to undergo looping was also reported, and tail malformation was observed as teratogenic category. Gross malformations resulting from exposure to toxicants included jaw reductions, presumptive skeletal defects, and edema. In the present study, heart malformation was a characteristic feature following exposure to H₂O₂ and AAPH toxicant, and this may reflect the fact that edema can accompany cardiovascular dysfunction because the osmoregulatory function of the skin and the circulatory function of the heart and vasculature are correlated. Moreover, zebrafish exposed to H₂O₂ and AAPH exhibited contorted tail and other tail malformation. This is the first report of H₂O₂ and AAPH toxicity in zebrafish. The malformations were caused by the irregular blood flow of the caudal vein and artery following H₂O₂ and AAPH exposure. In our studies, embryo exposure to H₂O₂ and AAPH elicited increased mortality (Fig. 1-1, Fig. 1-4), sublethal malformations (Fig 1-2, Fig. 1-3, Fig. 1-5, Fig. 1-6), and increased ROS (Fig. 1-7). Oxidative stress can lead to a variety of downstream effects including lipid

peroxidation, DNA and protein adduction and cellular death (**Kang et al., 2006**). Since there are limited tests that directly measure reactive oxygen species (ROS), researchers rely on detection of lipid peroxidation products and cell death as markers of oxidative stress. With few exceptions, underivatized H₂O₂ and AAPH are reportedly toxic due to pro-oxidant behavior that results in toxicity. Methods currently being developed to fluorescently detect ROS *in vivo*, will be applied to the embryonic zebrafish model in order to localize the stress in these transparent animals.





Part II

Zebrafish embryo as an alternative animal model
to evaluate antioxidant of functional food materials

Part II -1.

Protective effects of phlorotannins against H₂O₂-induced oxidative stress in zebrafish embryo

ABSTRACT

It overload with hydrogen peroxide (H₂O₂) induces oxidative stress and may initiate a cascade of intracellular toxic events leading to oxidation, lipid peroxidation and then subsequently cell death. Here, we have investigated the protective efficacy of phlorotannins including dieckol (DK), eckstolonol (ES), eckol (EK), triphloroethol A (TA), and phloroglucinol (PG), which are isolated from a brown seaweed *Ecklonia cava*, against H₂O₂-induced oxidative stress damage during zebrafish (*Danio rerio*) development. Zebrafish embryo exposed to H₂O₂ and compared with other groups that were co-exposed with phlorotannins until 2 day post fertilization (dpf). All phlorotannins were found to scavenge intracellular reactive oxygen species (ROS) and prevented lipid peroxidation. As a result, all phlorotannins reduced H₂O₂-induced cell death in zebrafish embryo. A H₂O₂ induced pericardial edema, yolk sac edema, and growth retardation in zebrafish embryos. In contrast, phlorotannins co-exposed groups did not show any morphological changes. These results clearly indicate that phlorotannins isolated from *E. cava* possesses prominent antioxidant activity against H₂O₂-mediated toxicity and which might be a potential therapeutic agent for treating or preventing several diseases implicated with oxidative stress. This study provides a new useful strategy for the protection of H₂O₂-induced oxidative stress in alternative animal model which is zebrafish.

INTRODUCTION

It is known that many human diseases can be caused by free radicals and natural antioxidants can act as free radical scavengers (**Chang et al. 2007; Meisel 1997**). Free radical-mediated lipid peroxidation oxidative stress and antioxidants are widely discussed in many current research areas. Lipid peroxidation is mostly an undesirable deteriorative reaction in food materials, which can produce rancidity odors and flavors during storage and processing. Lipid peroxidation is one example of oxidative stress caused by free radical reacting with lipid. Numerous studies revealed that lipid peroxidation is involved in the occurrence of many chronic diseases (**Butterfield et al. 2002**). Formation of free radicals such as hydroxyl radical ($\cdot\text{OH}$) or superoxide radical ($\text{O}_2^{\cdot-}$) is an unavoidable consequence in the respiration process of cells in aerobic organisms (**Je et al. 2007**). Moreover, $\cdot\text{OH}$ is known to be extremely reactive and more toxic than the others radical species, and can attack biologic molecules such as DNA, proteins, and lipids. The reactivity of $\cdot\text{OH}$ is marked and related to several human diseases such as rheumatoid arthritis, neurodegenerative disease, and diabetes (**Fig. 2-1**). Therefore, its scavenging activity has received much attention (**Kang et al. 2007**). Since free radicals are very unstable, they are immediately neutralized by antioxidant in the cell once they are generated in normal metabolism pathway. The free radical can cause damage of tissue by reacting with other chemicals in the body. Therefore, looking for functional ingredients that possess antioxidant activity in the food has become hot research subject in the food science (**Lindmark-Mansson and Akesson 2000**).

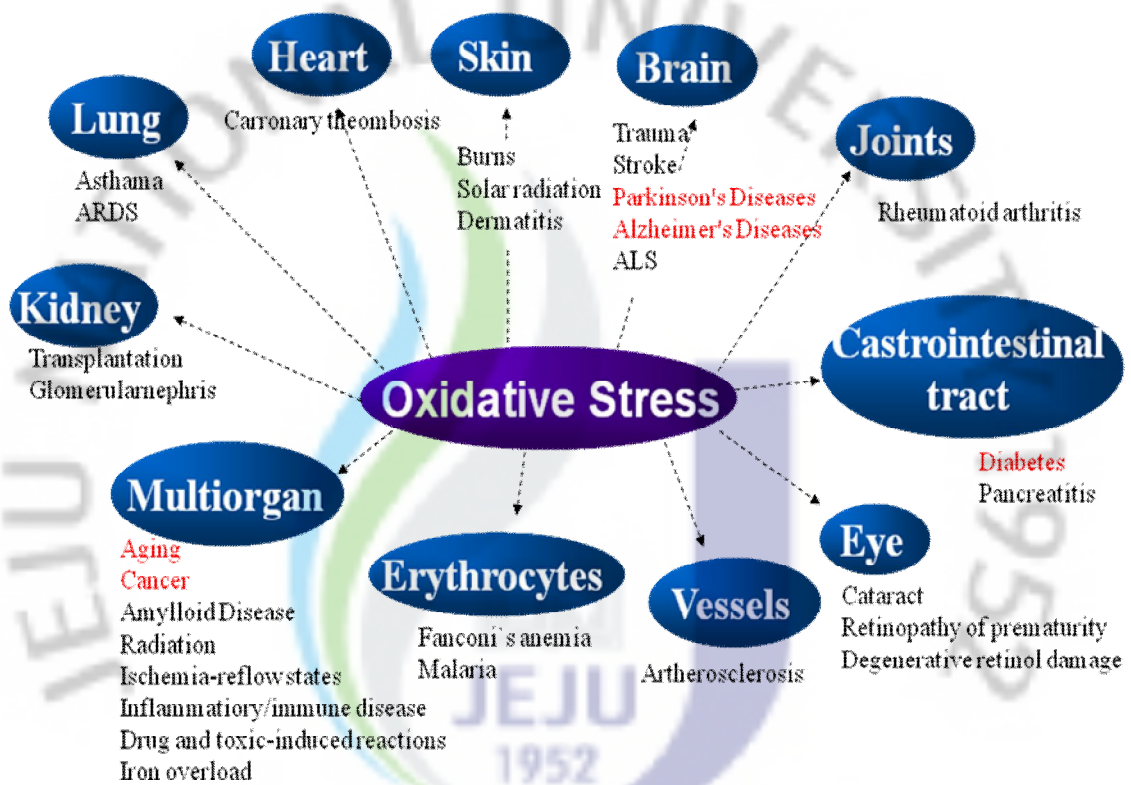


Fig. 2-1. Several human diseases caused by oxidative stress.

Nowadays, there is an increasing interest in detecting natural antioxidants, which are safe and effective in order to replace commercial synthetic antioxidants such as Butylated Hydroxyanisole (BHA) and Butylated Hydroxytoluen (BHT). The most commonly used antioxidants in lipid-containing food, with natural alternatives, because of their safety and toxicity problems (**Howell 1986; Amarowicz et al. 2000**). In fact, a number of marine algae have been used in Eastern Asia for thousands of years in traditional system of folk medicines, as antiviral, anticancer, anti-hypertension agent, and so on (**Jiang and Zhang 1994**). Meanwhile, marine organisms have been proven to be a rich source of structurally novel and biologically active secondary metabolites (**Takamatsu et al. 2003; Heo et al. 2008**). Marine algae have many phytochemicals with various bioactivities including antioxidant, anti-inflammatory and anticancer. Among them, antioxidant activity is intensively focused due to the current growing demand from the food and pharmaceutical industry where they are interested in antiaging and anticarcinogenic compounds, which possess health benefits. Therefore, many marine algae have been examined to identify new and effective antioxidant compounds, as well as to elucidate the mechanisms of cell proliferation and apoptosis (**Lee et al. 2004; Pietta et al. 1998**). Marine algae are also known to be rich in vitamins, minerals, polysaccharides, proteins, and polyphenols (**Nosedá et al. 1999; Barbarino and Lourenco 2005; Kuda et al. 2005**). Moreover, some brown algae (*Ecklonia cava*, *Eisenia bicyclis*, *Hizikia fusiformis* and *Sargassum* spp.) have been recognized as potential sources of antioxidants, including fucoxanthin, phlorotannins, chlorophylls, carotenoids, tocopherol derivatives such as vitamin E, and related isoprenoids (**Swanson and Druhl 2002; Takamatsu et al. 2003; Heo et al. 2008**). *Ecklonia cava* is a brown

alga (Laminariaceae) that is abundant in the subtidal regions of Jeju Island in Korea. Recently, it has been reported that *Ecklonia* species exhibits radical scavenging activity and, anti-plasmin inhibiting activity and, antimutagenic activity and, bactericidal activity, HIV-1 reverse transcriptase and protease inhibiting activity and tyrosinase inhibitory activity. Phlorotannin components, which is oligomeric polyphenol of phloroglucinol unit, are responsible for the biological activities of *Ecklonia* and phlorotannins such as eckol (a closed-chain trimer of phloroglucinol), 6,6'-bieckol (a hexamer), dieckol (a hexamer), phlorofucofuroeckol (a pentamer) were identified in *Ecklonia* species. During the investigation of antioxidative components in *E. cava*, we observed that eckol possessed very strong activity. Eckol, a trimeric compound of phloroglucinol with dibenzo-1,4-dioxin skeleton, is one of the major phlorotannins isolated from *E. cava*.

Physiologically H_2O_2 , a freely diffusible form of reactive oxygen species (ROS), is produced by many intracellular reactions, and an intermediate product of the degradation of ROS and a highly reactive molecule. Extracellular hydrogen peroxide is able to cross membranes, thus directly altering their intracellular concentrations (Li et al., 2000). Increased neurocellular load with ROS induces a number of intracellular events such as oxidative stress. Calcium is a potent pro-oxidant metal which stimulates production of ROS through inhibition of redox-sensitive enzymes such as catalase (Beyersmann and Hechtenberg, 1997).

2,2'-Azobis(2-amidopropane)dihydrochloride (AAPH), which generates two potent ROS capable of inducing LP, namely hydroxyl radical ($\cdot OH$) and peroxy radical ($ROO\cdot$). AAPH generates model peroxy radicals. These radicals are similar to such peroxy conditions that are physiologically active (Devasagayam et al.,

2003; Poli et al., 1987).

The vertebrate zebrafish (*Danio rerio*) is a small tropical freshwater fish that has emerged as a highly advantageous vertebrate model organism because of its small size, large clutches, transparent, low cost, and physiological similarity to mammals (Eisen, 1996; Fishman, 1999). Traditionally, zebrafish has been used in the fields of molecular genetics and developmental biology (Driever et al., 1996; Kimmel, 1989). However, its value as a model organism for drug discovery and toxicological studies has been recognized recently (den Hertog, 2005; Pichler et al., 2003). The application of drugs and/or small molecules to zebrafish is simple because the early stage embryo rapidly absorbs small molecular compounds diluted in the bathing media through the skin and gills. In contrast, relatively late stage zebrafish [from 7 d post-fertilization (dpf) to the adult stage] absorb the compounds orally rather than percutaneously (Langheinrich, 2003). In the present study, we have investigated the protective effect of phlorotannins on zebrafish embryos induced by H₂O₂- and AAPH-induced oxidative stress.

MATERIALS AND METHODS

Materials

The marine brown alga *E. cava* was collected along the coast of Jeju Island, Korea, between October 2007 and March 2008. The samples were washed three times with tap water to remove the salt, epiphytes, and sand attached to the surface. After then carefully rinsed with fresh water, and maintained in a medical refrigerator at -20°C. Thereafter, the frozen samples were lyophilized and homogenized with a grinder prior to extraction.

Preparation of phlorotannins from *Ecklonia cava*

The phlorotannins were isolated as previously described by **Ahn et al. (2007)** with slight modifications. Briefly, the dried *E. cava* powder (500 g) was extracted three times with 80% MeOH and then filtered. The filtrate was evaporated at 40°C to obtain the methanol extract. After, the extract was suspended on distilled water, and partitioned with ethyl acetate. The ethyl acetate fraction was mixed with celite. The mixed celite was dried and packed into a glass column, and eluted in the order of hexane, methylene chloride, diethyl ether, and methanol. The diethyl ether fraction was further purified by sephadex LH-20 column chromatography using stepwise gradient chloroform/methanol (2/1→0/1) solvents system. The phloroglucinol, eckol, triphloroethol A, eckstolonol and dieckol were purified by high performance liquid chromatography (HPLC) using a Waters HPLC system equipped with a Waters 996 photodiode array detector and C18 column (J'sphere ODSH80, 150× 20 mm, 4 μm; YMC Co.) by stepwise elution with methanol-water gradient (UV range: 230 nm,

flow rate: 0.8 ml/min). Finally, the purified compounds were identified by comparing their ^1H and ^{13}C NMR data to the literature report. The chemical structures of the phlorotannins are indicated in **Fig. 2-2**.

Origin and maintenance of parental zebrafish

Adult zebrafishes were obtained from a commercial dealer (Seoul aquarium, Korea) and 10 fishes were kept in 3 l acrylic tank with the following conditions; 28.5°C, with a 14/10 h light/dark cycle. Zebrafishes were fed three times a day, 6 d/week, with Tetramin flake food supplemented with live brine shrimps (*Artemia salina*). Embryos were obtained from natural spawning that was induced at the morning by turning on the light. Collection of embryos was completed within 30 min.

Waterborne exposure of embryos to phlorotannins and H_2O_2

From approximately 3 to 4 hour post-fertilization (3-4 hpf), embryos ($n=25$) were transferred to individual wells of a 24-well plate and maintained in embryo media containing 1 ml of vehicle (0.1% DMSO) or 50 μM phlorotannins for 1 h. Then treated with 5 mM H_2O_2 or co-treated H_2O_2 and phlorotannins for up to 48 hour post-fertilization (48 hpf).

Measurement of heart-beat rate

The heart-beating rate of both atrium and ventricle was measured at 35 hpf to determine the sample toxicity (Choi et al., 2007). Counting and recording of atrial and ventricular contraction were performed for 3 min under the microscope, and results were presented as the average heart-beating rate per min.

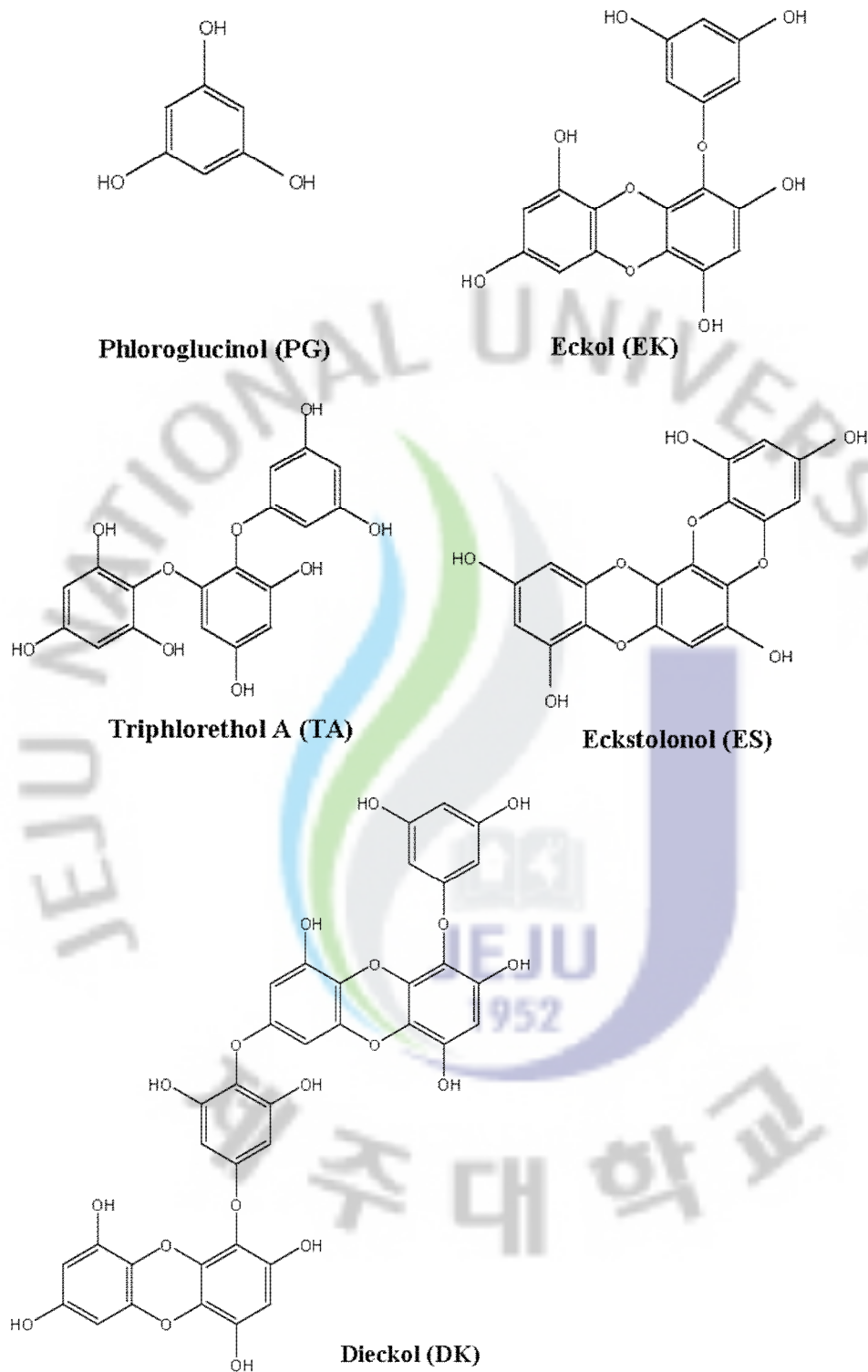


Fig. 2-2. The chemical structures of the phlorotannins.

Estimation of intracellular ROS generation and image analysis

Generation of reactive oxygen species (ROS) production of zebrafish embryos was analyzed using an oxidation-sensitive fluorescent probe dye, 2,7-dichlorofluorescein diacetate (DCF-DA). DCF-DA was deacetylated intracellularly by nonspecific esterase, which was further oxidized to the highly fluorescent compound dichlorofluorescein (DCF) in the presence of cellular peroxides (**Rosenkranz et al, 1992**). At 3-4 hpf, the embryos were treated with 50 μ M phlorotannins and 1 h later, 5 mM H_2O_2 was added to the plate. After treating embryos with 5 mM H_2O_2 for 6 h, the embryo media was changed and the embryos developed up to 2 dpf (day post-fertilization). The embryos were transferred in to 96 well plate and treated with DCF-DA solution (20 μ g/ml), and the plates were incubated for 1 h in the dark at 28.5°C. After incubation, the embryos were rinsed in fresh embryo media and anesthetized before visualization. Individual embryo fluorescence intensity was quantified using spectrofluorometer (Perkin–Elmer LS-5B, Austria) and the image of stained embryos were observed using a fluorescent microscope, which was equipped with a CoolSNAP-Pro color digital camera (Olympus, Japan).

Lipid peroxidation inhibitory activity and image analysis

Lipid peroxidation was measured to assess membrane damage according to **Wang et al. (2008)**. Morphological evaluation of the embryos was performed with Diphenyl-1-pyrenylphosphine (DPPP, Dojindo, Japan) is fluorescent probe for detection of cell membrane lipid peroxidation. DPPP is non-fluorescent, but it becomes fluorescent when oxidized. At 3-4 hpf, the embryos were treated with 50 μ M phlorotannins and 1 h later, 5 mM H_2O_2 was added to the plate. After treating

embryos with 5 mM H₂O₂ for 6 h, the embryo media was changed and the embryos developed up to 2 dpf. The embryos were transferred in to 96 well plate and treated with DPPP solution (25 µg/ml), and the plates were incubated for 1 h in the dark at 28.5 °C. After incubation, the embryos were rinsed in embryo media and anesthetized before visualization. Individual embryo fluorescence intensity was quantified using spectrofluorometer (Beckman DTX 800, USA) and image of embryos were observed using a fluorescent microscope, which was equipped with a CoolSNAP-Pro color digital camera (Olympus, Japan).

Measurement of oxidative stress-induced cell death in zebrafish embryo

Cell death was detected in live embryos using acridine orange staining, a nucleic acid selective metachromatic dye that interacts with DNA and RNA by intercalation or electrostatic attractions. Acridine orange stains cells with disturbed plasma membrane permeability so it preferentially stains necrotic or very late apoptotic cells. At 3-4 hpf, the embryos were treated with 50 µM phlorotannins and 1 h later, 5 mM H₂O₂ was added to the plate. After treating embryos with 5 mM H₂O₂ for 6 h, the embryo media was changed and the embryos developed up to 2 dpf. The embryos were transferred in to 96 well plate and treated with acridine orange (AO) solution (7 µg/ml), and the plates were incubated for 30 min in the dark at 28.5 °C. After incubation, the embryos were rinsed in embryo media and anesthetized before visualization. Individual embryo fluorescence intensity was quantified using spectrofluorometer (Perkin–Elmer LS-5B, Austria). The images of stained embryos were observed using a fluorescent microscope, which was equipped with a CoolSNAP-Pro color digital camera (Olympus, Japan).

Western blotting

The cells were harvested, washed twice with PBS, lysed on ice for 30 min in 100 ml lysis buffer [120 mM NaCl, 40 mM Tris (pH 8), 0.1% NP 40] and centrifuged at 13,000 X g for 15 min. The supernatants were collected from the lysates and the protein concentrations were determined. Aliquots of the lysates (40 mg of protein) were boiled for 5 min and electrophoresed in 10% sodium dodecyl sulfate-polyacrylamide gel. The blots in the gels were transferred onto nitrocellulose membranes (Bio-Rad, USA), which were incubated with the primary antibodies. The membranes were further incubated with the secondary immunoglobulin-G-horseradish peroxidase conjugates (Pierce, USA). Protein bands were detected using an enhanced chemiluminescence Western blotting detection kit (Amersham, UK), and then exposed onto X-ray film.

Statistical analysis

All the measurements were made in triplicate and all values were represented as mean±S.E. The results were subjected to an analysis of the variance using the Tukey test to analyze the difference. $P < 0.05$, $P < 0.01$ were considered significantly.

RESULTS

Toxicity of phlorotannins or H₂O₂ in zebrafish embryo

In order to determine the toxicity of the phlorotannins or H₂O₂, we monitored the survival rate and growth patterns of zebrafish embryos. The adopted endpoints experiment used to assess the toxicity of the compounds included embryo mortality, morphological malformations, and heart-beating disturbances. The survival rate of zebrafish embryos treated with H₂O₂ or co-treated with phlorotannins showed in **Fig. 2-3**. Significantly decreasing survival rate was observed survival in only H₂O₂ trearmnet embryos, in contrast, co-treatment with phlorotannins and H₂O₂ embryos survived about 90%. The phlorotannins were not associated with mortality in this experiment. When evaluating the morphological malformations, phlorotannins did not evidence conspicuous adverse effects. Whereas, zebrafish embryos exposed to H₂O₂ from 3-4 hpf to 9-10 hpf (6 h exposure) showed several typical morphological defects (**Fig. 2-4**). At 2 dpf, embryo treated with H₂O₂ showed short body leng and, in some case, incompletely differentiated tail ends, and spinal column curving. Heart curvature was unfolded and a dilated precardial sac was observed, suggesting precardial edema. Red blood cells accumulated in the side of york sac edema due to circulation failure. York consumption was slower than normal, suggesting growth retardation. Image analysis data showed that phlorotannins protected the morphological changes by H₂O₂. On the other hand, in the heart-beat test, H₂O₂ evidenced a marked increase in heart-beat rate, whereas phlorotannins did not generate any heat-beat rate disturbances as compared with the control (untreated phlorotannin or H₂O₂, **Fig. 2-5**). In simultaneous *in vivo* toxicity tests, toxicity was

not detected in the zebrafish treated with all phlorotannins, whereas toxicity was observed in the fish treated with H₂O₂.

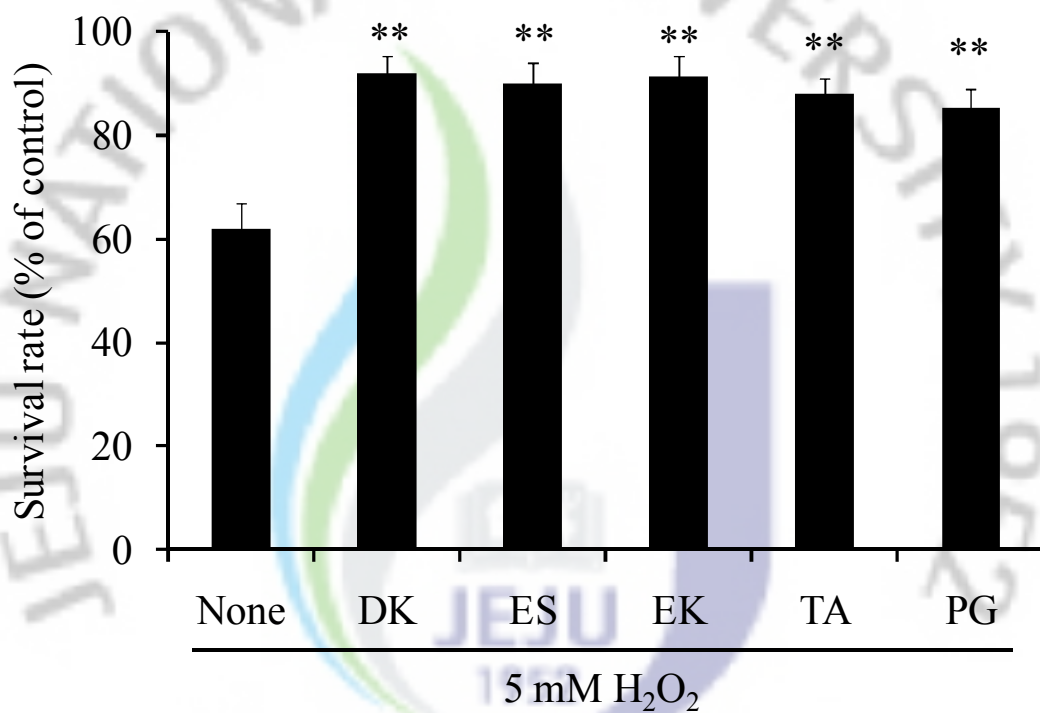


Fig. 2-3. Survival rate after treated with H₂O₂ or co-treated with phlorotannins.

The embryos were exposed to 5 mM H₂O₂ and phlorotannins treated. Dieckol (DK), Eckstolonol (ES), Eckol (EK), Triphlorethol A (TA), and Phloroglicinol (PG). Experiments were performed in triplicate and the data are expressed as mean± SE. ***p*<0.01.

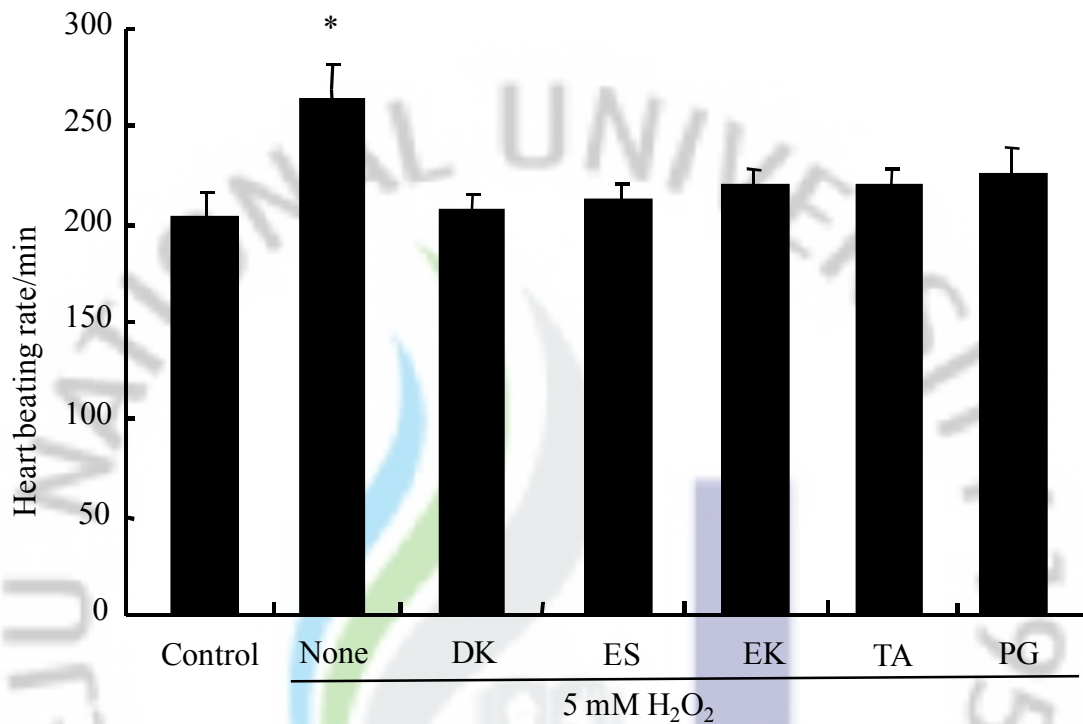


Fig. 2-4. Effects of phlorotannins on the heart-beat rate for measurement of the toxicity of the tested samples. The embryos were exposed to 5 mM H₂O₂ and phlorotannins treated. The heart-beat was measured at 48 hpf, under the microscopy. The number of heartbeat in 3 min was counted, and the results are expressed as the beats/min. Dieckol (DK), Eckstolonol (ES), Eckol (EK), Triphloethol A (TA), and Phloroglicinol (PG). Experiments were performed in triplicate and the data are expressed as mean± SE. * $p < 0.05$, ** $p < 0.01$.

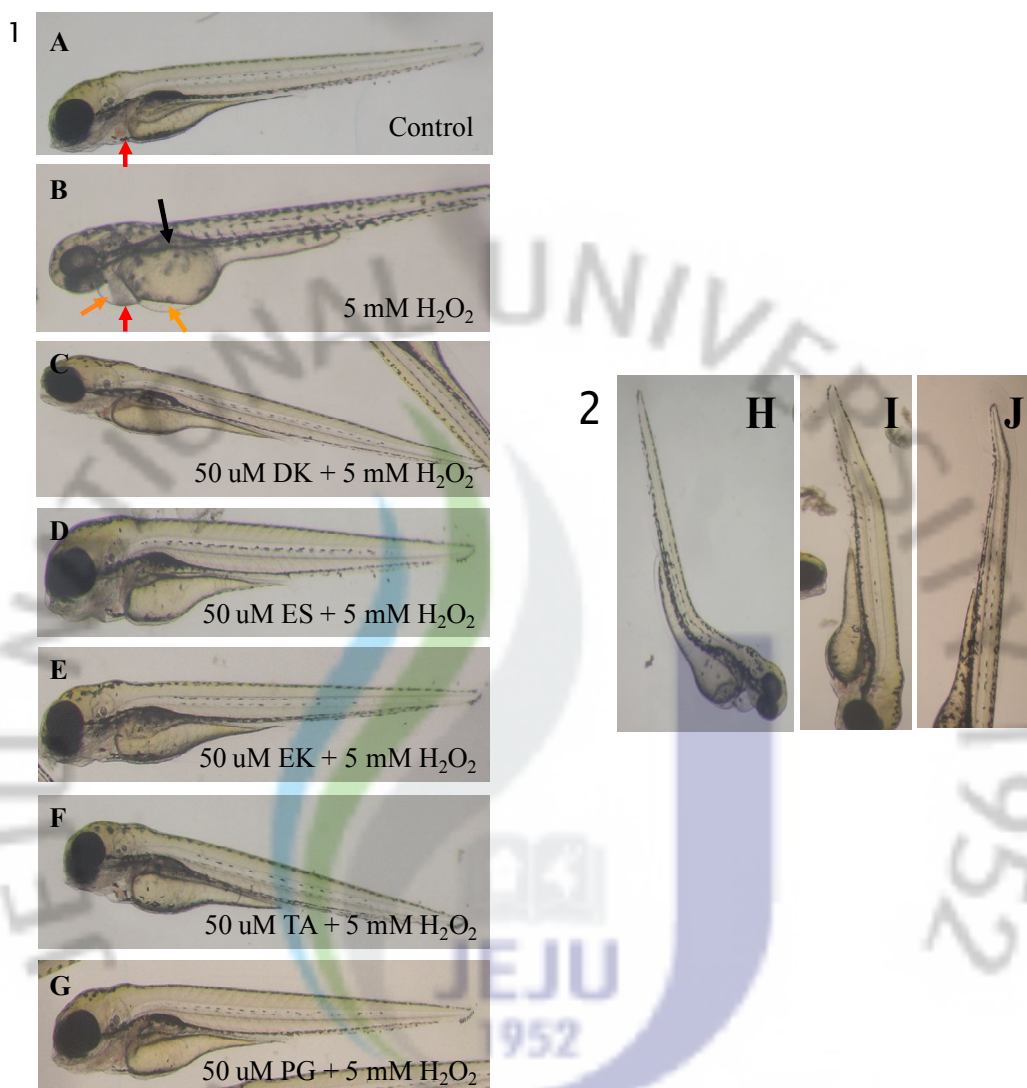


Fig. 2-5. Effects of the phlorotannins on the H₂O₂-mediated toxicity in zebrafish embryos. The embryos were treated to 5 mM H₂O₂ and co-treated phlorotannins. Images are representative of the morphological change in embryos exposure to vehicle, H₂O₂, phlorotannins + H₂O₂ (1). Incompletely differentiated tail ends, and spinal column curving (2). Dieckol (DK), Eckstolonol (ES), Eckol (EK), Triphlorethol A (TA), and Phloroglicinol (PG).

Inhibitory effect of ROS generation by H₂O₂-induced in zebrafish

The scavenging efficacy of phlorotannins including dieckol (DK), eckstolonol (ES), eckol (EK), triphlorethol A (TA), and phloroglicinol (PG), on ROS production in the H₂O₂-induced zebrafish embryo was measured. Treatment of the embryo with phlorotannins significantly inhibited the ROS production ($p < 0.05$, **Fig. 2-6**). Thus, it was shown mostly similar ROS level of the embryos compared with the control (without phlorotannins and H₂O₂) at the presence of 50 μ M phlorotannins. Fluorescence intensity of control embryo was recorded as 1951 whereas H₂O₂ treated embryo showed 5652. However, the addition of phlorotannins to the embryo mixed with H₂O₂ reduced intracellular ROS accumulation to 2909, 2807, 2880, 3010 and 3549, respectively. As shown in **Fig. 2-7**, it was taken typical fluorescence photographs of the zebrafish embryo. The negative control, which contained no phlorotannin or H₂O₂, generated clear image, whereas the positive control, which treated only H₂O₂, generated fluorescence image, which suggests that ROS took place in the presence of H₂O₂ in the zebrafish. However, the zebrafish were treated with phlorotannins prior to H₂O₂ treatment, a dramatic reduction in the amount of ROS was observed. This result reflects a reduction of ROS generation by phlorotannins. Hence these results indicate that phlorotannins has efficient antioxidant properties which can be developed into a potential bio-molecular candidate to inhibit ROS formation and zebrafish could possible visual analyzing animal model for antioxidant material screening. As shown **Fig 2-8**, by the Western blotting results, phlorotannins treatment in H₂O₂-treated zebrafish decreased the expression of phospho-JNK. These data suggest that phlorotannins protects zebrafish from H₂O₂ induced oxidative stress.

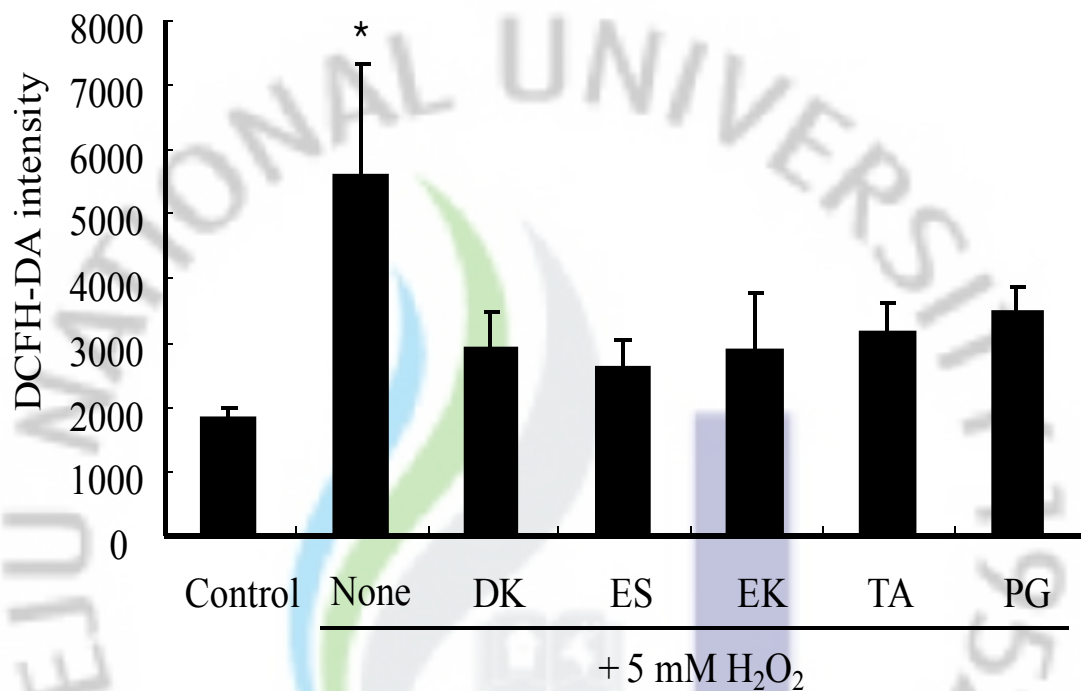


Fig. 2-6. Effect of phlorotannins isolated from *E. cava* on H₂O₂-induced ROS level in zebrafish embryos. The embryos were treated to 5 mM H₂O₂ and co-treated phlorotannins. After incubation, the intracellular ROS detected by fluorescence spectrophotometer after DCFH-DA staining. Dieckol (DK), Eckstolonol (ES), Eckol (EK), Triphloethol A (TA), and Phloroglicinol (PG). Experiments were performed in triplicate and the data are expressed as mean± SE. **p*<0.05.

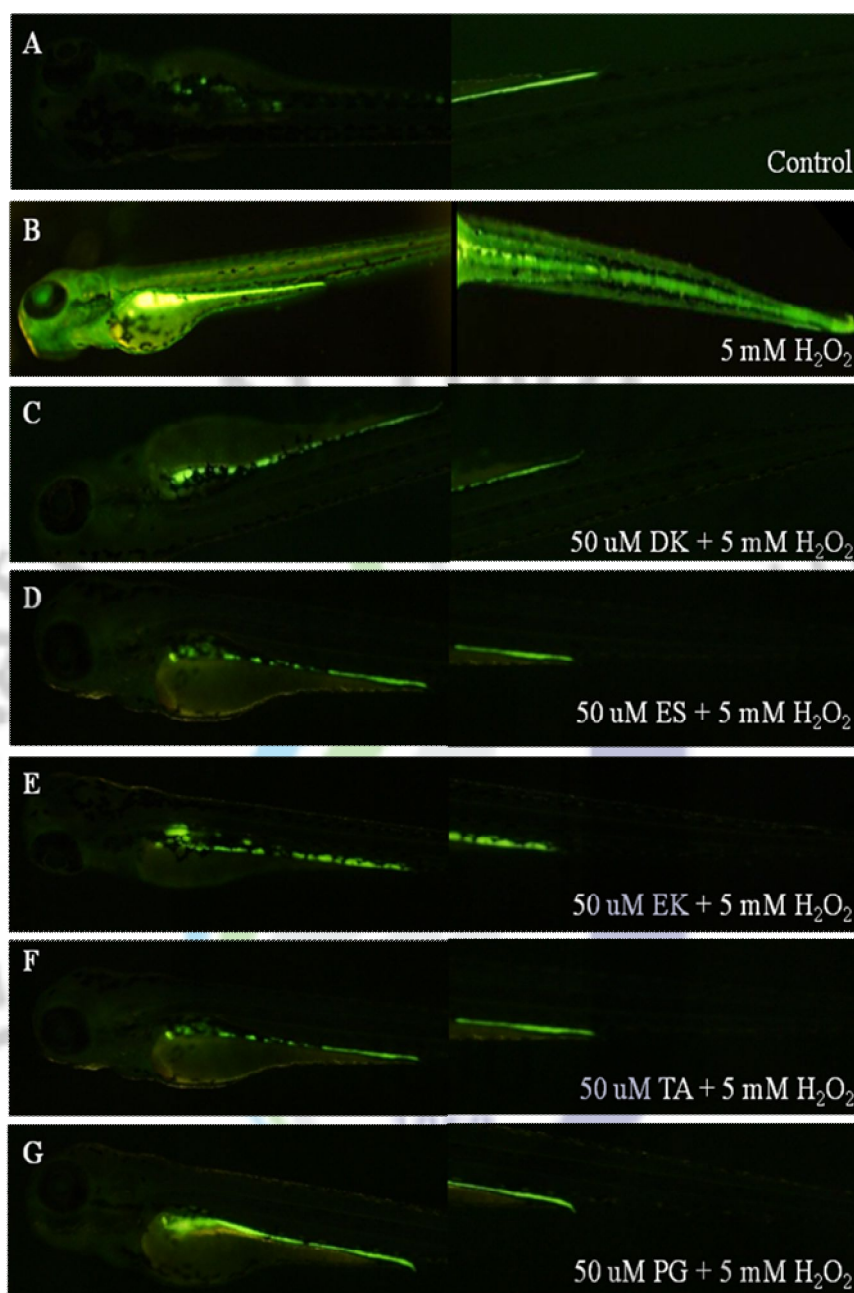


Fig. 2-7. Photographs of H_2O_2 -induced ROS level in zebrafish embryo. The embryos were treated to 5 mM H_2O_2 and co-treated phlorotannins. The ROS levels were measured by image analysis and fluorescence microscope. Dieckol (DK), Eckstolonol (ES), Eckol (EK), Triphlorethol A (TA), and Phloroglicinol (PG).

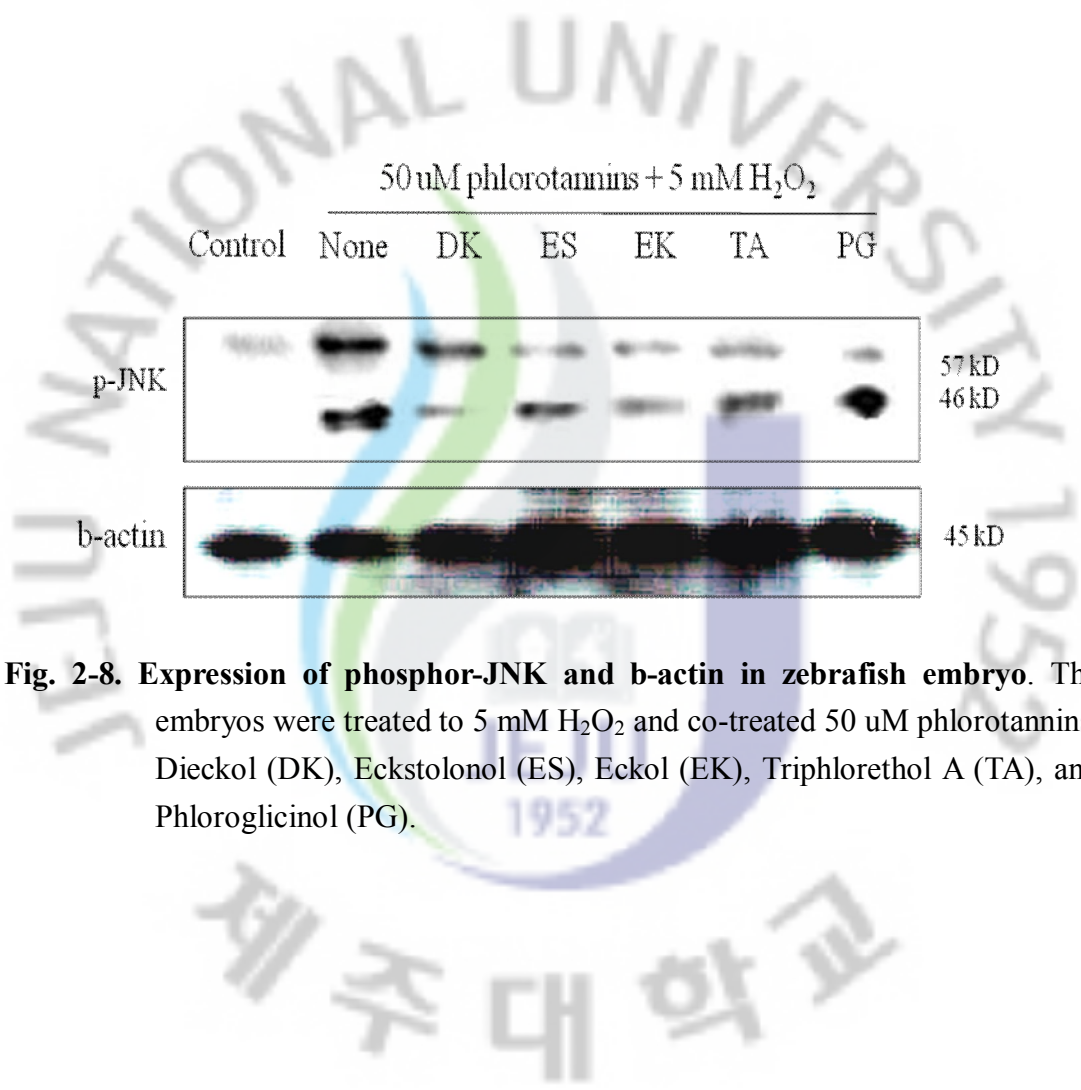


Fig. 2-8. Expression of phosphor-JNK and b-actin in zebrafish embryo. The embryos were treated to 5 mM H₂O₂ and co-treated 50 uM phlorotannins. Dieckol (DK), Eckstolonol (ES), Eckol (EK), Triphloretol A (TA), and Phloroglicinol (PG).

Lipid peroxidation inhibitory activity

The ability of phlorotannins to inhibit lipid peroxidation in H₂O₂-induced zebrafish embryo was investigated in **Fig. 2-9** and **Fig. 2-10**. The generation of thiobarbituric acid reactive substance (TBARS) was inhibited in the presence of phlorotannins (**Fig. 2-9**). In morphological evaluations, the lipid peroxidation inhibitory activity was observed using DPPP fluorescent dye and its results were shown in **Fig. 2-10**. The negative control, which contained no phlorotannin or H₂O₂, generated clear image, whereas the positive control, which treated only H₂O₂, generated fluorescence image, which suggests that lipid peroxidation took place in the presence of H₂O₂ in the zebrafish embryo. However, the zebrafish were treated with phlorotannins prior to H₂O₂ treatment, a reduction in the amount of lipid peroxidation was observed. This result reflects a reduction of lipid peroxidation generation by phlorotannins.

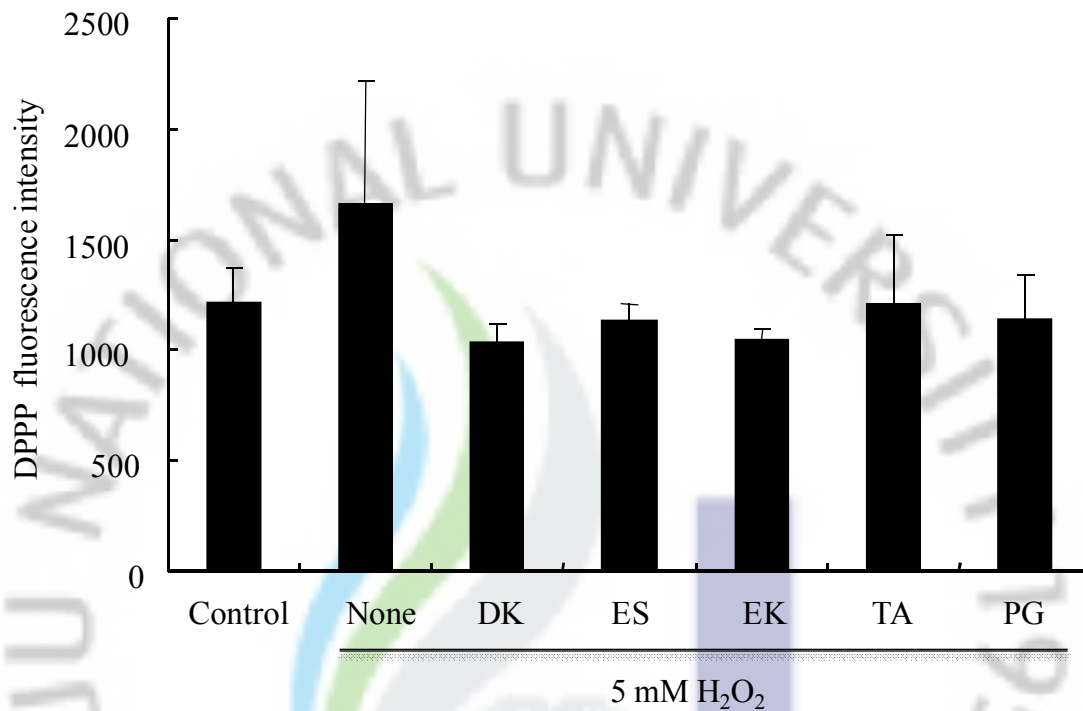


Fig. 2-9. Effect of phlorotannins isolated from *E. cava* on H₂O₂-induced lipid peroxidation level in zebrafish embryos. The embryos were treated to 5 mM H₂O₂ and co-treated phlorotannins. After incubation, the lipid peroxidation was detected by fluorescence spectrophotometer after DPPH staining. Dieckol (DK), Eckstolonol (ES), Eckol (EK), Triphlorethol A (TA), and Phloroglicinol (PG). Experiments were performed in triplicate and the data are expressed as mean±SE.

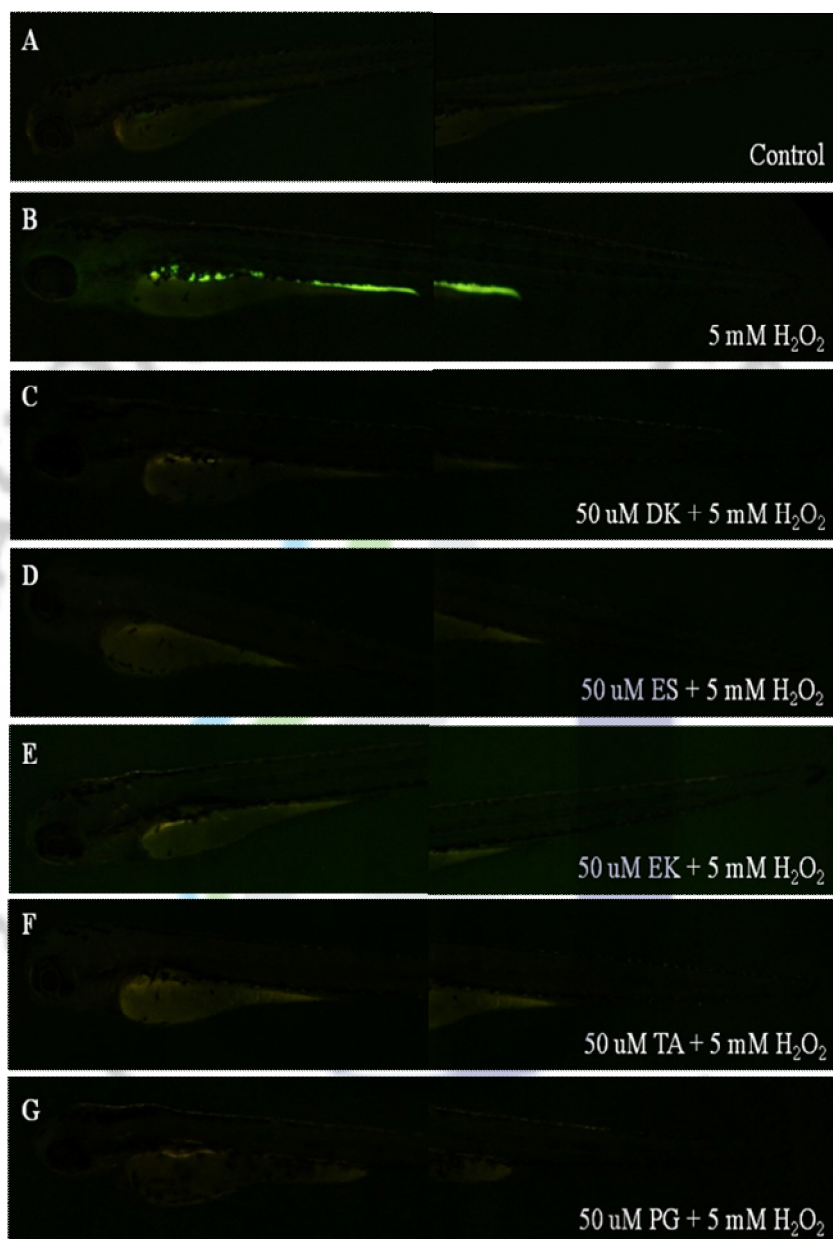


Fig. 2-10. Photographs of H₂O₂-induced lipid peroxidation level in zebrafish embryo. The embryos were treated to 5 mM H₂O₂ and co-treated phlorotannins. The lipid peroxidation levels were measured by image analysis and fluorescence microscope. Dieckol (DK), Eckstolonol (ES), Eckol (EK), Triphlorethol A (TA), and Phloroglicinol (PG).

Protective effects of phlorotannins on H₂O₂-induced cell death in live zebrafish

To evaluate whether phlorotannins protect against H₂O₂ treatment, cell death induced by H₂O₂ treatment was measured via acridine orange as fluorescence intensity in body of the zebrafish (**Fig. 2-11**). The H₂O₂-induced cell death in zebrafish was recorded as 15550 intensity (positive control), whereas the negative control presented as 9010 intensity. However, the cell death was reduced by the addition of phlorotannins to the zebrafish exposed to the H₂O₂. All phlorotannins showed protective effects against H₂O₂. Among the phlorotannins, DK, and TA showed higher protective effect against H₂O₂-induced cell death. The microscopic pictures have shown in **Fig. 2-12** that the control zebrafish had intact, and H₂O₂ treatment zebrafish showed significant increased the intensity of acridine orange. However, the zebrafish were treated with phlorotannins prior to H₂O₂ treatment, a dramatic decrease in cell death was observed. As shown **Fig 2-13**, by the Western blotting results, phlorotannins treatment in H₂O₂-treated zebrafish decreased the expression of cell death protein including Bcl-xL and PARP. These data suggest that phlorotannins protects zebrafish from H₂O₂ induced toxicity.

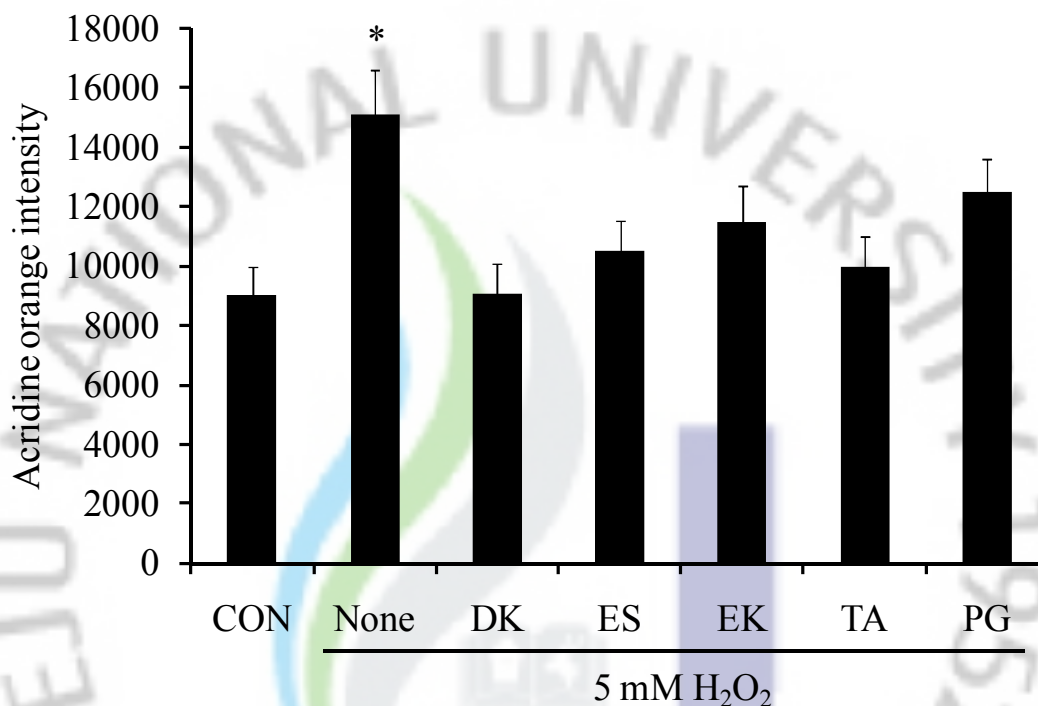


Fig. 2-11. Protective effect of phlorotannins isolated from *E. cava* on H₂O₂-induced cell death in live zebrafish embryo. The embryos were treated to 5 mM H₂O₂ and co-treated phlorotannins. After incubation, the cell death was detected by fluorescence spectrophotometer after acridine orange staining. Dieckol (DK), Eckstolonol (ES), Eckol (EK), Triphlorethol A (TA), and Phloroglicinol (PG). Experiments were performed in triplicate and the data are expressed as mean±SE. **p*<0.05.

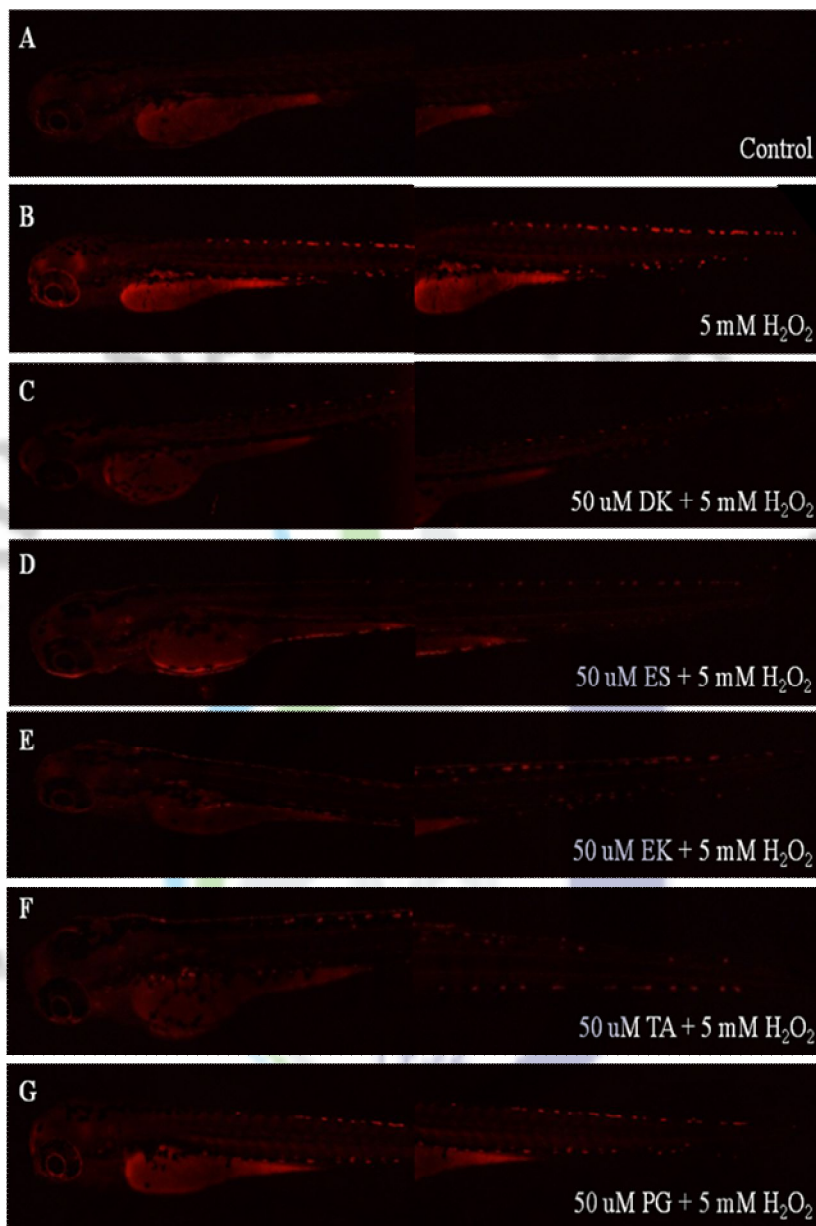


Fig. 2-12. Photographs of H₂O₂-induced cell death in live zebrafish embryo. The embryos were treated to 5 mM H₂O₂ and co-treated phlorotannins. The cell death levels were measured by image analysis and fluorescence microscope. Dieckol (DK), Eckstolonol (ES), Eckol (EK), Triphlorethol A (TA), and Phloroglicinol (PG).

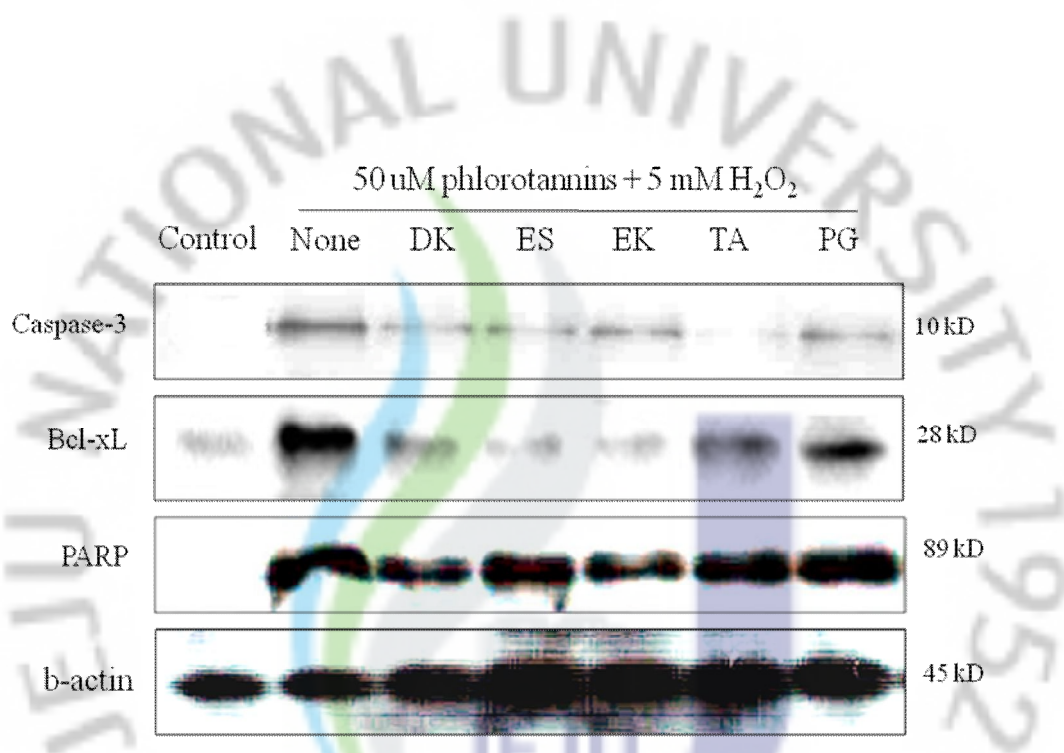


Fig. 2-13. Expression of Bcl-xL, PARP and b-actin in zebrafish embryo. The embryos were treated to 5 mM H₂O₂ and co-treated 50 uM phlorotannins. Dieckol (DK), Eckstolonol (ES), Eckol (EK), Triphloretol A (TA), and Phloroglicinol (PG).

DISCUSSION

Cells or live organism are protected from ROS-induced damage by a variety of endogenous ROS-scavenging enzymes, chemical compounds, and natural products. Recently, interest has been increased in the therapeutic potential of natural products to be used as natural antioxidants in the reduction of such free radical-induced tissue injuries, thereby suggesting that many natural products may prove to possess therapeutically useful antioxidant compounds (Coyle and Puttfarcken, 1993; Satoh et al., 1999; Satoh and Lipton, 2007). H₂O₂ has been extensively used as an inducer of oxidative stress in *in vitro* models (Whittemore et al., 1995; Li et al., 2000; Cole and Perez-Polo, 2002; Xu et al., 2004; Malecki et al., 2000; Liu et al., 2000; Neely et al., 2005). It readily crosses the cellular membranes giving rise to the highly reactive hydroxyl radical, which has the ability to react with macromolecules, including DNA, proteins, and lipids, and ultimately damage to whole cell (Kang et al., 2003; Kang et al., 2005, 2006; Kim et al., 2006; Kong et al., 2009). Several studies have shown that oxidative stress is a major cause of cellular injuries in a variety of human diseases including cancer, neurodegenerative, and cardiovascular disorders. Recently, many researchers have made considerable efforts to search natural antioxidants. Many studies have revealed that seaweeds have potential to be used as a candidate for natural antioxidant. Potent antioxidative compounds have already been isolated from seaweeds and identified as phylophoeophytin in *Eisenia bicyclis* (daehwang), fucoxanthine in *Hijikia fusiformis* (tot), phlorotannin in *Ecklonia stolonifera*, bromophenols in *Polysiphonia urceolata*, and sulfated polysaccharides. Among these antioxidants, phlorotannins, well known marine algal

polyphenols, are recognized to have defensive or protective functions against oxidative stress (Kang et al., 2003). The physiological benefits of phlorotannins are generally thought to be due to their antioxidant and free radical scavenging properties, even though phlorotannins displaying other biological activities (Kang et al., 2005, 2006; Kim et al., 2006; Kong et al., 2009). The efficacy of phlorotannins have been studied extensively in which ROS are produced either chemically (Kang et al., 2006) or radiolysis (Heo et al., 2009), and the elimination of ROS by *E. cava* are monitored directly or by measuring lipids peroxidation levels (Kang et al., 2006, Kim et al., 2006). Although some reports suggest that phlorotannins from algae exhibit antioxidant effect on free radicals, there are no reports on the zebrafish study of the phlorotannins. In this study, we investigated the antioxidant effects of phlorotannins, after the administration of H₂O₂ in zebrafish embryo. 2',7'-Dichlorodihydrofluorescein diacetate was used as a probe for ROS measurement. DCFH-DA crosses cell membranes and is hydrolyzed enzymatically by intracellular esterase to nonfluorescent DCFH (Veerman et al., 2004). In the presence of ROS, DCFH is oxidized to highly fluorescent DCF. It is well known that H₂O₂ is the principal ROS responsible for the oxidation of DCFH to DCF. As phlorotannins were found to exert a ROS scavenging effect, it was further evaluated with regard to its protective effects against H₂O₂-induced oxidative stress in zebrafish embryo. In the present study, we investigated scavenging activity of phlorotannins on intracellular ROS and the results are illustrated in Fig. 2-6. It showed mostly similar ROS level of the cells compared with the control (without phlorotannins and H₂O₂ treatment) at the presence of 50 μM phlorotannins. As shown in Fig. 2-7, it was taken typical fluorescence photographs of the zebrafish embryo. The negative control, which contained no phlorotannin or

H₂O₂ treatment, generated clear image, whereas the positive control, which irradiated only H₂O₂ treatment, generated fluorescence image, which suggests that ROS took place in treatment of H₂O₂ in the zebrafish embryo. However, the zebrafish embryos were treated with phlorotannins prior to H₂O₂ treatment, a dramatic reduction in the amount of ROS was observed. Moreover, the expression levels of phospho-JNK was reduced by phlorotannins (**Fig. 2-8**). This result reflects a reduction of ROS generation by phlorotannins. To evaluate whether phlorotannins protect lipid peroxidation induced by H₂O₂, zebrafish embryos were pretreated with phlorotannins in the absence or presence of oxidative stress. As shown in **Fig. 2-9** and **Fig. 2-10**, the generation of thiobarbituric acid reactive substance (TBARS) was inhibited in the presence of phlorotannins (**Fig. 2-9**). In morphological evaluations, the lipid peroxidation inhibitory activity was observed using DPPH fluorescent dye and its results were shown in **Fig. 2-10**. The negative control, which contained no phlorotannin or H₂O₂, generated clear image, whereas the positive control, which treated only H₂O₂, generated fluorescence image, which suggests that lipid peroxidation took place in the presence of H₂O₂ in the zebrafish embryo. However, the zebrafish were treated with phlorotannins prior to H₂O₂ treatment, a reduction in the amount of lipid peroxidation was observed. This result reflects a reduction of lipid peroxidation generation by phlorotannins. To evaluate whether phlorotannins protect from cellular damage induced by H₂O₂, zebrafish embryos were pretreated with phlorotannins for 1 h in the absence or presence of oxidative stress. As shown in **Fig. 2-11** and **Fig. 2-12**, H₂O₂ treatment without phlorotannins decreased cell death intensity, while phlorotannins prevented zebrafish embryo from H₂O₂-induced cell death. Phlorotannins treatment in H₂O₂-treated zebrafish decreased the expression of

cell death protein (**Fig. 2-13**). These results suggest that phlorotannins have ability to protect zebrafish embryo from oxidative stress-related cellular injuries. In a previous study, **Kang et al. (2006)** reported that some natural compounds from brown seaweeds have an ability to increase catalase located at peroxisome in cell that converts H_2O_2 into molecular oxygen and water. In this study, we showed that phlorotannins have prominent effect on the H_2O_2 -induced toxicity. In conclusion, we investigated the protective effects of phlorotannins against H_2O_2 -induced oxidative stress in zebrafish embryos for the first time. Our results demonstrated that H_2O_2 induces toxicities in the zebrafish embryos and phlorotannin can protect zebrafish embryos against H_2O_2 by inhibit intracellular ROS formation, lipid peroxidation, and cell death. Moreover, phlorotannins showed evidence in survival rate of embryos and reduced morphological changes. We conclude that zebrafish embryos are valuable laboratory alternative animals.

Part II -2.

Protective effects of phlorotannins against 2,2'-Azobis (2-amidopropane) dihydrochloride (AAPH)-induced oxidative stress in zebrafish embryo

ABSTRACT

2,2'-Azobis (2-amidopropane) dihydrochloride (AAPH), which generates two potent ROS capable of inducing lipid peroxidation, namely hydroxyl radical ($\cdot\text{OH}$) and peroxy radical ($\text{ROO}\cdot$). AAPH generates model peroxy radicals. These radicals are similar to such peroxy conditions that are physiologically active and might initiate a cascade of intracellular toxic events leading to oxidation, lipid peroxidation and then subsequently cell death. Here, we have investigated the protective efficacy of phlorotannins including dieckol (DK), eckstolonol (ES), eckol (EK), triphloroethol A (TA), and phloroglucinol (PG) which are isolated from a brown algal *Ecklonia cava*, against AAPH-induced oxidative stress toxicity in zebrafish embryo. Zebrafish embryo exposed to AAPH and compared with other groups that were co-exposed with phlorotannins until 2 day post fertilization (dpf). All phlorotannins were found to scavenge intracellular reactive oxygen species (ROS) and prevented lipid peroxidation. As a result, all phlorotannins reduced AAPH-induced cell death in zebrafish embryo. AAPH induced pericardial edema, yolk sac edema, and growth retardation in zebrafish embryos. In contrast, phlorotannins co-exposed groups did not show any morphological changes. These results clearly indicate that phlorotannins isolated from *E. cava* possesses prominent antioxidant activity against AAPH-

mediated toxicity and which might be a potential therapeutic agent for treating or preventing several diseases implicated with oxidative stress. This study provides a new useful strategy for the protection of AAPH-induced oxidative stress in alternative animal model which is zebrafish.



MATERIALS AND METHODS

Materials

The marine brown alga *E. cava* was collected along the coast of Jeju Island, Korea, between October 2007 and March 2008. The samples were washed three times with tap water to remove the salt, epiphytes, and sand attached to the surface. After then carefully rinsed with fresh water, and maintained in a medical refrigerator at -20°C. Thereafter, the frozen samples were lyophilized and homogenized with a grinder prior to extraction.

Preparation of phlorotannins from *Ecklonia cava*

The phlorotannins were isolated as previously described by **Ahn et al. (2007)** with slight modifications. Briefly, the dried *E. cava* powder (500 g) was extracted three times with 80% MeOH and then filtered. The filtrate was evaporated at 40°C to obtain the methanol extract. After, the extract was suspended on distilled water, and partitioned with ethyl acetate. The ethyl acetate fraction was mixed with celite. The mixed celite was dried and packed into a glass column, and eluted in the order of hexane, methylene chloride, diethyl ether, and methanol. The diethyl ether fraction was further purified by sephadex LH-20 column chromatography using stepwise gradient chloroform/methanol (2/1→0/1) solvents system. The phloroglucinol, eckol, triphloroethol A, eckstolonol and dieckol were purified by high performance liquid chromatography (HPLC) using a Waters HPLC system equipped with a Waters 996 photodiode array detector and C18 column (J'sphere ODSH80, 150× 20 mm, 4 μm; YMC Co.) by stepwise elution with methanol-water gradient (UV range: 230 nm,

flow rate: 0.8 ml/min). Finally, the purified compounds were identified by comparing their ^1H and ^{13}C NMR data to the literature report. The chemical structures of the phlorotannins are indicated in **Fig. 1**.

Origin and maintenance of parental zebrafish

Adult zebrafishes were obtained from a commercial dealer (Seoul aquarium, Korea) and 10 fishes were kept in 3 l acrylic tank with the following conditions; 28.5°C, with a 14/10 h light/dark cycle. Zebrafishes were fed three times a day, 6 d/week, with Tetramin flake food supplemented with live brine shrimps (*Artemia salina*). Embryos were obtained from natural spawning that was induced at the morning by turning on the light. Collection of embryos was completed within 30 min.

Waterborne exposure of embryos to phlorotannins and H_2O_2

From approximately 3 hour post-fertilization (3 hpf), embryos ($n=25$) were transferred to individual wells of a 24-well plate and maintained in embryo media containing 1 ml of vehicle (0.1% DMSO) or 50 μM phlorotannins for 1 h. Then treated with 5 mM H_2O_2 or co-treated H_2O_2 and phlorotannins for up to 120 hour post-fertilization (120 hpf).

Measurement of heart-beat rate

The heart-beating rate of both atrium and ventricle was measured at 35 hpf to determine the sample toxicity (Choi et al., 2007). Counting and recording of atrial and ventricular contraction were performed for 3 min under the microscope, and results were presented as the average heart-beating rate per min.

Estimation of intracellular ROS generation and image analysis

Generation of reactive oxygen species (ROS) production of zebrafish embryos was analyzed using an oxidation-sensitive fluorescent probe dye, 2,7-dichlorofluorescein diacetate (DCF-DA). DCF-DA was deacetylated intracellularly by nonspecific esterase, which was further oxidized to the highly fluorescent compound dichlorofluorescein (DCF) in the presence of cellular peroxides (**Rosenkranz et al, 1992**). At 3-4 hpf, the embryos were treated with 50 μ M phlorotannins and 1 h later, 25 mM AAPH was added to the plate. After treating embryos with 25 mM AAPH for 6 h, the embryo media was changed and the embryos developed up to 2 dpf (day post-fertilization). The embryos were transferred in to 96 well plate and treated with DCF-DA solution (20 μ g/ml), and the plates were incubated for 1 h in the dark at 28.5°C. After incubation, the embryos were rinsed in fresh embryo media and anesthetized before visualization. Individual embryo fluorescence intensity was quantified using spectrofluorometer (Perkin–Elmer LS-5B, Austria) and the image of stained embryos were observed using a fluorescent microscope, which was equipped with a CoolSNAP-Pro color digital camera (Olympus, Japan).

Lipid peroxidation inhibitory activity and image analysis

Lipid peroxidation was measured to assess membrane damage according to **Wanget et al (2008)**. Morphological evaluation of the embryos was performed with Diphenyl-1-pyrenylphosphine (DPPP, Dojindo, Japan) is fluorescent probe for detection of cell membrane lipid peroxidation. DPPP is non-fluorescent, but it becomes fluorescent when oxidized. At 3-4 hpf, the embryos were treated with 50 μ M phlorotannins and 1 h later, 25 mM AAPH was added to the plate. After treating

embryos with 25 mM AAPH for 6 h, the embryo media was changed and the embryos developed up to 2 dpf. The embryos were transferred in to 96 well plate and treated with DPPP solution (25 $\mu\text{g}/\text{ml}$), and the plates were incubated for 1 h in the dark at 28.5°C. After incubation, the embryos were rinsed in embryo media and anesthetized before visualization. Individual embryo fluorescence intensity was quantified using spectrofluorometer (Beckman DTX 800, USA) and image of embryos were observed using a fluorescent microscope, which was equipped with a CoolSNAP-Pro color digital camera (Olympus, Japan).

Measurement of oxidative stress-induced cell death in zebrafish embryo

Cell death was detected in live embryos using acridine orange staining, a nucleic acid selective metachromatic dye that interacts with DNA and RNA by intercalation or electrostatic attractions. Acridine orange stains cells with disturbed plasma membrane permeability so it preferentially stains necrotic or very late apoptotic cells. At 3-4 hpf, the embryos were treated with 50 μM phlorotannins and 1 h later, 25 mM AAPH was added to the plate. After treating embryos with 25 mM AAPH for 6 h, the embryo media was changed and the embryos developed up to 2 dpf. The embryos were transferred in to 96 well plate and treated with acridine orange (AO) solution (7 $\mu\text{g}/\text{ml}$), and the plates were incubated for 30 min in the dark at 28.5°C. After incubation, the embryos were rinsed in embryo media and anesthetized before visualization. Individual embryo fluorescence intensity was quantified using spectrofluorometer (Perkin–Elmer LS-5B, Austria). The images of stained embryos were observed using a fluorescent microscope, which was equipped with a CoolSNAP-Pro color digital camera (Olympus, Japan).

Statistical analysis

All the measurements were made in triplicate and all values were represented as mean±S.E. The results were subjected to an analysis of the variance using the Tukey test to analyze the difference. $P < 0.05$, $P < 0.01$ were considered significantly.



RESULTS

Toxicity of phlorotannins or AAPH in zebrafish embryo

In order to determine the toxicity of the phlorotannins or AAPH, we monitored the survival rate and growth patterns of zebrafish embryos. The adopted endpoints experiment used to assess the toxicity of the compounds included embryo mortality, and heart-beating disturbances. The survival rate of zebrafish embryos treated with AAPH or co-treated with phlorotannins showed in **Fig. 2-14**. Significantly decreasing survival rate was observed survival in only AAPH treatment embryos, in contrast, co-treatment with phlorotannins and AAPH embryos survived about 90%. The phlorotannins were not associated with mortality in this experiment. When evaluating the morphological malformations, phlorotannins did not evidence conspicuous adverse effects. Whereas, zebrafish embryos exposed to AAPH from 3-4 hpf to 9-10 hpf (6 h exposure) showed several typical morphological defects. At 48 hpf, embryo treated with 25 mM AAPH showed short body length and, in some case, incompletely differentiated tail ends, and spinal column curving. Heart curvature was unfolded and a dilated precardial sac was observed, suggesting precardial edema. Red blood cells accumulated in the side of yolk sac edema due to circulation failure. Yolk consumption was slower than normal, suggesting growth retardation. Image analysis data showed that phlorotannins protected the morphological changes by AAPH. On the other hand, in the heart-beat test, AAPH generated a slight increase whereas phlorotannins did not generate any heart-beat rate disturbances as compared with the control (untreated phlorotannin or AAPH, **Fig. 2-15**). In simultaneous *in vivo* toxicity tests, toxicity was not detected in the fish treated with

all phlorotannins, whereas toxicity was observed in the fish treated with the positive controls.

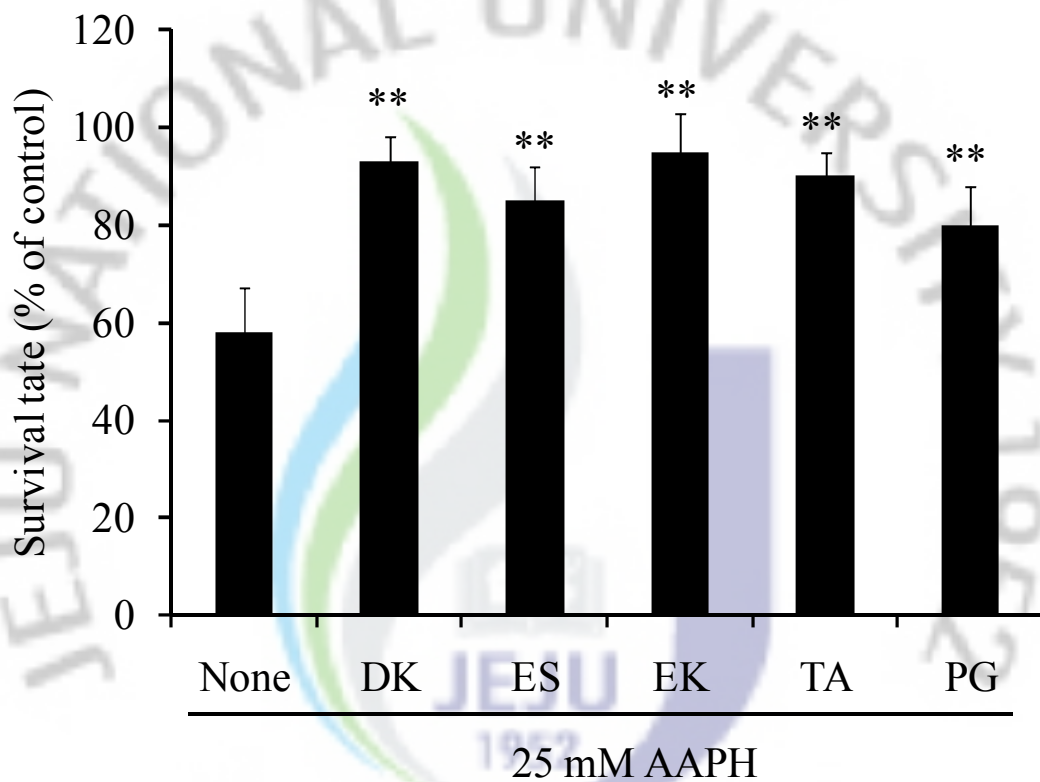


Fig. 2-14. Survival rate after treated with AAPH or co-treatment with phlorotannins. The embryos were treated to 25 mM AAPH and co-treated phlorotannins. Dieckol (DK), Eckstolonol (ES), Eckol (EK), Triphlorethol A (TA), and Phloroglicinol (PG). Experiments were performed in triplicate and the data are expressed as mean \pm SE. ** p <0.01.

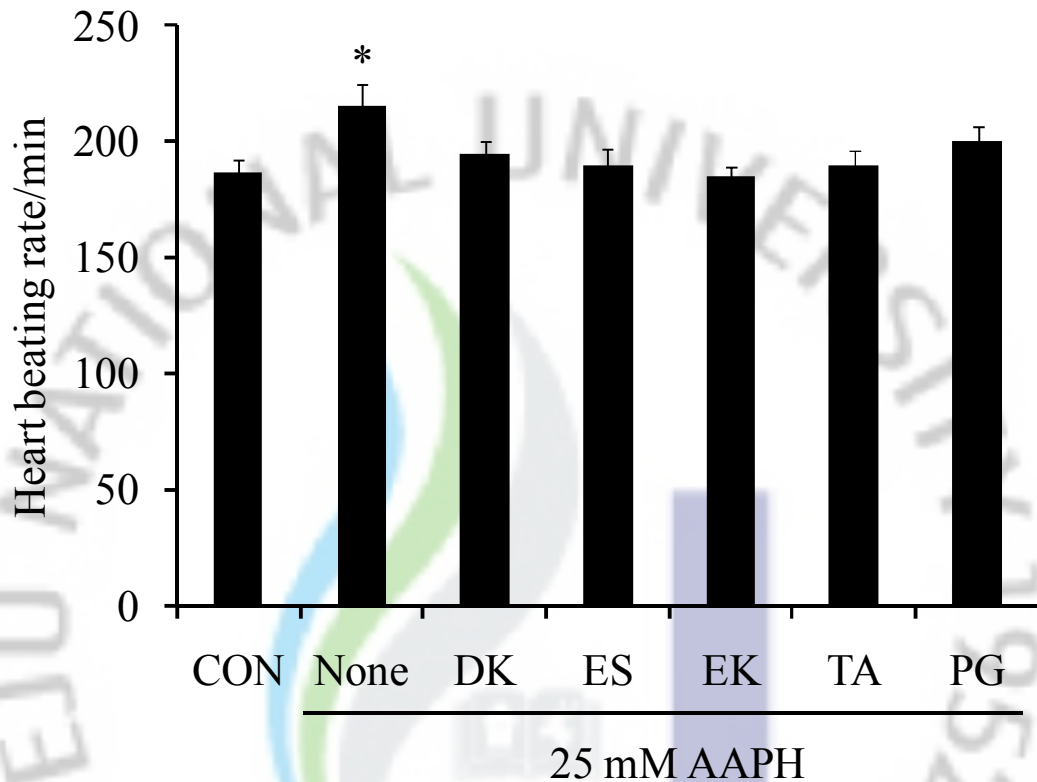


Fig. 2-15. Effects of phlorotannins on the heart-beat rate for measurement of the toxicity of the tested samples. The embryos were treated to 25 mM AAPH and co-treated phlorotannins. The heart-beat was measured at 48 hpf, under the microscopy. The number of heartbeat in 3 min was counted, and the results are expressed as the beats/min. Dieckol (DK), Eckstonol (ES), Eckol (EK), Triphlorethol A (TA), and Phloroglicinol (PG). Experiments were performed in triplicate and the data are expressed as mean±SE. * $p < 0.05$.

Inhibitory effect of ROS generation by AAPH-induced in zebrafish

The scavenging efficacy of phlorotannins including dieckol (DK), eckstolonol (ES), eckol (EK), triphlorethol A (TA), and phloroglicinol (PG), on ROS production in the AAPH-induced zebrafish embryo was measured. Treatment of the embryo with phlorotannins inhibited the ROS production (**Fig. 2-16**). Thus, it was shown mostly similar ROS level of the embryos compared with the control (without phlorotannins and AAPH) at the presence of 50 μ M phlorotannins. Fluorescence intensity of control embryo was recorded as 1591 whereas AAPH treated embryo showed 3568. However, the addition of phlorotannins to the embryo mixed with AAPH reduced intracellular ROS accumulation to 1568, 2346, 1703, 1540 and 2262, respectively. Among the phlorotannins, the fluorescence intensity recovered as similar to that of control (without phlorotannins and AAPH) in the treatment of DK, EK and TA.

As shown in **Fig. 2-17**, it was taken typical fluorescence photographs of the zebrafish embryo. The negative control, which contained no phlorotannin or AAPH, generated clear image, whereas the positive control, which treated only AAPH, generated fluorescence image, which suggests that ROS took place in the presence of AAPH in the zebrafish embryo. However, when the zebrafish embryos were treated with phlorotannins prior to AAPH treatment, a dramatic reduction in the amount of ROS observed. This result reflects a reduction of ROS generation by phlorotannins. Hence these results indicate that phlorotannins has efficient antioxidant properties which can be developed into a potential bio-molecular candidate to inhibit ROS formation of cellular.

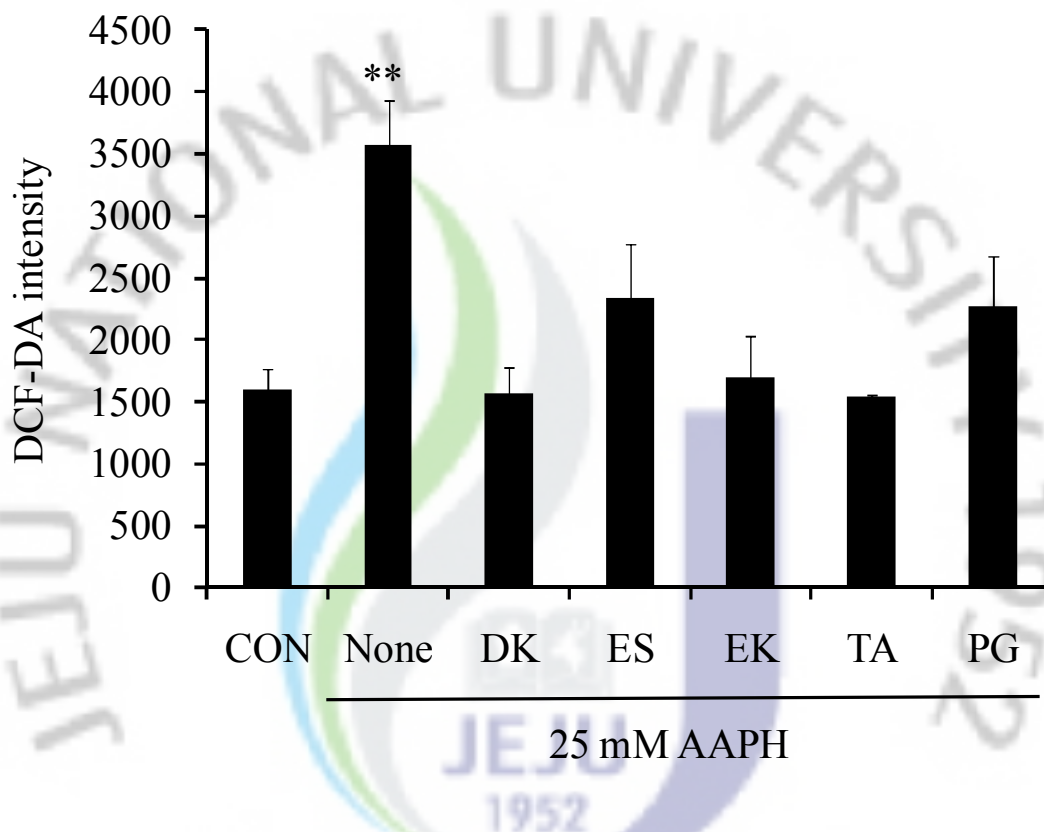


Fig. 2-16. Effect of phlorotannins isolated from *E. cava* on AAPH-induced ROS level in zebrafish embryos. The embryos were treated to 25 mM AAPH and co-treated phlorotannins. After incubation, the intercellular ROS detected by fluorescence spectrophotometer after DCFH-DA staining. Dieckol (DK), Eckstolonol (ES), Eckol (EK), Triphlorethol A (TA), and Phloroglicinol (PG). Experiments were performed in triplicate and the data are expressed as mean±SE. ** $p < 0.01$.

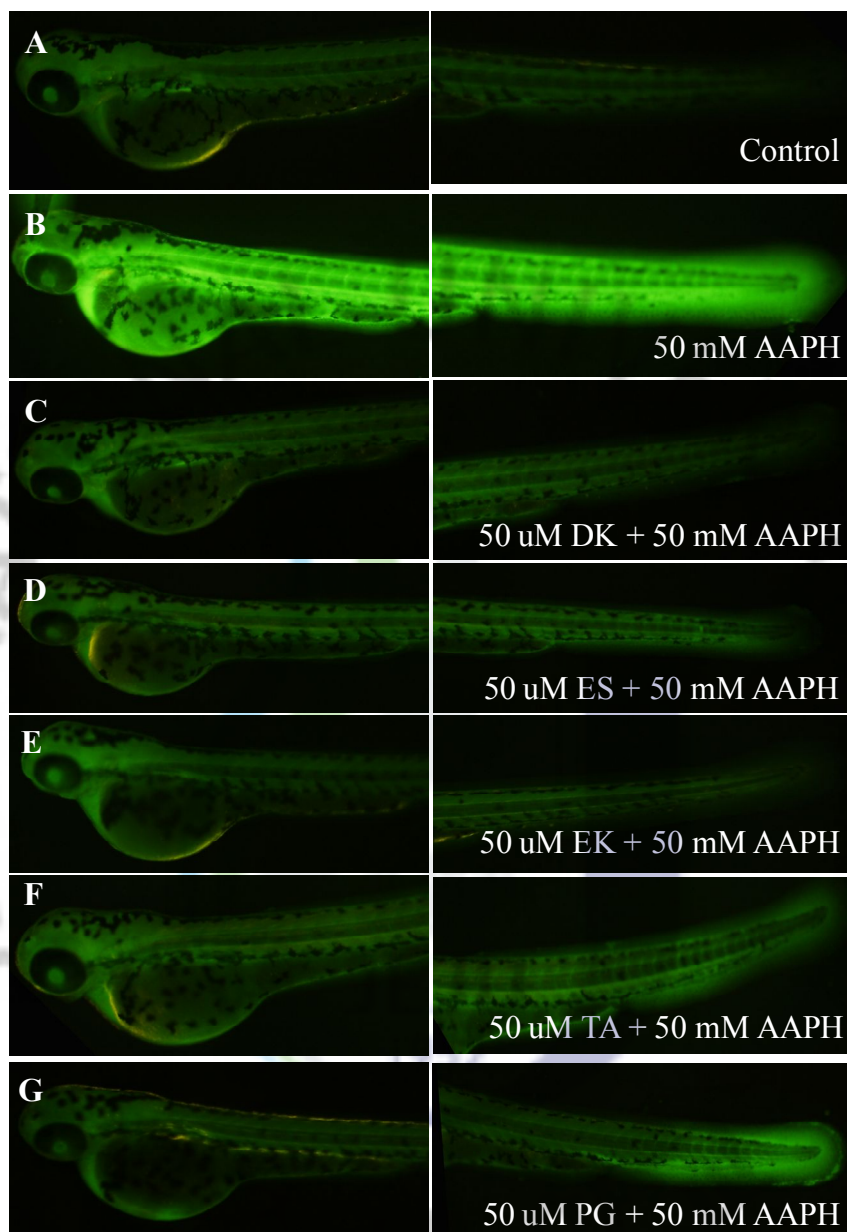


Fig. 2-17. Photographs of AAPH-induced ROS level in zebrafish embryo. The embryos were treated to 25 mM AAPH and co-treated phlorotannins. The ROS levels were measured by image analysis and fluorescence microscope. (A) Control, (B) AAPH (positive control), (C) Dieckol (DK), (D) Eckstolonol (ES), (E) Eckol (EK), (F) Triphlorethol A (TA), and (G) Phloroglicinol (PG).

Lipid peroxidation inhibitory activity

The ability of phlorotannins to inhibit lipid peroxidation in AAPH-induced zebrafish embryo was investigated in **Fig. 2-18** and **Fig. 2-19**. The generation of thiobarbituric acid reactive substance (TBARS) was inhibited in the presence of phlorotannins (**Fig. 2-18**). It showed mostly similar lipid peroxidation level of the embryos compared with the control (without phlorotannins and AAPH) at the presence of 50 μ M phlorotannins. Fluorescence intensity of control embryo was recorded as 1447 whereas AAPH treated embryo showed 2199. However, the addition of phlorotannins to the embryo mixed with AAPH reduced intracellular lipid peroxidation accumulation to 1249, 1163, 1671, 1586 and 1681 (DK, ES, EK, TA and PG), respectively. Among the phlorotannins, the fluorescence intensity even lowered in DK and ES treatment embryos than that of the control (without phlorotannins and AAPH). In morphological evaluations, the lipid peroxidation inhibitory activity was observed using DPPP fluorescent dye and its results were shown in **Fig. 2-19**. The negative control, which contained no phlorotannin or AAPH, generated clear image, whereas the positive control, which treated only AAPH, generated fluorescence image, which suggests that lipid peroxidation took place in the presence of AAPH in the zebrafish embryo. However, when the zebrafish were treated with phlorotannins prior to AAPH treatment, a dramatic reduction in the amount of lipid peroxidation was observed. This result reflects a reduction of lipid peroxidation generation by phlorotannins.

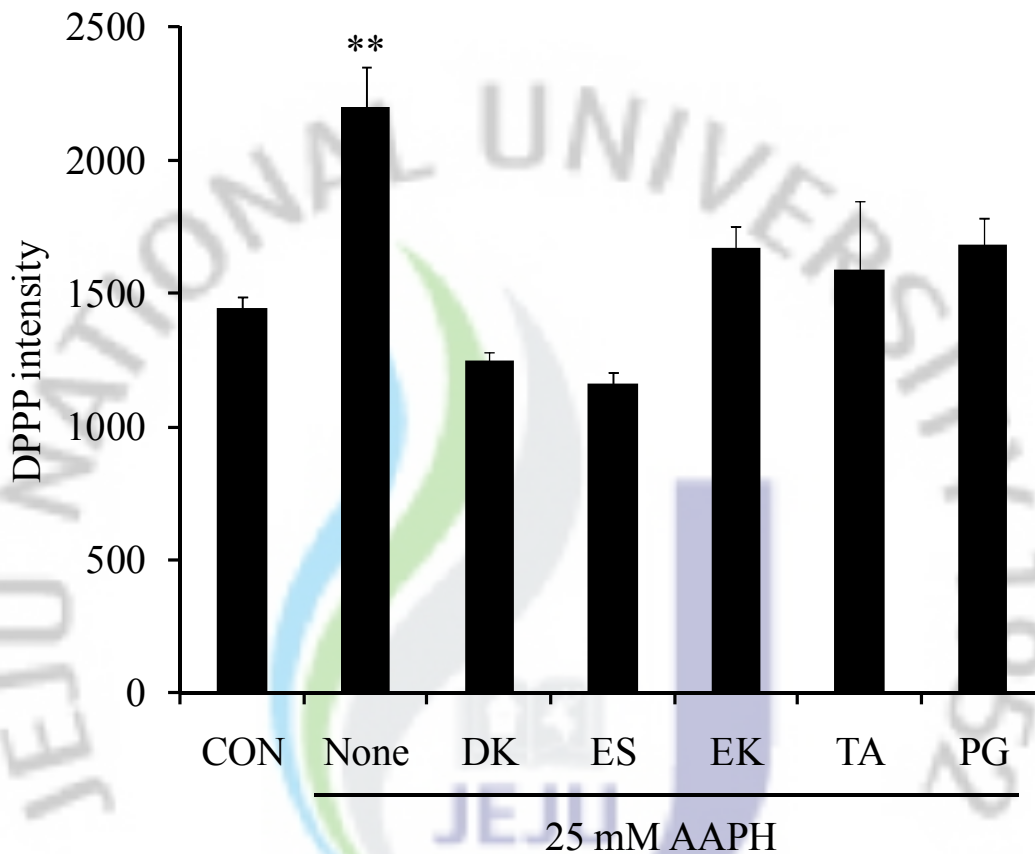


Fig. 2-18. Effect of phlorotannins isolated from *E. cava* on AAPH-induced lipid peroxidation level in zebrafish embryos. The embryos were treated to 25 mM AAPH and co-treated phlorotannins. After incubation, the lipid peroxidation was detected by fluorescence spectrophotometer after DPPH staining. The embryos were exposed to 25 mM AAPH and phlorotannins treated. Dieckol (DK), Eckstolonol (ES), Eckol (EK), Triphlorethol A (TA), and Phloroglicinol (PG). Experiments were performed in triplicate and the data are expressed as mean \pm SE. ** p <0.01.

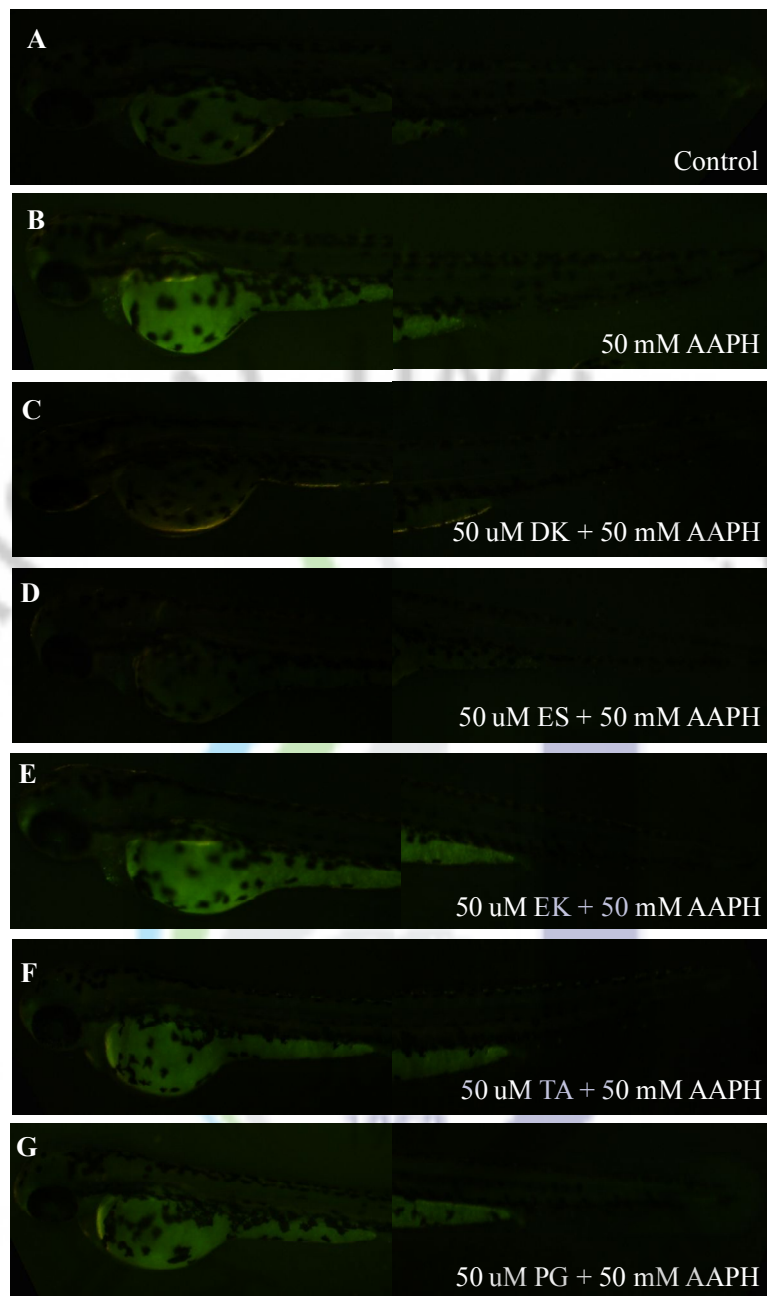


Fig. 2-19. Photographs of AAPH-induced lipid peroxidation level in zebrafish embryo. The embryos were treated to 25 mM AAPH and co-treated phlorotannins. The lipid peroxidation levels were measured by image analysis and fluorescence microscope. (A) Control, (B) AAPH (positive control), (C) Dieckol (DK), (D) Eckstolonol (ES), (E) Eckol (EK), (F) Triphlorethol A (TA), and (G) Phloroglicinol (PG).

Protective effects of phlorotannins on AAPH-induced cell death in live zebrafish

To evaluate whether phlorotannins protect against AAPH treatment, cell death induced by AAPH treatment was measured via acridine orange as fluorescence intensity in body of the zebrafish (**Fig. 2-20**). The AAPH-induced cell death in zebrafish was recorded as 5539 intensity (positive control), whereas the negative control presented as 4279 intensity. However, the cell death was reduced by the addition of phlorotannins to the zebrafish exposed to the AAPH. All phlorotannins showed protective effects against AAPH. Among the phlorotannins, ES and EK showed higher protective effect against AAPH-induced cell death in live zebrafish. The microscopic pictures have shown in **Fig. 2-21** that the control zebrafish had intact, and AAPH treatment zebrafish have shown significant increased the intensity of acridine orange. However, when the fish were treated with phlorotannins prior to AAPH treatment, a dramatic decrease in cell death was observed.

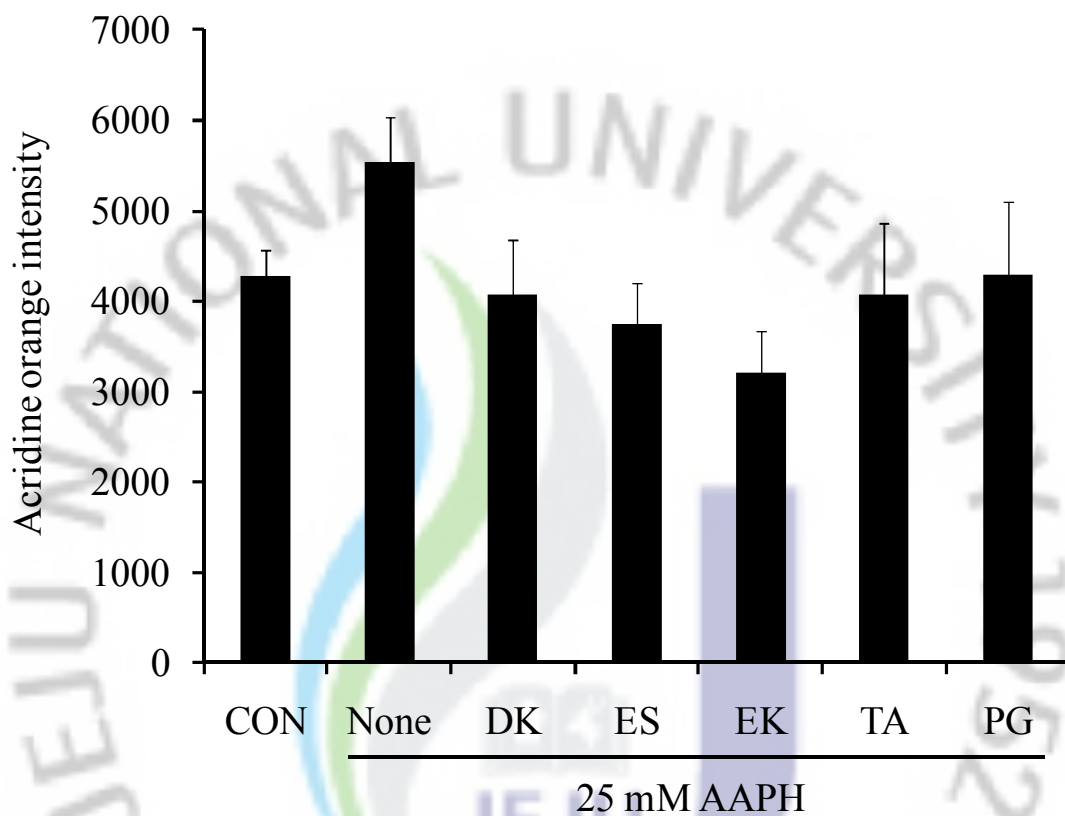


Fig. 2-20. Protective effect of phlorotannins isolated from *E. cava* on AAPH-induced cell death in live zebrafish embryo. The embryos were treated to 25 mM AAPH and co-treated phlorotannins. After incubation, the cell death was detected by fluorescence spectrophotometer after acridine orange staining. Dieckol (DK), Eckstolonol (ES), Eckol (EK), Triphlorethol A (TA), and Phloroglicinol (PG). Experiments were performed in triplicate and the data are expressed as mean \pm SE.

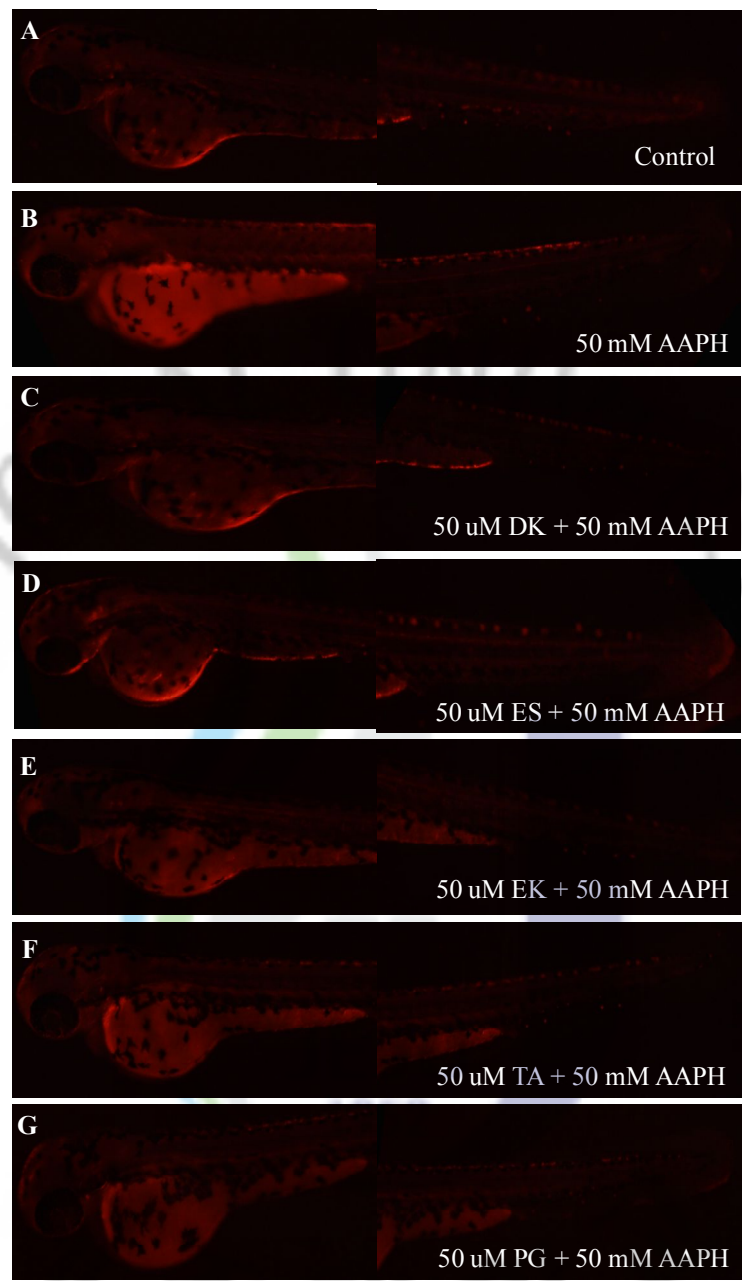


Fig. 2-21. Photographs of AAPH-induced cell death in live zebrafish embryo. The embryos were treated to 25 mM AAPH and co-treated phlorotannins. The cell death levels were measured by image analysis and fluorescence microscope. (A) Control, (B) AAPH (positive control), (C) Dieckol (DK), (D) Eckstolonol (ES), (E) Eckol (EK), (F) Triphlorethol A (TA), and (G) Phloroglicinol (PG).

DISCUSSION

Cells or live organism are protected from ROS-induced damage by a variety of endogenous ROS-scavenging enzymes, chemical compounds, and natural products. Recently, interest has been increased in the therapeutic potential of natural products to be used as natural antioxidants in the reduction of such free radical-induced tissue injuries, thereby suggesting that many natural products may prove to possess therapeutically useful antioxidant compounds (**Beyersmann and Hechtenberg, 1997; Stohs and Bagchi, 1995; Kim et al., 2006**). AAPH has been extensively used as an inducer of oxidative stress in *in vivo* models. Prevention of free-radical formation and maintenance of cellular structural integrity and of chemical environment are fundamental requirements of all cells. In biological systems, radiation-induced free radicals impair antioxidant defence leading to increased membrane lipid peroxidation (**Devasagayam et al., 2003; Poli et al., 1987**). Generation of ROS by ionizing radiation (especially with low-LET radiation) and AAPH and its profound impact on cellular biomolecules are well established. The present investigation demonstrates that AAPH and radiation induced significant lipid peroxidation in mitochondria. Increase in peroxidation is observed. Several studies have shown that oxidative stress is a major cause of cellular injuries in a variety of human diseases including cancer, neurodegenerative, and cardiovascular disorders. Recently, many researchers have made considerable efforts to search natural antioxidants. Many studies have revealed that seaweeds have potential to be used as a candidate for natural antioxidant. Potent antioxidative compounds have already been isolated from seaweeds and identified as phylophoeophytin in *Eisenia bicyclis*

(arame), fucoxanthine in *Hijikia fusiformis* (hijiki), phlorotannin in *Ecklonia stolonifera*, bromophenols in *Polysiphonia urceolata*, and sulfated polysaccharides. Among these antioxidants, phlorotannins, well known marine algal polyphenols, are recognized to have defensive or protective functions against oxidative stress (**Kang et al., 2003**). The physiological benefits of phlorotannins are generally thought to be due to their antioxidant and free radical scavenging properties, even though phlorotannins displaying other biological activities (**Kang et al., 2005, 2006; Kim et al., 2006; Kong et al., 2009**). The efficacy of phlorotannins have been studied extensively in which ROS are produced either chemically (**Kang et al., 2006**) or radiolysis (**Heo, 2009**), and the elimination of ROS by *E. cava* are monitored directly or by measuring lipids peroxidation levels (**Kang et al., 2006, Kim et al., 2006a**). Although some reports suggest that phlorotannins from algae exhibit antioxidant effect on free radicals, there are no reports on the neuroprotective effects of the phlorotannins, and the underlying mechanism of phlorotannins. In this study, we investigated the antioxidant effects of phlorotannins, after the administration of AAPH in zebrafish embryo. 2',7'-Dichlorodihydrofluorescein diacetate was used as a probe for ROS measurement. DCFH-DA crosses cell membranes and is hydrolyzed enzymatically by intracellular esterase to nonfluorescent DCFH. In the presence of ROS, DCFH is oxidized to highly fluorescent DCF. It is well known that H₂O₂ is the principal ROS responsible for the oxidation of DCFH to DCF. As phlorotannins were found to exert a ROS scavenging effect, it was further evaluated with regard to its protective effects against AAPH-induced oxidative stress in zebrafish embryo. In the present study, we investigated scavenging activity of phlorotannins on intracellular ROS and the results are illustrated in **Fig. 2-16**. It showed mostly similar ROS level

of the cells compared with the control (without phlorotannins and AAPH treatment) at the presence of 50 μ M phlorotannins. As shown in **Fig. 2-17**, it was taken typical fluorescence photographs of the zebrafish embryo. The negative control, which contained no phlorotannin or AAPH treatment, generated clear image, whereas the positive control, which irradiated only AAPH treatment, generated fluorescence image, which suggests that ROS took place in treatment of AAPH in the zebrafish embryo. However, the zebrafish embryos were treated with phlorotannins prior to H_2O_2 treatment, a dramatic reduction in the amount of ROS was observed. This result reflects a reduction of ROS generation by phlorotannins. To evaluate whether phlorotannins protect lipid peroxidation induced by AAPH, zebrafish embryos were pretreated with phlorotannins for 1 h in the absence or presence of oxidative stress. After then, fluorescence intensity was recorded after dying with DPPP. As shown in **Fig. 2-18** and **Fig. 2-19**, the generation of thiobarbituric acid reactive substance (TBARS) was inhibited in the presence of phlorotannins (**Fig. 2-18**, $p < 0.05$). In morphological evaluations, the lipid peroxidation inhibitory activity was observed using DPPP fluorescent dye and its results were shown in **Fig. 2-19**. The negative control, which contained no phlorotannin or AAPH, generated clear image, whereas the positive control, which treated only AAPH, generated fluorescence image, which suggests that lipid peroxidation took place in the presence of AAPH in the zebrafish embryo. However, when the zebrafish were treated with phlorotannins prior to AAPH treatment, a dramatic reduction in the amount of lipid peroxidation was observed. This result reflects a reduction of lipid peroxidation generation by phlorotannins. To evaluate whether phlorotannins protect from cellular damage induced by AAPH, zebrafish embryos were pretreated with phlorotannins in the

absence or presence of oxidative stress. As shown in **Fig. 2-20** and **Fig. 2-21**, AAPH treatment without phlorotannins decreased cell death intensity, while phlorotannins prevented zebrafish embryo from AAPH-induced cell death. These results suggest that phlorotannins have ability to protect zebrafish embryo from oxidative stress-related cellular injuries. In a previous study, **Kang et al. (2006)** reported that some natural compounds from brown seaweeds have an ability to increase catalase located at peroxisome in cell that converts AAPH into molecular oxygen and water. In this study, we showed that phlorotannins have prominent effect on the AAPH -induced cell death. In conclusion, the results obtained in the present study show that phlorotannins isolated from *E. cava* could effectively inhibit intracellular ROS formation, lipid peroxidation, and cell death induced by AAPH. These results revealed that phlorotannins could be used not only as the easily accessible source of natural antioxidants but also as an ingredient of the functional food related to the prevention and control oxidative stress. In conclusion, we investigated the protective effects of phlorotannins against AAPH-induced oxidative stress in zebrafish embryos for the first time. Our results demonstrated that AAPH induces toxicities in the zebrafish embryos and phlorotannins can protect zebrafish embryos against AAPH by inhibit intracellular ROS formation, lipid peroxidation, and cell death. Moreover, phlorotannins showed evidence in survival rate of embryos. We conclude that zebrafish embryos are valuable laboratory alternative animals. The antioxidant mechanisms underlying the protective efficacies afforded by phlorotannins in this experiment remain to elucidate.



Part III

Zebrafish embryo as an alternative *in vivo*
model to evaluate cosmetic materials

Part III-1.

Whitening effects of phlorotannins using zebrafish as an alternative *in vivo* model

ABSTRACT

Although many hypo-pigmenting agents are currently available, the demand for novel whitening agents is increasing, in part due to the weak effectiveness and unwanted side effects of currently available compounds. To examine the possibility of phlorotannins as a whitening agent, we adopted zebrafish as an alternative experimental *in vivo* model. All the tested samples evidenced excellent inhibitory effects on the pigmentation of zebrafish, most likely due to their potential tyrosinase inhibitory activity. In simultaneous *in vivo* toxicity tests, no toxicity was observed in all phlorotannin treated groups, on the other hand, toxicity was observed in positive controls treated group. Moreover, *E. cava* has been proved to possess excellent antioxidant activities and high phenolic content according to the previous study so that it could potentially be the candidates for cosmetic ingredients and anti-hyperpigmentation applications. Together, zebrafish are valuable alternative *in vivo* model for dermatology.

INTRODUCTION

Cosmetics are commercially available products that are used to improve the appearance of the skin. Recently, a number of women concerning about whiter skin complexion, especially in Asia have increased dramatically (**Tengamnuay et al., 2006**). Melanin is the major pigment which is largely responsible for the color of human skin. It has been known to be overproduced with chronic sun exposure, melasma, or other hyperpigmentation diseases. Therefore, a number of depigmenting agents have been developed in cases of undesirable skin discolorations. Tyrosinase, a copper-containing monooxygenase, is a key enzyme that catalyzes melanin synthesis in melanocytes. It catalyzes the hydroxylation of tyrosine into dihydroxyphenylalanine (DOPA) and other intermediates (**Sturm et al., 2001; Kajiwara et al., 2006; Wang et al., 2006**). Thus, inhibition of tyrosinase activity or its production can prevent melanogenesis. Skin is the preferred target of oxidative stress as continuously exposed to ultraviolet (UV) radiation from sunlight and environmental oxidizing pollutants (**Thiele et al., 1997**). It is well established that overexposure to UV radiation provokes acute sunburn reaction, which clinically manifests itself as erythema. Chronically irradiated skins by UV radiation are associated with abnormal cutaneous reactions such as epidermal hyperplasia, accelerated breakdown of collagen, and inflammatory responses (**Longstreth et al., 1998; Marrot et al., 2001; Tanaka et al., 2007**). UV radiation has a strong oxidative component and photo-oxidative stress has been directly linked to the onset of skin photodamage (**Fuchs, 1998; Caddeo et al., 2008**). Hence, regular intake of dietary antioxidants or treatment of the skin with products containing antioxidant

ingredients could possibly be a useful strategy for preventing UV-induced damages. Oxidative stress might be induced by increasing generation of ROS and other free radicals. UV radiation can induce formation of ROS in skin such as singlet oxygen and superoxide anion, promoting biological damage in exposed tissues via iron-catalyzed oxidative reactions (Yasui and Sakurai, 2003). These ROS enhance melanin biosynthesis, damage DNA, and may induce proliferation of melanocytes. A previous study (Yamakoshi et al., 2003) also found evidence for a role of oxidative stress in pathogenesis of skin disorders. It is known that ROS scavengers or inhibitors such as antioxidants may reduce hyperpigmentation (Ma et al., 2001).

Several chemical compounds of plant origin have been reported as tyrosinase inhibitors. Ellagic acid (Shimogaki et al., 2000), oxyresveratrol (Kim et al., 2002), chlorophorin, and norartocarpanone (Shimizu et al., 1998) were described for their tyrosinase inhibition properties. Despite a large number of tyrosinase inhibitors reported, the identification and isolation of tyrosinase inhibitors from natural sources are one of the most important approach (Son et al., 2000). Furthermore, it has been reported that tyrosinase might contribute to the dopamine neurotoxicity and neurodegeneration associated with Parkinson's disease (Xu et al., 1997). These facts led us to focus our research work on the exploration of natural tyrosinase inhibitors from marine algae.

In recent years, many marine resources have been attracted attentions in the search for bioactive compounds for the development of new drugs and health foods. Marine algae are known to be rich in vitamins, minerals, and a variety of functional polysaccharides and polyphenols (Noseda et al., 1999; Barbarino and Lourenco, 2005; Kuda et al., 2005; Heo and Jeon, 2008; Heo et al., 2005).

The vertebrate zebrafish (*Danio rerio*) is a small tropical freshwater fish which has emerged as a highly advantageous vertebrate model organism because of its small size, large clutches, transparent, low cost, and physiological similarity to mammals (**Eisen, 1996; Fishman, 1999**). Traditionally, zebrafish has been used in the fields of molecular genetics and developmental biology (**Driever et al., 1996; Kimmel, 1989**). However, its value as a model organism for drug discovery and toxicological studies has been recognized recently (**den Hertog, 2005; Pichler et al., 2003**). The application of drugs and/or small molecules to zebrafish is uncomplicated because the early stage embryo rapidly absorbs small molecular compounds diluted in the bathing media through the skin and gills. In contrast, relatively late stage zebrafish [from 7 d post-fertilization (dpf) to the adult stage] absorbs the compounds orally rather than percutaneously. Therefore, the use of early stage larva provides another advantage of testing percutaneous effects of medicinal and/or cosmetic compounds. In addition, zebrafish has melanin pigments on the surface, allowing simple observation of the pigmentation process without complicated experimental procedures (**Choi et al., 2007**).

The characteristic external pigment pattern of zebrafish is generated by an array of three types of pigment cells, all of which are derived from the neural crest. These include melanophores (melanin-containing melanocytes), xanthophores (containing yellow pigment), and iridophores (containing reflecting platelets) (**Jin and Thibaudau, 1999**). The combination of xanthophores and iridophores makes the yellowish-silver interstripes, while melanophores contribute to the longitudinal dark stripes of the epidermis (**Hirata et al., 2005; Kelsh et al., 1996**). Developmentally, pigment formation begins first from the retinal pigment epithelium (RPE), followed

by the melanocytes located on dorsolateral skin. Skin melanin could be seen at approximately 24 h post-fertilization (hpf). However, tyrosinase gene transcription and translation occur at earlier times; the mRNA for tyrosinase is detected approximately 7 h before visible pigmentation in the RPE, and tyrosinase enzymatic activity is detected 3 h before visible pigmentation (**Camp and Lardelli, 2001**).

The aim of this study is to develop natural whitening and UV protecting materials from *Ecklonia cava*, zebrafish adopted as an alternative *in vivo* model.



MATERIAL AND METHOD

Materials

The marine brown alga *E. cava* was collected along the coast of Jeju Island, Korea, between October 2007 and March 2008. The samples were washed three times with tap water to remove the salt, epiphytes, and sand attached to the surface. After that, these samples were carefully rinsed with fresh water, and maintained in a medical refrigerator at -20°C. Thereafter, the frozen samples were lyophilized and homogenized with a grinder prior to extraction.

Preparation of phlorotannins from *Ecklonia cava*

The phlorotannins were isolated as previously described by Ahn et al. (2007) with slight modifications. Briefly, the dried *E. cava* powder (500 g) was extracted three times with 80% MeOH and then filtered. The filtrate was evaporated at 40°C to obtain the methanol extract. After that, the extract was suspended on distilled water, and partitioned with ethyl acetate. The ethyl acetate fraction was mixed with celite. The mixed celite was dried and packed into a glass column, and eluted in the order of hexane, methylene chloride, diethyl ether, and methanol. The diethyl ether fraction was further purified by sephadex LH-20 column chromatography using stepwise gradient chloroform/methanol (2/1→0/1) solvents system. The phloroglucinol, eckol, triphloroethol A, eckstolonol and dieckol were purified by high performance liquid chromatography (HPLC) using a Waters HPLC system equipped with a Waters 996 photodiode array detector and C18 column (J'sphere ODSH80, 150× 20 mm, 4 μm; YMC Co.) by stepwise elution with methanol-water gradient (UV range: 230 nm,

flow rate: 0.8 ml/min). Finally, the purified compounds were identified by comparing their ^1H and ^{13}C NMR data to the literature report. The chemical structures of the phlorotannins are indicated in **Fig. 1**.

Origin and maintenance of parental zebrafish

Adult zebrafishes were purchased from a commercial dealer (Seoul aquarium, Korea) and 10 fishes were kept in 3 l acrylic tank with the following conditions; 28.5°C, with a 14/10 h light/dark cycle. Zebrafishes were fed three times a day, 6 d/week, with Tetramin flake food supplemented with live brine shrimps (*Artemia salina*). Embryos were obtained from natural spawning that was induced at the morning by turning on the light. Collection of embryos was completed within 30 min. All other chemicals were used reagent grade chemicals.

Zebrafish pigmentation evaluating

Embryos were collected and arrayed by pipette, 10 to 15 embryos per well, in 24-well plates containing 475 μl embryo medium. Test compounds were dissolved in 0.1% DMSO, and then added to the embryo medium from 9 to 35 hpf. Control animals were exposed to vehicle (0.1% DMSO) only. The effects on the pigmentation of zebrafish were observed under the microscope. In all experiments, PTU (1-phenyl-2-thiourea) and arbutin were used to generate transparent zebrafish without interfering the developmental process, and considered as positive controls. Phenotype-based evaluations of body pigmentation were carried out at 35 hpf. For observation, embryos were dechorionated in 2 mg/ml pronase (non-specific enzyme, Sigma, USA), anesthetized in tricaine methanesulfonate solution (Sigma, USA), and

photographed under the microscope AX100 (Zeiss, Gemany).

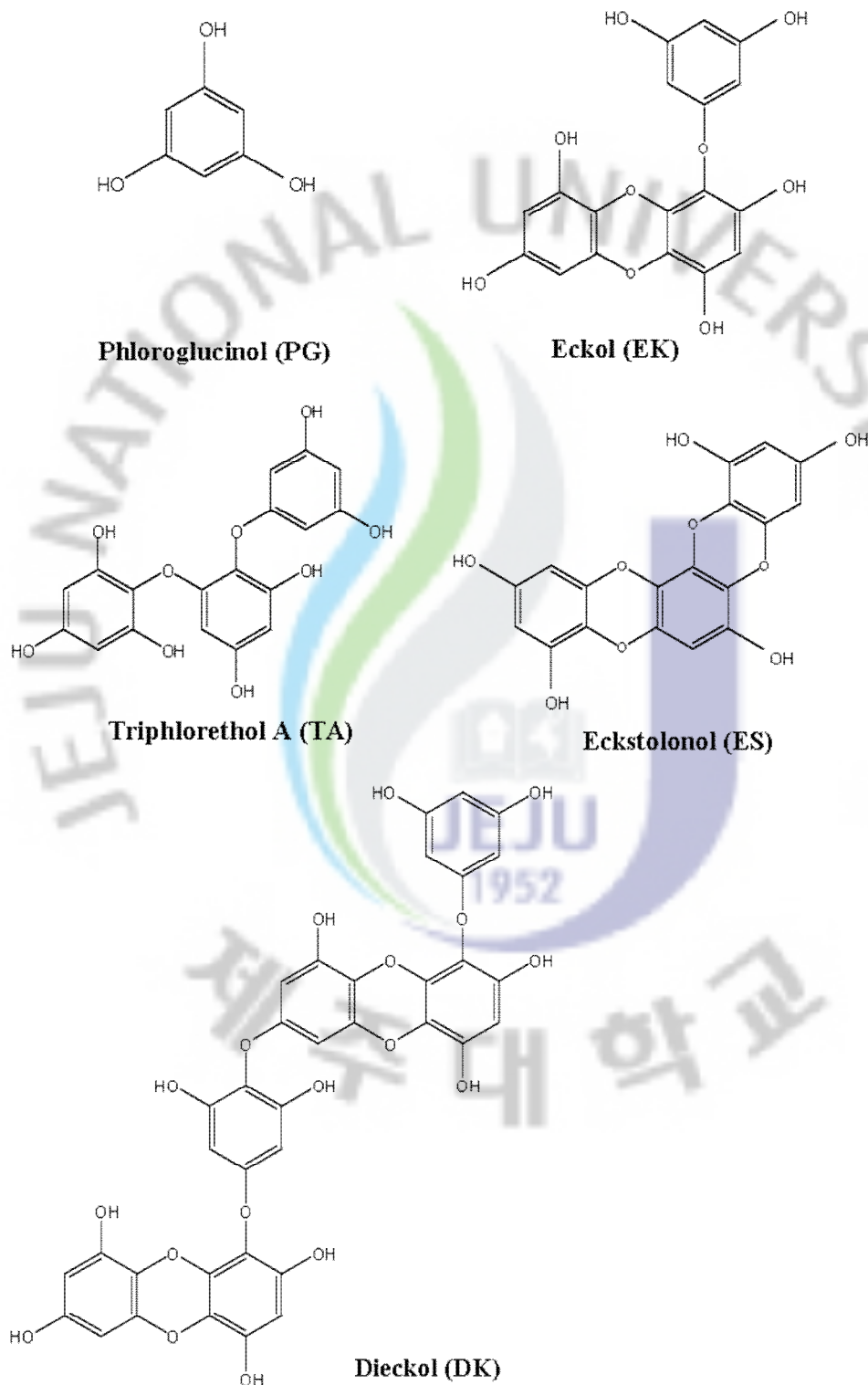


Fig. 3-1. Chemical structure of phlorotannins isolated from *Ecklonia cava*.

Melanin synthesis inhibitory activity of phlorotannins in zebrafish embryos

Melanin content was determined as described previously (Choi et al., 2007). Briefly, about 100 zebrafish embryos were treated without or with melanogenic inhibitors (phlorotannins or PTU and arbutin) from 9 to 35 hpf, and sonicated in Pro-Prep protein extraction solution (Intron, Korea). After the centrifugation, pellet was dissolved in 1 ml of 1 N NaOH at 100°C for 30 min. The mixture was then vigorously vortexed to solubilize the melanin pigment. Optical density of the supernatant was measured at 490 nm using the micro-reader (Packard spectrocount™, Austria). The melanin content was calibrated by protein amount, and expressed as a percentage of the control.

Tyrosinase inhibitory activity of phlorotannin in zebrafish embryos

Tyrosinase inhibitory activity was spectrometrically determined as described previously.²⁰ Briefly, about 100 zebrafish embryos were treated without or with melanogenic inhibitors (phlorotannins or PTU and arbutin) from 9 to 35 hpf, and sonicated in Pro-Prep protein extraction solution (Intron, Korea). The lysate was clarified by centrifuging at 10,000 × g for 5 min. A 250 µg of total protein in 100 µl of lysis buffer was transferred into the 96-well plate, and 100 µl of 1 mM *l*-DOPA was added. Control well contained 100 µl of lysis buffer and 100 µl of 1 mM *l*-DOPA. After incubation for 60 min at 28°C, absorbance was measured at 475 nm using the micro-reader (Packard spectrocount™, Austria). PTU and arbutin were used as positive controls. The tyrosinase was calibrated by protein amount, and expressed as a percentage of the control.

Measurement of heart-beating rate

The heart-beating rate of both atrium and ventricle was measured at 35 hpf to determine the sample toxicity.²⁰ Counting and recording of atrial and ventricular contraction were performed for 3 min under the microscope, and the results were presented as the average heart-beating rate per min.

Statistical analysis

Data were evaluated statistically using Student's *t*-test followed by Fisher's least significance was set at $p < 0.001$ or $p < 0.05$. The data were the mean \pm SD of three independent experiments.



RESULTS

Melanin synthesis inhibitory activity of phlorotannins in zebrafish embryo

In order to estimate the inhibitory activities, we measured the melanin synthesis using whole zebrafish extracts. We noted substantial reductions in tyrosinase activity after the treatment with phlorotannins including dieckol (DK), eckstolonol (ES), eckol (EK), triphloethol A (TA), and phloroglicinol (PG) from *Ecklonia cava* (**Fig. 3-1**). PTU as a positive control, as anticipated, reduced melanin synthesis (87.73%) to a marked degree. Arbutin also reduced melanin synthesis (61.36%). DK, ES, EK, TA, and PG also inhibited tyrosinase activity (73.64%, 69.55%, 79.09%, 69.54% and 61.36%, respectively) (**Fig. 3-2**). Interestingly, DK, ES, EK, and TA have shown higher melanin synthesis inhibitory activity than arbutin. All of them showed around 70% of inhibition. And PG has shown similar activity as arbutin. EK showed the highest melanin synthesis inhibitory activity among phlorotannins, and DK showed the second highest inhibitory activity. This is shown in **Fig. 3-3**, which contains an image of the morphologic findings. The positive controls, including PTU and arbutin evidenced a remarkable inhibition of trunk and yolk sac pigmentation. On the other hand, phlorotannins were utilized the melanin shrank on the surface of the trunk. In particular, the yolk sac pigmentation was inhibited dramatically after treatment with the phlorotannins.

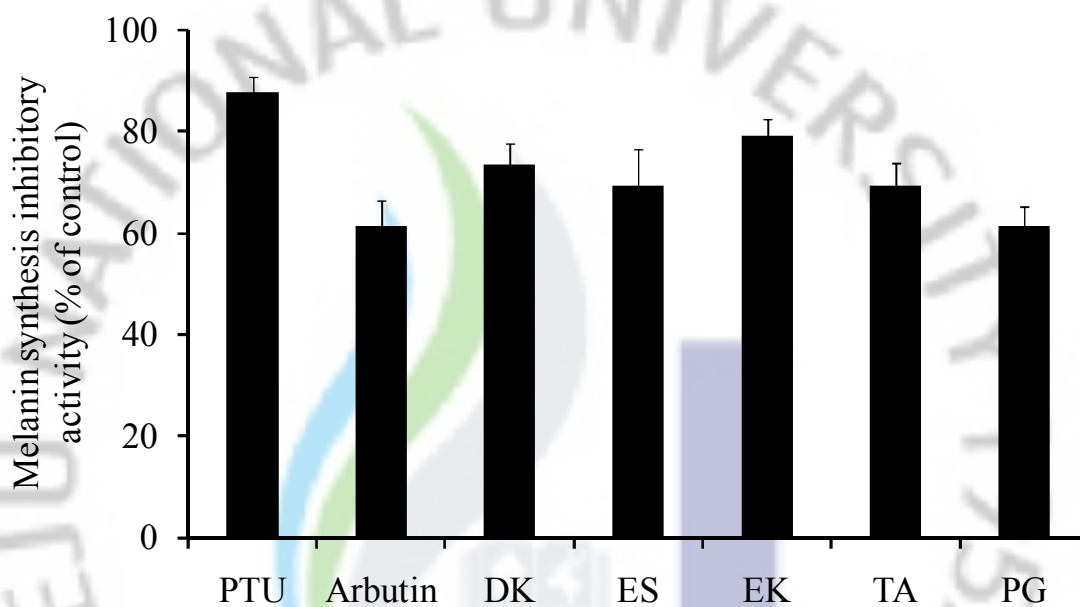


Fig. 3-2. Melanin synthesis inhibitory activity of phlorotannins in zebrafish embryos. 1-phenyl-2-thiourea (PTU) and arbutin utilized as positive controls. Dieckol (DK), Eckstolonol (ES), Eckol (EK), Triphlorethol A (TA), and Phloroglicinol (PG). Experiments were performed in triplicate and the data are expressed as mean \pm SE.

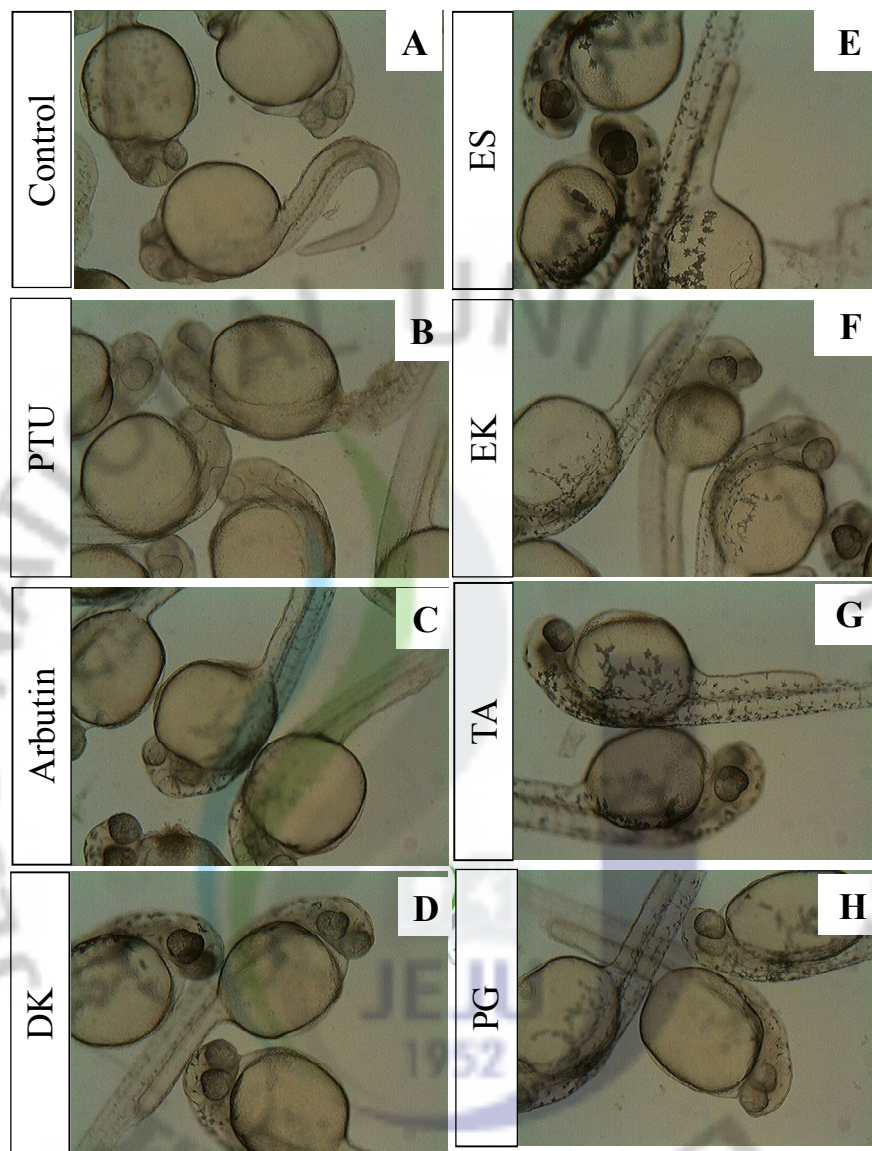


Fig. 3-3. Effects of melanogenic inhibitors on the pigmentation of zebrafish. The effects of the pigmentation of zebrafish were observed at 35 hpf (hour post-fertilization) under microscope. (A) Untreated zebrafish embryos as a control, (B, C) 1-phenyl-2-thiourea (PTU), arbutin as positive controls, (D) dieckol (DK), (E) eckstolonol (ES), (F) eckol (EK), (G) triphlorethol A (TA), and (H) phloroglicinol (PG).

Tyrosinase inhibitory activity of phlorotannins in zebrafish embryo

In order to estimate the inhibitory activities, we measured the tyrosinase activity using whole zebrafish extracts. We noted substantial reductions in tyrosinase activity after the treatment with phlorotannins including dieckol (DK), eckstolonol (ES), eckol (EK), triphlorethol A (TA), and phloroglicinol (PG) from *Ecklonia cava* (**Fig. 3-1**). PTU as a positive control, as anticipated, reduced tyrosinase activity (48.75%). Arbutin also reduced tyrosinase activity (58.78%). On the other hand, DK, ES, EK, TA, and PG also inhibited tyrosinase activity (40.86%, 62.72%, 43.37%, 56.27 and 62.01%, respectively) (**Fig. 3-4**). ES, TA, and PG have shown higher tyrosinase inhibitory activity than PTU. In particular, ES and PG have shown higher tyrosinase inhibitory activity than the positive controls.

Toxicity of melanogenic inhibitors in zebrafish embryo

In order to determine the toxicity of the melanogenic inhibitors, we monitored the growth patterns of zebrafish. The adopted endpoints experiment used to assess the toxicity of the compounds included embryo mortality, morphological malformations, and heart-beating disturbances. The melanogenic inhibitors (PTU, arbutin, DK, ES, EK, TA, and PG) were not associated with mortality in this experiment. When evaluating the morphological malformations, inhibitors did not evidence conspicuous and adverse effects (data not shown). On the other hand, in the heart-beat test, arbutin generated a slight disturbance, and PTU evidenced a marked increase in heart-beat rate, whereas DK, ES, EK, TA, and PG did not generate any heart-beat rate disturbances as compared with the controls (untreated control, **Fig. 3-5**). In simultaneous *in vivo* toxicity tests, toxicity was not detected in the fish treated with

all phlorotannins, whereas toxicity was observed in the fish treated with the positive controls including PTU and arbutin.



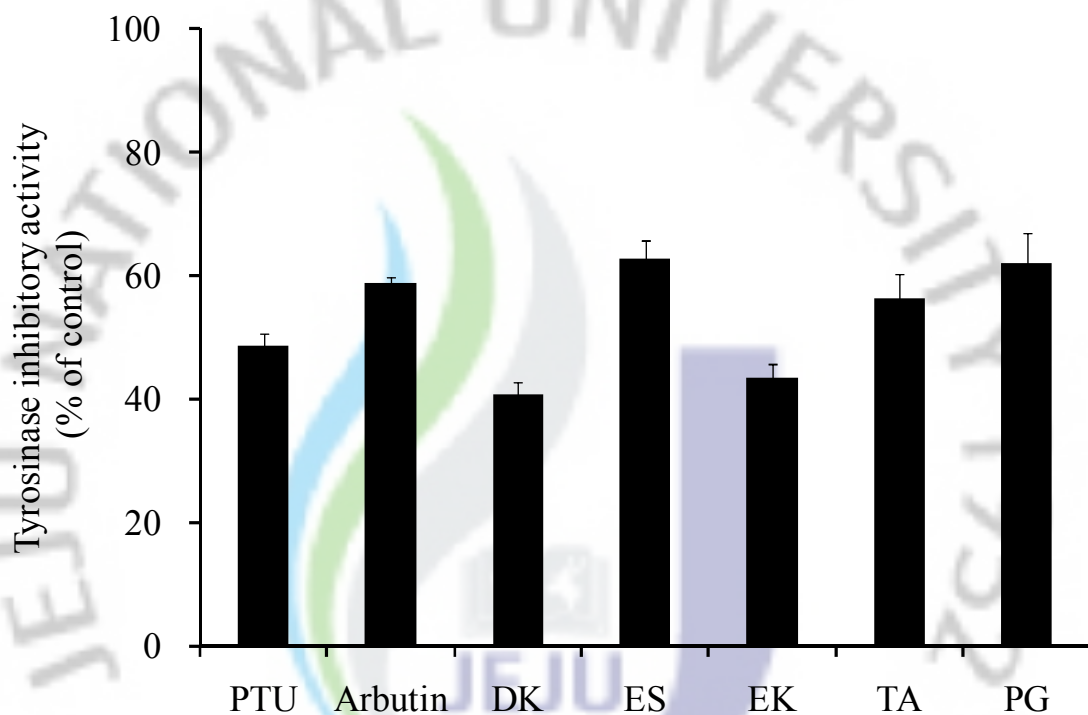


Fig. 3-4. Tyrosinase inhibitory activity of phlorotannins in zebrafish embryos. 1-phenyl-2-thiourea (PTU) and arbutin utilized as positive controls. Dieckol (DK), Eckstolonol (ES), Eckol (EK), Triphlorethol A (TA), and Phloroglicinol (PG). Experiments were performed in triplicate and the data are expressed as mean \pm SE. * p <0.05, ** p <0.01.

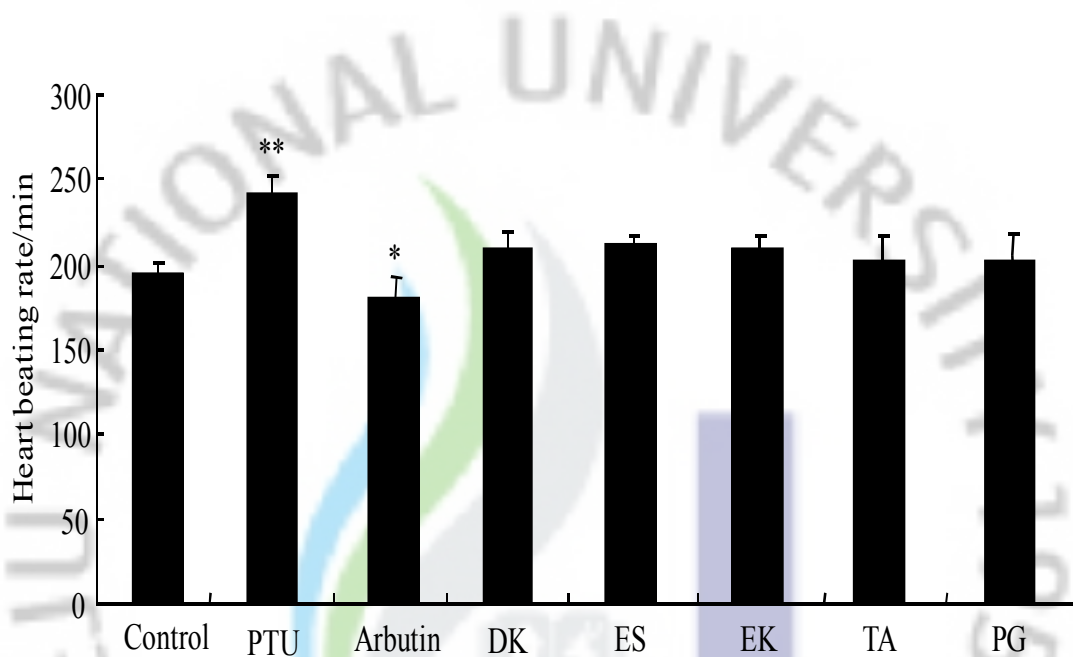


Fig. 3-5. Effects of melanogenic inhibitors on the heart-beating rate. The heart-beating rate was measured under the microscope. The number of heart-beating for 3 min was counted, and the result represented as the beat/min. 1-phenyl-2-thiourea (PTU) and arbutin utilized as positive controls. Dieckol (DK), Eckstolonol (ES), Eckol (EK), Triphlorethol A (TA), and Phloroglicinol (PG). Experiments were performed in triplicate and the data are expressed as mean \pm SE. * p <0.05, ** p <0.01.

DISCUSSION

Marine algal extracts and their bioactive constituents have been previously explored with regard to tyrosinase inhibitory activity. According to **Kang et al., (2004)** *Ecklonia stolonifera* showed inhibitory activity with an IC₅₀ value of 345 µg/ml. By way of contrast, our new findings reveal that inhibitors evidenced tyrosinase inhibitory effects that were dramatically more profound than those of *E. stolonifera*.

Despite its successful applications, the cell model has some disadvantages in terms of its physiological and economic relevance. For example, the data acquired from *in vitro* studies using cultured cells may not be directly extrapolated from the *in vivo* results. Clearly, *in vivo* tests using animal models or humans are the most physiologically relevant. However, these tests are expensive, labor intensive and tedious, as well as it requires large amounts of precious compounds, particularly during the screening and compound evaluation steps. Furthermore, pressure to limit the use of animals is increasing, except for tests of preclinical toxicity and safety assessments (**Zon and Peterson, 2005**). Thus, we proposed zebrafish model as an *in vivo* animal model for evaluation of the melanogenic regulatory compounds from marine algae. The value of the zebrafish as an animal model for drug discovery and toxicological studies has been recently recognized (**den Hertog, 2005; Pichler et al., 2003**). Additionally, the zebrafish has melanin pigmentations on its surface, allowing for simple observation of the pigmentation process without needs for any complicated experimental procedures. The characteristic external pigmentation pattern of the zebrafish is generated by an array of three types of pigment cells, all of

which are derived from the neural crest. These include melanophores (melanin-containing melanocytes), xanthophores (containing yellow pigment), and iridophores (containing reflecting platelets) (**Jin, 1999**). The combination of xanthophores and iridophores generate the yellowish-silver interstripes, whereas melanophores contribute to the formation of the characteristic longitudinal dark stripes of the epidermis.³⁹⁻⁴⁰ Recognizing the advantages of this model, which includes a rapid pigmentation process, permeability to small molecules and ease of handling, we propose that zebrafish can be employed as a phenotype-based model for the screening of melanogenic regulatory compounds (**Choi et al., 2007**). Additionally, the toxicity of certain compounds can be simultaneously determined by assessing the morphological malformations and heart-beat disturbance (**Zon and Peterson, 2005**). In the previous studies, a variety of materials has been developed and currently utilized as cosmetic additives or as medicinal products for the treatment of hyperpigmentation (**An et al., 2005; Wang et al., 2007**). Recently, the demand for natural products which inhibit or prevent skin pigmentation is rapidly increasing all over the world. A variety of natural or synthetic substances are currently utilized as ingredients of preparations designed to control hyperpigmentation, but none of these have proven completely satisfactory, either due to their limited efficacy or owing to safety concerns (**Briganti et al., 2003**). For instance, hydroquinone, which was used widely and considered as the standard depigmenting agent, has recently been banned for cosmetic uses in Europe and some Asian countries, as well as it is available only by prescription. Kojic acid, another tyrosinase inhibitor, has a high sensitizing potential and has also been prohibited in some countries, citing mutagenic concerns (**Petit and Pierard, 2003**). Arbutin, a natural compound, is used extensively in the

cosmetic industry as a response to increasing global demand for skin-whitening agent substances for the development of new depigmenting, cosmeceutical, and skin lighting agents (Seo et al., 2003; Aburjai and Natsheh, 2003). Marine algae have been used in food for centuries; they are frequently utilized to maintain good health or to treat a variety of diseases. In this study, the cosmetic potential of phlorotannins from *E. cava* were used in subsequent experiments. Therefore, we evaluated their inhibitory effects on tyrosinase and melanin synthesis in a zebrafish embryo. We evaluated the feasibility of zebrafish as an animal model system to determine the effects of marine algae for melanogenic inhibition. PTU is a sulfur-containing tyrosinase inhibitor which has been extensively utilized in zebrafish research as a pigment inhibitor (Karlsson et al., 2001; Elsalini and Rohr, 2003). Arbutin was also utilized as a positive control.

Tyrosinase is an important constituent of cosmetics and a known skin-lightening agent (An et al., 2005). Pigment synthesis involves the conversion of tyrosine to melanin synthesis in melanocytes (Li et al., 2007). We utilized *l*-DOPA as the substrate for the detection of this tyrosinase inhibitory effect. Among the phlorotannins, ES and PG have shown to exert potent tyrosinase inhibitory effects (Fig. 3-4). PTU and arbutin function as whitening agents and evidenced tyrosinase inhibitory activity. The tested phlorotannins evidenced inhibitory activities higher than those of PTU and arbutin. TA also has shown tyrosinase inhibitory activity as similar to arbutin. Melanin formation is the most important determining factor in mammalian skin color (Hearing, 2005). In melanogenesis, the proximal pathway consists of the enzymatic oxidation of tyrosine or *l*-DOPA to its corresponding *o*-dopaquinone catalyzed via tyrosinase (Kim and Uyama, 2005).

In the current study, zebrafish embryos were utilized to assess melanin synthesis inhibitory activity. All of the tested samples exerted profound inhibitory effects on zebrafish pigmentation, most likely as the consequence of their tyrosinase activity-inhibitory potential (**Fig. 3-4, Fig. 3-5**). Interestingly, this ability of DK, ES, EK, and TA were more profound than observed in the positive control (arbutin). Arbutin is a natural product, which it is a glucosylated hydroquinone, and may pose similar risks of cancer (**O'Donoghue, 2006**). In addition, the zebrafish were allowed to continue to develop, the PTU-treated zebrafish were all dead after 4 days, and the arbutin-treated fish survived at a rate of approximately 60% over the same period, whereas the phlorotannins-treated zebrafish was evidenced a survival rate of approximately 90%. In simultaneous *in vivo* toxicity tests, toxicity was not detected in the fish treated with phlorotannins, whereas toxicity was observed in the fish treated with the positive controls. Additionally, *E. cava* has shown in a previously study that it possesses excellent antioxidant activities and high phenolic content (**Heo et al., 2005**), thus making them potential candidates for cosmetic application.

In summary, phlorotannins from *E. cava* were evaluated in regard to their potential efficacy as whitening agents, and they evidenced profound inhibitory effects against tyrosinase and melanin synthesis in zebrafish *in vivo* model. It can be surmised that these algae are likely to be useful for the cosmetic and medicinal industries. Together, zebrafish are valuable alternative *in vivo* model.

Part III-2.

UV-B protective effects of phlorotannins using zebrafish as an alternative *in vivo* model

ABSTRACT

In the present study, five kinds of phlorotannins, marine algal polyphenol, were estimated their protective effect against photo-oxidative stress induced by UV-B radiation was investigated. Among the phlorotannins, ES showed higher effect than that of the other phlorotannins in the the assay and all phlorotannins were showed relatively lower than that of a control (only UV-B radiation). The UV-B protection effect was evaluated via DCFH-DA, DAF-FM DA, acridine orange and morphological changes in zebrafish as an alternative *in vivo* model. ROS and NO induced by UV-B radiation were reduced by the addition of phlorotannins. Moreover, all phlorotannins demonstrated strong protective properties against UV-B radiation-induced cell death in zebrafish. Hence, these results indicated that phlorotannins isolated from *E. cava* has potential protective effects on UV-B radiation-induced cell death, which might be used in pharmaceutical and cosmeceutical industries.

MATERIAL AND METHOD

Materials

The marine brown alga *E. cava* was collected along the coast of Jeju Island, Korea, between October 2007 and March 2008. The samples were washed three times with tap water to remove the salt, epiphytes, and sand attached to the surface, and then carefully rinsed with fresh water, and maintained in a medical refrigerator at -20°C. Thereafter, the frozen samples were lyophilized and homogenized with a grinder prior to extraction.

Preparation of phlorotannins from *Ecklonia cava*

The phlorotannins were isolated as previously described by Ahn et al. (2007) with slight modifications. Briefly, the dried *E. cava* powder (500 g) was extracted three times with 80% MeOH and then was filtered. The filtrate was evaporated at 40°C to obtain the methanol extract. After, the extract was suspended on distilled water, and partitioned with ethyl acetate. The ethyl acetate fraction was mixed with celite. The mixed celite was dried and packed into a glass column, and eluted in the order of hexane, methylene chloride, diethyl ether, and methanol. The diethyl ether fraction was further purified by sephadex LH-20 column chromatography using stepwise gradient chloroform/methanol (2/1→0/1) solvents system. The phloroglucinol, eckol, triphloroethol A, eckstolonol and dieckol were purified by high performance liquid chromatography (HPLC) using a Waters HPLC system equipped with a Waters 996 photodiode array detector and C18 column (J'sphere ODSH80, 150× 20 mm, 4 μm; YMC Co.) by stepwise elution with methanol-water

gradient (UV range: 230 nm, flow rate: 0.8 ml/min). Finally, the purified compounds were identified by comparing their ^1H and ^{13}C NMR data to the literature report. The chemical structures of the phlorotannins are indicated in **Fig. 3-1**.

Origin and maintenance of parental zebrafish

Adult zebrafishes were obtained from a commercial dealer (Seoul aquarium, Korea) and 10 fishes were kept in 3 l acrylic tank with the following conditions; 28.5°C, with a 14/10 h light/dark cycle. Zebrafishes were fed three times a day, 6 d/week, with Tetramin flake food supplemented with live brine shrimps (*Artemia salina*). Embryos were obtained from natural spawning that was induced at the morning by turning on the light. Collection of embryos was completed within 30 min.

UV-B irradiation

Zebrafish were exposed to UV-B (312 nm) range at a dose rate of 10–100 mJ/cm² (UV Lamp, VL-6LM, Vilber Lourmat, France) and 50 mJ/cm² dose were identified as the optimum irradiation dose. Therefore, the 50 mJ/cm² dose of UV-B was used for further experiments.

Waterborne exposure of embryos to phlorotannins

From approximately 2 days post-fertilization (2 dpf), embryos ($n=25$) were transferred to individual wells of a 24-well plate and maintained in embryo media containing 1 ml of vehicle (0.1% DMSO) or 50 uM phlorotannins for 1 h. Then irradiated with UV-B (312 nm) or co-irradiated UV-B and phlorotannins for 1 h.

Measurement of heart-beat rate

The heart-beating rate of both atrium and ventricle were measured after UV-B irradiation. Counting and recording of atrial and ventricular contraction were performed for 3 min under the microscope, and results were presented as the average heart-beating rate per min.

Zebrafish pigmentation evaluating

Phenotype-based evaluations of body pigmentation were carried out. For observation, embryos were anesthetized in tricaine methanesulfonate solution (Sigma, USA), and photographed under the microscope SZX9 (Olympus, Japan).

Determination of UV-B induced melanin contents in zebrafish

Melanin content was determined according to **Choi et al., (2007)** with slight modification. Briefly, at 2 d pf zebrafish embryos were irradiated UV-B, and then sonicated in Pro-Prep protein extraction solution (Intron, Korea). After the centrifugation, pellet was dissolved in 1 ml of 1 N NaOH at 100°C for 30 min. The mixture was then vigorously vortexed to solubilize the melanin pigment. Optical density of the supernatant was measured at 490 nm using the micro-reader (Packard spectrocountTM, Austria). The melanin content was calibrated by protein amount, and expressed as a percentage of the control.

Estimation of UV-B induced intracellular ROS generation and image analysis

Generation of reactive oxygen species (ROS) production of zebrafish embryos was analyzed using an oxidation-sensitive fluorescent probe dye, 2,7-

dichlorofluorescein diacetate (DCF-DA). DCF-DA was deacetylated intracellularly by nonspecific esterase, which was further oxidized to the highly fluorescent compound dichlorofluorescein (DCF) in the presence of cellular peroxides (Rosenkranz et al., 1992). At 2 dpf, the embryos were treated with phlorotannins and 1 h later, UV-B (312 nm) was irradiated to the plate. After irradiating embryos with UV-B for 1 h, the embryos were transferred in to 96 well plate and treated with DCF-DA solution (20 µg/ml), and the plates were incubated for 1 h in the dark at 28.5 °C. After incubation, the embryos were rinsed in embryo media and anesthetized before visualization. Individual embryo fluorescence intensity was quantified using spectrofluorometer (Perkin–Elmer LS-5B, Austria). The images of stained embryos were observed using a fluorescent microscope, which was equipped with a CoolSNAP-Pro color digital camera (Olympus, Japan).

Estimation of UV-B induced intracellular NO generation and image analysis

In order to visualize NO to analyze its spatial and temporal localization in living cells, fluorescent probes have been developed. They permit a reliable detection, bioimaging, and quantification of NO with nanomolar sensitivity. Generation of nitric oxide (NO) production of zebrafish embryos was analyzed using a fluorescent probe dye, 2',7'-difluorofluorescein diacetate (DAF-FM DA). DAF transformation by NO in the presence of dioxygen generates highly fluorescent triazole derivatives. At 2 dpf, the embryos were treated with phlorotannins and 1 h later, UV-B (312 nm) was irradiated to the plate. After irradiating embryos with UV-B for 1 h, the embryos were transferred in to 96 well plate and treated with DAF-FM DA solution (5 µM), and the plates were incubated for 1 h in the dark at 28.5 °C. After incubation, the

embryos were rinsed in embryo media and anesthetized before visualization. Individual embryo fluorescence intensity was quantified using spectrofluorometer (Perkin–Elmer LS-5B, Austria). The image of stained embryos were observed using a fluorescent microscope, which was equipped with a CoolSNAP-Pro color digital camera (Olympus, Japan).

Measurement of UV-B induced cell death in zebrafish embryo

Cell death was detected in live embryos using acridine orange staining, a nucleic acid selective metachromatic dye that interacts with DNA and RNA by intercalation or electrostatic attractions. Acridine orange stains cells with disturbed plasma membrane permeability so it preferentially stains necrotic or very late apoptotic cells.

At 2 dpf, the embryos were treated with phlorotannins and 1 h later, UV-B (312 nm) was irradiated to the plate. After irradiating embryos with UV-B for 1 h, the embryos were transferred in to 96 well plate and treated with acridine orange (AO) solution (7 µg/ml), and the plates were incubated for 1 h in the dark at 28.5°C. After incubation, the embryos were rinsed in embryo media and anesthetized before visualization. Individual embryo fluorescence intensity was quantified using spectrofluorometer (Perkin–Elmer LS-5B, Austria). The image of stained embryos were observed using a fluorescent microscope, which was equipped with a CoolSNAP-Pro color digital camera (Olympus, Japan).

Statistical analysis

All the measurements were made in triplicate and all values were represented as mean±S.E. The results were subjected to an analysis of the variance using the Tukey

test to analyze the difference. $P < 0.05$, $P < 0.001$ were considered significantly.



RESULTS

Toxicity of phlorotannins in zebrafish after UV-B radiation

In order to determine the toxicity of phlorotannins in zebrafish after UV-B radiation, we monitored the morphological malformations of zebrafish and heart-beating disturbances. During UV-B radiation with or without phlorotannins, there was no association of mortality in this experiment. When evaluating the morphological malformations, UV-B radiation did not evidence conspicuous adverse effects (data not shown). On the other hand, in the heart-beat test, UV-B radiation evidenced a marked increase in heart-beat rate, whereas the zebrafish pre-treated with phlorotannins before UV-B radiation did not generate any heart-beat rate disturbances as compared with the control (UV-B non radiation, **Fig. 3-6**).

Inhibitory effect of phlorotannins on melanogenesis after UV-B radiation in zebrafish

The inhibition of melanogenesis was evaluated in **Fig. 3-7** and **Fig. 3-8**. The inhibitory effect of the DK, ES, EK, TA, and PG and recorded as 149.25%, 137.5%, 153.5%, 149.5%, and 150.5%, respectively at the concentrations of 50 μ M. Whereas, the inhibitory effect of melanogenesis recorded as 202.5% on UV-B radiation zebrafish. Out of the phlorotannins, ES possess higher inhibitory activity than those of the other phlorotannins, and all phlorotannins showed protective effect of melanogenesis against UV-B radiation.

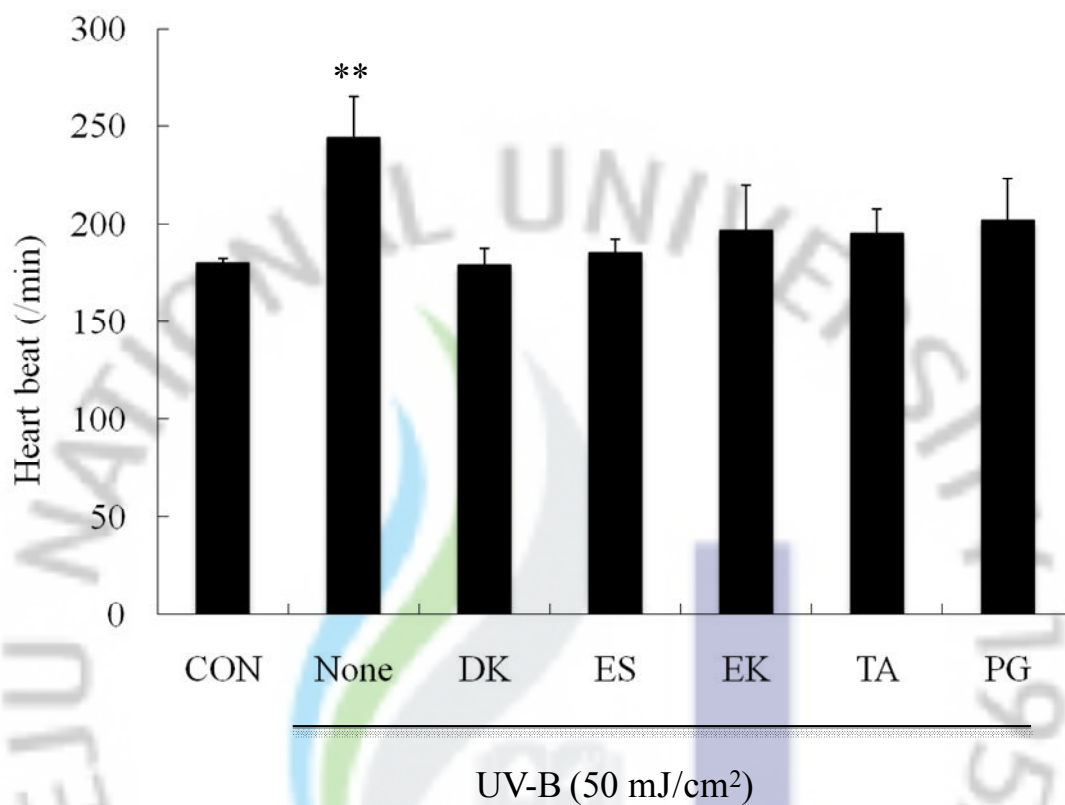


Fig. 3-6. Protective effect of phlorotannins isolated from *E. cava* on UV-B radiation-induced heart-beat disturbance in zebrafish. The embryos were exposed to UV-B (50 mJ/cm²) and phlorotannins treated. The heart-beat was measured at 48 hpf, under the microscopy. The number of heartbeat in 3 min was counted, and the results are expressed as the beats/min. Dieckol (DK), Eckstolonol (ES), Eckol (EK), Triphlorethol A (TA), and Phloroglicinol (PG). Experiments were performed in triplicate and the data are expressed as mean±SE. ** $p < 0.01$.

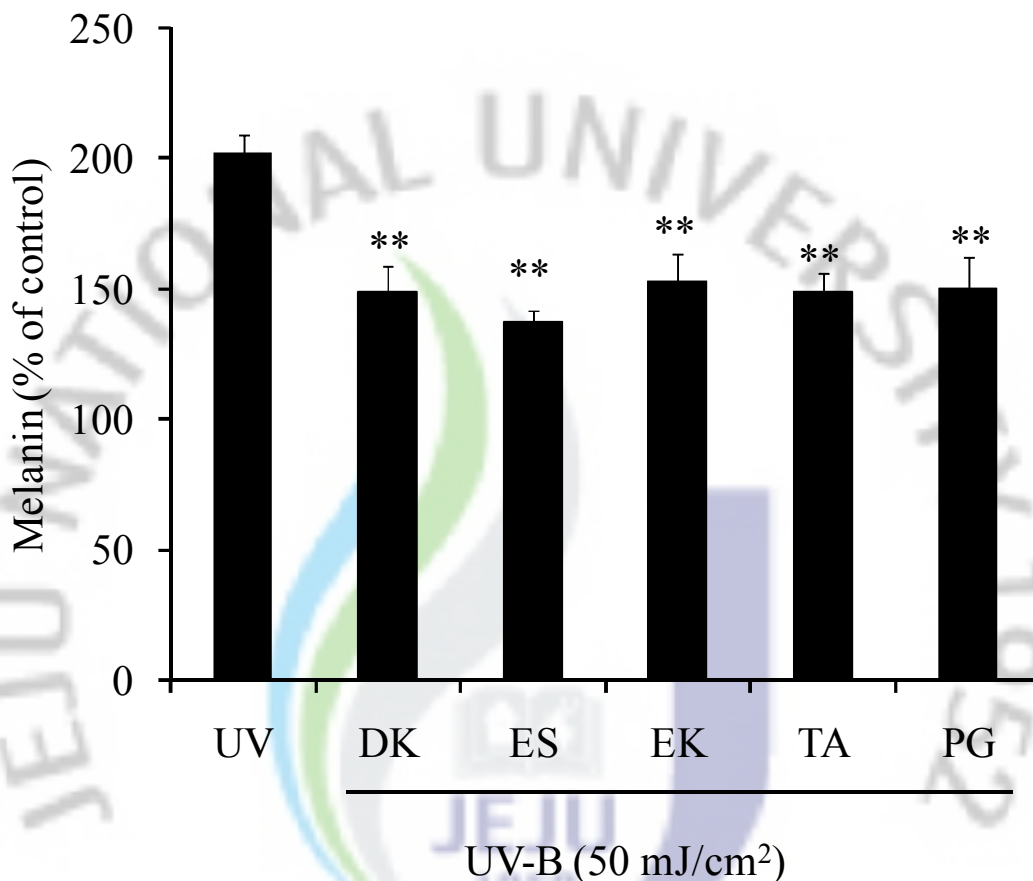


Fig. 3-7. Inhibitory effect of phlorotannins on melanogenesis after UV-B radiation in zebrafish embryos. The embryos were exposed to UV-B (50 mJ/cm²) and phlorotannins treated. After incubation, melanin contents were detected by spectrophotometer after dissolved in 1N NaOH. Dieckol (DK), Eckstolonol (ES), Eckkol (EK), Triphlorethol A (TA), and Phloroglicinol (PG). Experiments were performed in triplicate and the data are expressed as mean±SE. ***p*<0.01.

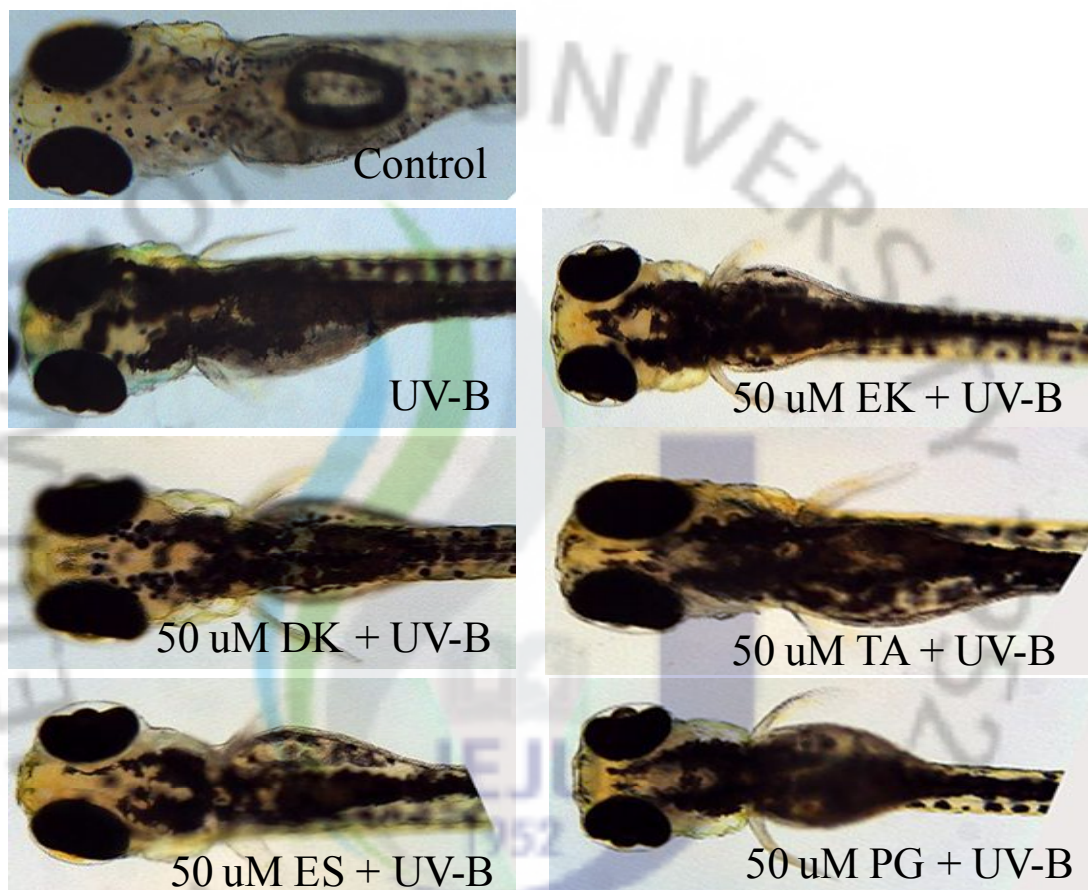


Fig. 3-8. Inhibitory effect of phlorotannins on melanogenesis after UV-B radiation in zebrafish embryos. The embryos were exposed to UV-B (50 mJ/cm²) and phlorotannins treated. Dieckol (DK), Eckstolonol (ES), Eckol (EK), Triphlorethol A (TA), and Phloroglicinol (PG).

Inhibitory effect of ROS generation by UV-B radiation in zebrafish embryos

The scavenging efficacy of phlorotannins including dieckol (DK), eckstolonol (ES), eckol (EK), triphlorethol A (TA), and phloroglicinol (PG), on ROS production in the UV-B radiation-induced zebrafish was measured. Treatment of zebrafish with phlorotannins inhibited the ROS production. (**Fig. 3-9**). Thus, it showed mostly similar ROS level of the cells compared with the control (without phlorotannins and UV-B radiation) at the presence of 50 μ M phlorotannins. As shown in **Fig. 3-10**, it was taken typical fluorescence photographs of the zebrafish. The negative control, which contained no phlorotannin or UV-B radiation, generated clear image, whereas the positive control, which irradiated only UV-B, generated fluorescence image, which suggests that ROS took place in the radiation of UV-B in the zebrafish. However, the zebrafish were treated with phlorotannins prior to UV-B radiation, a dramatic reduction in the amount of ROS was observed. This result reflects a reduction of ROS generation by phlorotannins.

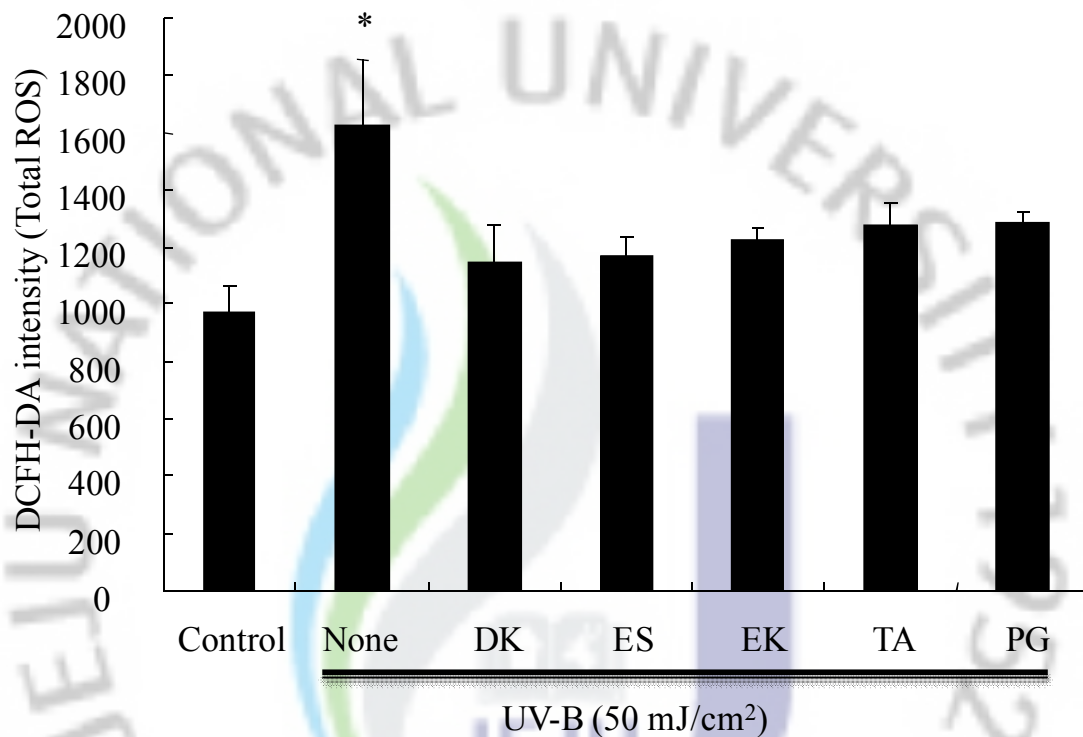


Fig. 3-9. Effect of phlorotannins isolated from *E. cava* on UV-B radiation-induced ROS level in zebrafish. The embryos were exposed to UV-B (50 mJ/cm²) and phlorotannins treated. After incubation, the intracellular ROS detected by fluorescence spectrophotometer after DCFH-DA staining. Dieckol (DK), Eckstolonol (ES), Eckol (EK), Triphlorethol A (TA), and Phloroglicinol (PG). Experiments were performed in triplicate and the data are expressed as mean± SE. **p*<0.05.

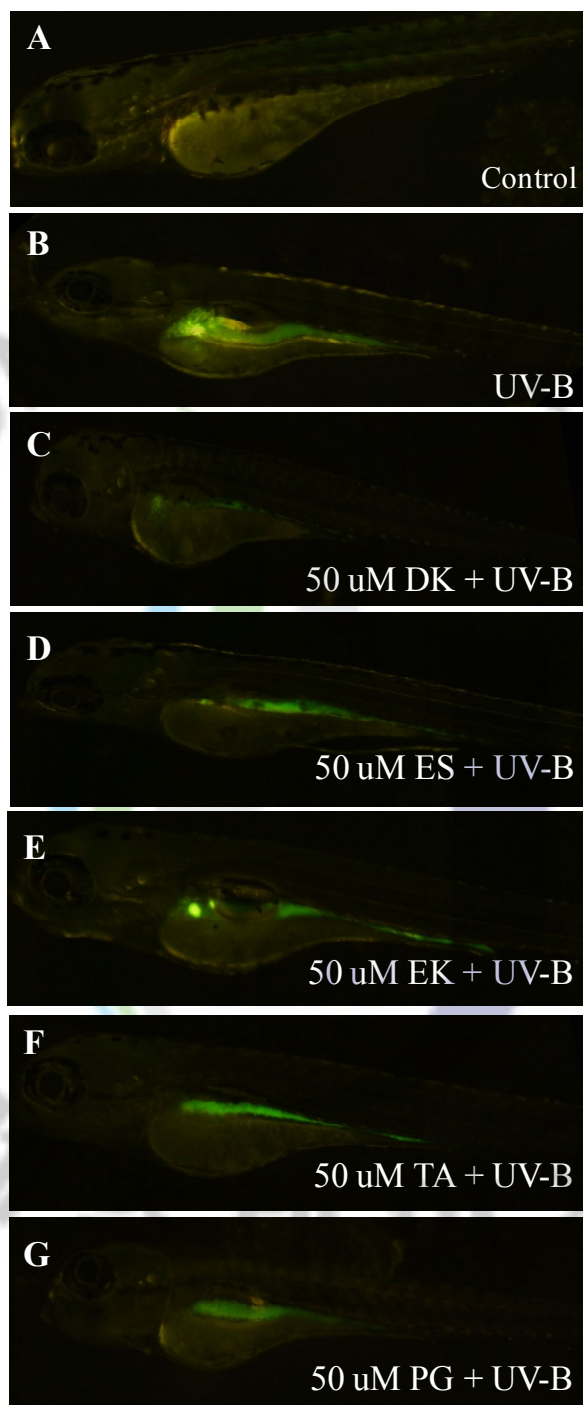


Fig. 3-10. Photographs of UV-B radiation-induced ROS level in zebrafish. The embryos were exposed to UV-B (50 mJ/cm^2) and phlorotannins treated. The ROS levels were measured by image analysis and fluorescence microscope.

Inhibitory effect of NO generation by UV-B radiation in zebrafish

The scavenging efficacy of phlorotannins including dieckol (DK), eckstolonol (ES), eckol (EK), triphloethol A (TA), and phloroglicinol (PG), on NO production in the UV-B radiation-induced zebrafish was measured. Treatment of zebrafish with phlorotannins inhibited the NO production (**Fig. 3-11**). All phlorotannins showed no scavenging effect against UV-B radiation. Thus, DK, ES, and PG showed mostly similar NO level of the zebrafish compared with the control (without phlorotannins and UV-B radiation) at the presence of 50 μ M phlorotannins. As shown in **Fig. 3-12**, it was taken typical fluorescence photographs of the zebrafish. The negative control, which contained no phlorotannin or UV-B radiation, generated clear image, whereas the positive control, which irradiated only UV-B, generated fluorescence image, which suggests that NO took place in the radiation of UV-B in the zebrafish. However, when the zebrafish were treated with phlorotannins prior to UV-B radiation, a dramatic reduction in the amount of NO was observed. This result reflects a reduction of NO generation by phlorotannins.

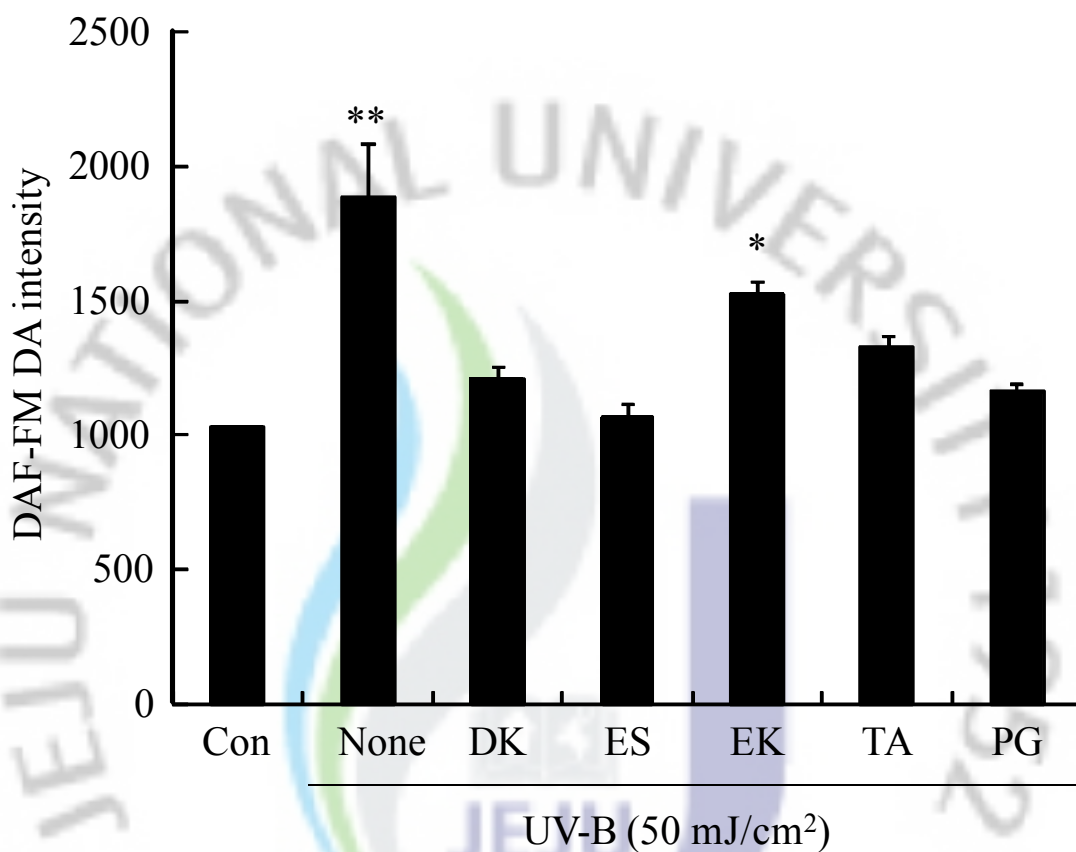


Fig. 3-11. Effect of phlorotannins isolated from *E. cava* on UV-B radiation-induced NO level in zebrafish. The embryos were exposed to UV-B (50 mJ/cm²) and phlorotannins treated. After incubation, the intracellular ROS detected by fluorescence spectrophotometer after DAF-FM DA staining. Dieckol (DK), Eckstolonol (ES), Eckol (EK), Triphlorethol A (TA), and Phloroglicinol (PG). Experiments were performed in triplicate and the data are expressed as mean±SE. * p <0.05, ** p <0.01.

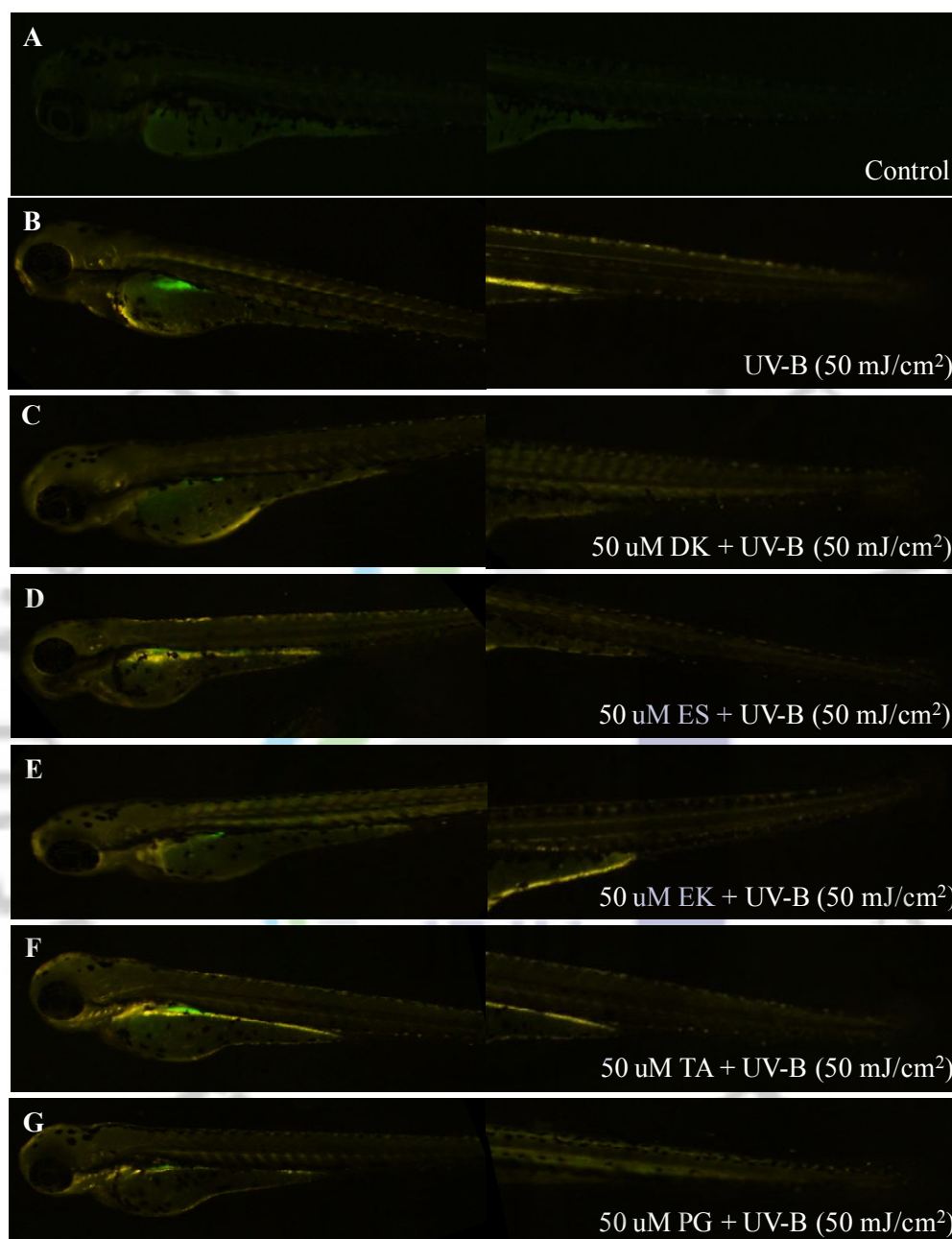


Fig. 3-12. Photographs of UV-B radiation-induced NO level in zebrafish. The embryos were exposed to UV-B (50 mJ/cm^2) and phlorotannins treated. The ROS levels were measured by image analysis and fluorescence microscope. Dieckol (DK), Eckstolonol (ES), Eckol (EK), Triphlorethol A (TA), and Phloroglicinol (PG).

Protective effects of phlorotannins on UV-B radiation-induced cell death in live zebrafish

To evaluate whether phlorotannins protect against UV-B radiation, cell death induced by UV-B radiation was measured via acridine orange as fluorescence intensity in body of the zebrafish (**Fig. 3-13**). The UV-B radiation-induced cell death in zebrafish was recorded as 2010 intensity (positive control), whereas the negative control presented as 1000 intensity. However, the cell death was reduced by the addition of phlorotannins to the zebrafish exposed to the UV-B radiation. All phlorotannins showed protective effects against UV-B radiation. Among the phlorotannins, DK, ES, and TA showed higher protective effect against UV-B radiation induced cell death. The microscopic pictures have shown in **Fig. 3-14** that the control zebrafish had intact, and UV-B radiation zebrafish have shown significant increased the intensity of acridine orange. However, the fish were treated with phlorotannins prior to UV-B radiation, a dramatic decrease in cell death was observed.

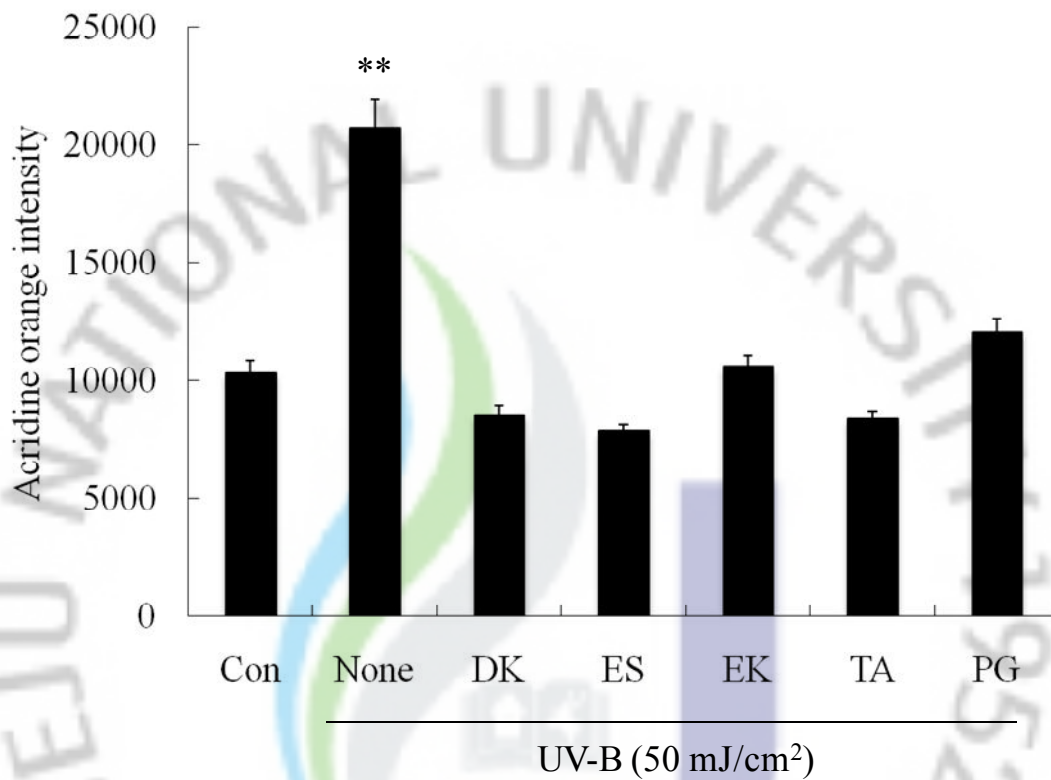


Fig. 3-13. Protective effect of phlorotannins isolated from *E. cava* on UV-B radiation-induced cell death in live zebrafish. The embryos were exposed to UV-B (50 mJ/cm²) and phlorotannins treated. After incubation, the cell death was detected by fluorescence spectrophotometer after acridine orange staining. Dieckol (DK), Eckstolonol (ES), Eckol (EK), Triphlorethol A (TA), and Phloroglicinol (PG). Experiments were performed in triplicate and the data are expressed as mean±SE. ***p*<0.01.

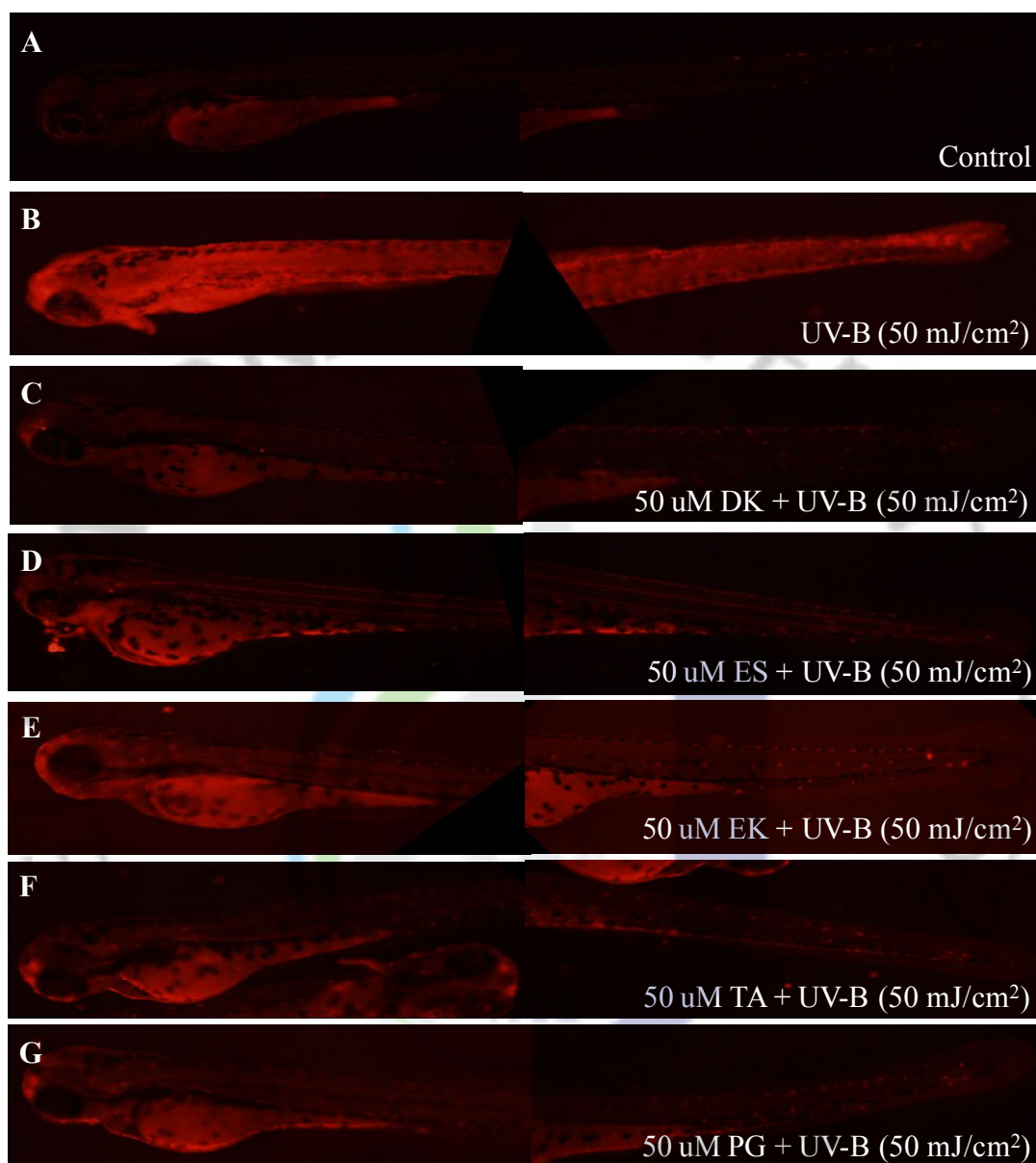


Fig. 3-14. Photographs of UV-B radiation-induced cell death in live zebrafish.

The embryos were exposed to UV-B (50 mJ/cm^2) and phlorotannins treated. The cell death levels were measured by image analysis and fluorescence microscope. Dieckol (DK), Eckstolonol (ES), Eckol (EK), Triphlorethol A (TA), and Phloroglicinol (PG).

DISCUSSION

Marine algae have been well-known as an important source to produce natural bioactive secondary metabolites including phenols and polyphenols with unique linkages (Torres et al., 2008). *E. cava*, an edible brown alga with a long history as folk medicine in Korea, is abundantly distributed only in Korea and Japan according to the latest statistics. The previous reports on *E. cava* have revealed that it contains variety of phlorotannin derivatives which are commonly known to have defensive or protective functions against herbivores (Li et al., 2009). Although some reports suggest that phlorotannins from algae exhibit antioxidant effect on free radicals, there are no reports on the effects of the phlorotannins on melanogenesis and their photo-protective effect on the cell damage induced by UV-B radiation, as well as the underlying mechanism of phlorotannins. Thus, in this study, the potential sun light protective effect of phlorotannins isolated from *E. cava* was investigated in zebrafish as an alternative animal model system. Melanins play a critical role in the absorption of free radicals and melanogenesis in the skin in a kind of process that produces photo-protective agents against damaging effect from UV. Many cosmetic and pharmaceutical companies have tried to find inhibitors for melanogenesis. The regulation of cellular pigmentation can be controlled at the different stages of melanogenesis. In the present study, phlorotannins isolated from *E. cava* were examined for their ability to inhibit melanin contents in zebrafish. From these results, it was reduced that all phlorotannins inhibited pigmentation more effectively than that of the positive control (only UV-B radiation). Hence, phlorotannins can be applied as a natural sunlight protecting material. Oxidative stress may be induced by

increasing generation of ROS and other free radicals. UV radiation can induce the formation of ROS such as singlet oxygen and superoxide anion in the skin, promoting biological damage in exposed tissues via iron-catalyzed oxidative reactions (**Wang et al., 2006**). Generation of intracellular ROS can be detected using oxidation sensitive dye DCFH-DA as the substrate. Fluorescent probes have been widely employed to monitor oxidative activity in cells. During labeling, non-fluorescent DCFH-DA dye which penetrates freely into the cells gets hydrolyzed by intracellular esterase to DCFH, and traps inside the cells (**Veerman et al., 2004**). Therefore, an increase in the cellular fluorescence level reveals the elevated levels of ROS. Many types of death stimuli induce the increasing cellular levels of ROS, and the elimination of the induced ROS through the use of antioxidants protects the cells from those stimuli. Therefore, ROS are believed to act as key mediators of cell death (**Martindale and Holbrook, 2002; Kim et al., 2008**). A variety of stresses such as chemicals, pathogens, and others can induce NO production. These results suggest that phlorotannins can be developed into a potential bio-molecular candidate to inhibit ROS formation. As phlorotannins were found to exert a ROS scavenging effect, it was further evaluated with regard to its protective effects against UV-B radiation-induced cell death in zebrafish.

Phlorotannins, well known marine algal polyphenols, are recognized to have defensive or protective functions against oxidative stress (**Kang et al., 2003**). Although some reports suggest that the phlorotannins from algae exhibit antioxidant effect on free radicals and H₂O₂, there are no reports on the protective effects against UV-B radiation of phlorotannins in zebrafish. These results demonstrated that phlorotannins possess the potential inhibitory effects on oxidative damage induced

by UV-B radiation. Also the antioxidant activities were associated with the improvement of the cell viability as compared to our previous study (**Ahn et al., 2007**). The skin possesses an elaborate antioxidant defense system to protect it from oxidative stress. However, excessive exposure to reactive oxygen species can shift the prooxidant–antioxidant balance of the skin toward the more oxidative state. Resulting oxidative stress causes many adverse effects and pathological conditions (**Ananthaswamy and Kanjilal, 1996; Finkel and Holbrook, 2000**). Under these circumstances, regular intake of dietary antioxidants or treatment of the skin with products containing UV protective ingredients could be a useful strategy for preventing UV-B induced damage. Oxidative stress is associated with cell death which occurs during several pathological situations. When evaluating a compound with therapeutical potential, the screening of toxicity has a special relevance. Therefore, in this study, we report the protective effect of phlorotannins as antioxidant and UV protective agent for UV-B radiation-induced cell death via acridine orange dye and morphological analysis. It was clearly demonstrated that phlorotannins reduced cell death induced by UV-B radiation. Several natural compounds have gained considerable attention as skin photo-protective agents. Plants can change their phenolic metabolisms under UV-B radiation, which supply enough phenolic compounds to screen UV-B light, and sometimes these molecules might function as antioxidant to quench ROS generated by UV-B radiation (**Booij-James et al., 2000; Sudheer et al., 2007; Skandrani et al., 2009**). Phlorotannins are well known polyphenols in marine algae, which have various biological activities including antioxidant, antitumor, antihypertension, and anti-inflammatory effects. Among them, antioxidant activity related to UV protection is intensively focused due

to the currently growing demand from the cosmeceutical industry where they are interested in anti-aging and whitening natural products. Therefore, the phlorotannins can easily be applied in antioxidant and cosmeceutical industries as a natural compound from marine biomass. We conclude that zebrafish embryos are valuable laboratory alternative *in vivo* model. The antioxidant mechanisms underlying the protective efficacies afforded by phlorotannins in this experiment remain to elucidate.



REFERENCES

- Aburjai T., Natsheh F.M., 2003. Plants used in cosmetics. *Phytotherapy Research* 17, 987–1000.
- Ahn, G.N., Kim, K.N., Cha, S.H., Song, C.B., Lee, J., Heo, M.S., Yeo, I.K., Lee, N.H., Lee, Y.H., Kim, J.S., Heu, M.S., Jeon, Y.J., 2007. Antioxidant activities of phlorotannins purified from *Ecklonia cava* on free radical scavenging using ESR and H₂O₂- mediated DNA damage. *European Food Research and Technology* 226, 71–79.
- Amarowicz R., Naczek M., Shahidi F., 2000. Antioxidant activity of various fractions of non-tannin phenolics of Canola hulls. *Journal of Agricultural Food and Chemistry* 48, 2755-2759.
- An, B.J., Kwak, J.H., Park, J.M., Lee, J.Y., Park, T.S., Lee, J.T., Son, J.H., Jo, C., Byun, M.W., 2005. Inhibition of enzyme activities and the antiwrinkle effect of polyphenol isolated from the persimmon leaf (*Diospyros kaki* folium) on human skin. *Dermatologic Surgery* 31, 848–854.
- Ananthaswamy, H.N., Kanjilal, S., 1996. Oncogenes and tumor suppressor genes in photocarcinogenesis. *Photochemistry and Photobiology* 63, 428–432.
- Antkiewicz DS, Burns CG, Carney SA, Peterson RE, Heideman W., 2005. Heart malformation in an early response to TCDD in embryonic zebrafish. *Toxicology Science* 84, 368-377.
- Barbarino E., Lourenco S.O., 2005. An evaluation of methods for extraction and quantification of protein from marine macro- and microalgae. *Journal Applied Phycology* 17, 447-460.
- Beyersmann D., S. Hechtenberg, 1997. Cadmium, gene regulation, and cellular signalling in mammalian cells. *Toxicology Applied Pharmacology* 144, 247–261.
- Booij-James, I.S., Dube, S.K., Jansen, M.A.K., Edelman, M., Mattoo, A.K., 2000. Ultraviolet-B radiation impacts light-mediated turnover of the photosystem II reaction center heterodimer in *Arabidopsis* mutants altered in phenolic metabolism. *Plant Physiology* 124, 1275–1283.
- Bradbury J., 2004. Small Fish, Big Science. *PLoS Biology* 2, e148.
- Butterfield D.A., Castenga A., Pocernich C.B., Drake J., Scapagnini G., Calabrese V., 2002. Nutritional approaches to combat oxidative stress in Alzheimer's disease. *The Journal of Nutritional Biochemistry* 13, 444-461.
- Caddeo, C., Teskac̆, K., Sinico, C., Kristl, J., 2008. Effect of resveratrol

- incorporated in liposomes on proliferation and UV-B protection of cells. *International Journal of Pharmaceutics* 363, 183–191.
- Camp E., Lardelli M., 2001. Tyrosinase gene expression in zebrafish embryos. *Development Genes Evolution* 211, 150-153.
- Chang C.Y., Wu K.C., Chiang S.H., 2007. Antioxidant properties and protein compositions of porcine haemoglobin hydrolysates. *Food Chemistry* 100, 1537-1543.
- Chen J.N., Haffter P., Odenthal J., Vogelsang E., Brand M., van Eeden F.J., Furutani-Seiki M., Granato M., Hammerschmidt M., Heisenberg C.P., Jiang Y.J., Kane D.A., Kelsh R.N., Mullins M.C., Nüsslein-Volhard C., 1996. Mutations affecting the cardiovascular system and other internal organs in zebrafish. *Development* 123, 293-302.
- Choi T.Y., Kim J.H., Ko D.H., Kim C.H., Hwang J.S., Ahn S., Kim S.Y., Kim C.D., Lee J.H., Yoon T.J., 2007. Zebrafish as a new model for phenotypic-based screening of melanogenic regulatory compounds. *Pigment Cell Research* 20, 120-127.
- Cole, K.K., Perez-Polo, J.R., 2002. Poly (ADP-ribose) polymerase inhibition prevents both apoptotic-like delayed neuronal death and necrosis after H₂O₂ injury. *Journal of Neurochemistry* 82, 19–29.
- Coyle J.T., Puttfarcken P., 1993. Oxidative stress, glutamate, and neurodegenerative disorders, *Science* 262, 689–695.
- den Hertog J. 2005. Chemical genetics: drug screens in zebrafish. *Bioscience Rep* 25, 289–297.
- Devasagayam, T. P. A., Boloor, K. K. and Ramasarma, T., 2003. Methods for estimating lipid peroxidation: An analysis of merits and demerits (mini review). *Indian Journal of Biochemistry and Biophys* 40, 300–308.
- Driever W., Solnica-Krezel L., Schier A.F., 1996. A genetic screen for mutations affecting embryogenesis in zebrafish. *Development* 123, 37–46.
- Eisen J.S., 1996. Zebrafish make a big splash. *Cell* 87, 969–977.
- Elsalini O.A., Rohr K.B., 2003. Phenylthiourea disrupts thyroid function in developing zebrafish. *Development Genes Evolution* 212, 593–598.
- Finkel, T., Holbrook, N.J., 2000. Oxidants, oxidative stress and the biology of ageing. *Nature* 408, 239–247.
- Fishman M.C., 1999. Zebrafish genetics: the enigma of arrival. *Proc Natl Acad Sci* 96, 10554–10556.
- Fleming A., 2007. Zebrafish as an alternative model organism for disease modelling

- and drug discovery: implications for the 3Rs.
- Frayssé B., Mons R., Garric J., 2006. Development of a zebrafish 4-day embryonal bioassay to assess toxicity of chemicals. *Ecotoxicology and Environmental Safety* 63, 253–267.
- Fuchs, J., 1998. Potentials and limitations of the natural antioxidants RRR- α -tocopherol, L-ascorbic acid and β -carotene in cutaneous photoprotection. *Free Radical Biology and Medicine* 25, 848–873.
- Hearing, V.J., 2005. Biogenesis of pigment granules: a sensitive way to regulate melanocyte function. *Journal of Dermatological Science* 37, 3–14.
- Heo S.J., Cha S.H., Lee K.W., Cho K.S.M., Jeon Y.J., 2005. Antioxidant activities of chlorophyta and phaeophyta from Jeju Island. *Algae* 20, 251-260.
- Heo S.J., Jeon Y.J., 2008. Identification of Chemical Structure and Free Radical Scavenging Activity of Diphlorethohydroxycarmalol Isolated from a Brown Alga, *Ishige okamurae*. *Journal Microbiology and Biotechnology* 18, 676-681.
- Heo SJ, Jeon YJ. Radical scavenging capacity and cytoprotective effect of enzymatic digests of *Ishige okamurae*. *J Appl Phycol* 2008; 20: 1087-1095.
- Heo, S.J., Ko, S.C., Cha, S.H., Kang, D.H., Park, H.S., Choi, Y.U., Kim, D., Jung, W.K., Jeon, Y.J., 2009. Effect of phlorotannins isolated from *Ecklonia cava* on melanogenesis and their protective effect against photo-oxidative stress induced by UV-B radiation. *Toxicology in Vitro* 23, 1123-1130.
- Hill A., Howard C.V., Strahle U., Cossins A., 2003. Neurodevelopmental defects in zebrafish (*Danio rerio*) at environmentally relevant dioxin (TCDD) concentrations. *Toxicology Science* 76, 392–399.
- Hill A.J., Teraoka H., Heideman W., Peterson R.E., 2005. Zebrafish as a model vertebrate for investigating chemical toxicity. *Toxicology Science* 86, 6-19.
- Hirata M., Nakamura K., Kondo S., 2005. Pigment cell distributions in different tissues of the zebrafish, with special reference to the striped pigment pattern. *Development Dynamics*. 234 293– 300.
- Howell J.C., 1986. Food antioxidants: international perspectives—welcome and introductory remarks. *Food Chemistry Toxicology* 24,997-1002.
- Incardona J.P., Collier T.K., Scholz N.L., 2004. Defects in cardiac function precede morphological abnormalities in fish embryos exposed to polycyclic aromatic hydrocarbons. *Toxicology Applied Pharmacology* 196, 191-205.
- Je J.Y., Qian Z.J., Byun H.G., Kim S.K., 2007. Purification and characterization of an antioxidant peptide obtained from tuna backbone protein by enzymatic hydrolysis. *Process Biochemistry* 42, 840–846.

- Jiang F.W., Zhang Y.S., 1994. A dictionary of chinese marine drugs. China Ocean Press, Beijing, p 507
- Jin E.J., Thibaudeau G., 1999. Effects of lithium on pigmentation in the embryonic zebrafish (*Brachydanio rerio*). *Biochimistry Biophys Acta* 1449, 93–99.
- Kajiwara, T., Matsui, K., Akakabe, Y., Murakawa, T., Arai, C., 2006. Antimicrobial browning-inhibitory effect flavor compounds in seaweeds. *Journal of Applied Phycology* 18, 413–422.
- Kang H.S., Chung H.Y., Kim J.Y., Son B.W., Jung H.A., Choi J.S., 2004. Inhibitory phlorotannins from the edible brown alga *Ecklonia stolonifera* on total reactive oxygen species (ROS) generation. *Arch Pharm Research* 27, 194–198.
- Kang K.S., Yokozawa T., Yamabe T., Kim H.Y., Park J.H., 2007. ESR Study on the Structure and Hydroxyl Radical-Scavenging Activity Relationships of Ginsenosides Isolated from Panax ginseng C. A. MEYER *Biology and Pharmacy Bulletin* 30, 917-921.
- Kang, K., Park, Y., Hwang, H.J., Kim, S.H., Lee, J.G., Shin, H.C., 2003. Antioxidative properties of brown algae polyphenolics and their perspectives as chemopreventive agents against vascular risk factors. *Archives of Pharmacal Research* 26, 286-293.
- Kang, K.A., Lee, K.H., Chae, S, Koh, Y.S., Kim J.H., Ham Y.M., Baik, J.S., Lee, N.H., Hyun, J.W., 2005. Triphlroethol-A from *Ecklonia cava* protects V79-4 lung fibroblast hydrogen peroxide induced cell damage. *Free Radical Research* 39, 883-892.
- Kang, K.A., Lee, K.H., Chae, S., Zhang, R., Jung, M.S., Ham, Y.M., Baik, J.S., Lee, N.H., Hyun, J.W., 2006. Cytoprotective effect of phloroglucinol on oxidative stress induced cell damage via catalase activation. *Journal of cellular biochemistry* 97, 609-620.
- Karlsson J., von Hofsten J, Olsson P.E., 2001. Generating transparent zebrafish: a refined method to improve detection of gene expression during embryonic development. *Marine Biotechnology* 3, 522–527.
- Kelsh R.N., Brand M., Jiang Y.J., 1996. Zebrafish pigmentation mutations and the processes of neural crest development. *Development* 123, 369–389.
- Kent M., Spitsbergen J., 2003. The State of the Art of the Zebrafish Model for Toxicology and Toxicologic Pathology Research--Advantages and Current Limitations. *Toxicology Pathology* 31, 62-87.
- Kim E.M., Yang H.S., Kang S.W., Ho J.N., Lee S.B., Um H.D., 2008. Amplification of the c-irradiation-induced cell death pathway by reactive oxygen species in

- human U937 cells. *Cellular Signalling* 20, 916–924.
- Kim K.N., Heo S.J., Song C.B., Lee J., Heo M.S., Yeo I.K., Kang K.A., Hyun J.W., Jeon Y.J., 2006a. Protective effect of *Ecklonia cava* enzymatic extracts on hydrogen peroxide-induced cell damage. *Process Biochemistry* 41, 2393–2401.
- Kim M., Yun J., Lee C.K., Lee H., Min K.R., Ki Y.m, 2002. Oxyresveratrol and hydroxystibene compounds. Inhibitory effect on tyrosinase and mechanism of action. *Journal of Biology Chemistry* 277, 16340–16344.
- Kim Y.J., Hwang S.Y., Oh E.S., Oh S., Han I.O., 2006. IL-1beta, an immediate early protein secreted by activated microglia, induces iNOS/NO in C6 astrocytoma cells through p38 MAPK and NF-kappaB pathways. *Journal of Neuroscience Reseach* 84, 1037–1046.
- Kim Y.J., Uyama H., 2005. Tyrosinase inhibitors from natural and synthetic sources: structure, inhibition mechanism and perspective for the future. *Cellular and Molecular Life Sciences* 62, 1707–1723.
- Kimmel C., Ballard W., Kimmel S., Ullmann B., Schilling T., 1995. Stages of embryonic development of the zebrafish. *Developmental Dynamics* 203, 253–310.
- Kimmel C.B., 1989. Genetics and early development of zebrafish. *Trends. Genet* 5, 283–288.
- Kong, C.S., Kim, J.A., Yoon, N.Y., Kim, S.K., 2009. Induction of apoptosis by phloroglucinol derivative from *Ecklonia cava* in MCF-7 human breast cancer cells *Food and Chemical Toxicology* 47, 1653-1658.
- Kuda T., Tsunekawa M., Goto H., Araki Y., 2005. Antioxidant properties of four edible algae harvested in the Noto Peninsula, Japan. *Journal of Food Composition Analysis* 18, 625-633.
- Langenheinrich U., 2003. Zebrafish: a new model on the pharmaceutical catwalk. *BioEssays* 25, 904-912.
- Lee J.Y., Hwang W.I., Lim S.T., 2004. Antioxidant and anticancer activities of organic extracts from *Platycodon grandiflorum* A. De Candolle roots. *Journal of Ethnopharmacol* 93, 409-415.
- Lele Z., Krone P.H., 1996. The zebrafish as a model system in developmental, toxicological and transgenic research. *Biotechnol Adv* 14, 57-72.
- Li J, Wang X.Q., Watson M.B., Assmann S.M., 2000. Regulation of abscisic acid-induced stomatal closure and anion channels by guard cell AAPK kinase. *Science* 287, 300–303
- Li Y., Qian Z.J., Ryu B., Lee S.H., Kim M.M., Kim S.K., 2009. Chemical

- components and its antioxidant properties in vitro: an edible marine brown alga, *Ecklonia cava*. *Bioorganic and Medicinal Chemistry* 17, 1963–1973.
- Li Y.P., Hsu F.L., Chen C.S., Chern J.W., Lee M.H., 2007. Constituents from the Formosan apple reduce tyrosinase activity in human epidermal melanocytes. *Phytochemistry* 68, 1189–1199.
- Li, J., Huang, C.Y., Zheng, R.L., Cui, K.R., Li, J.F., 2000. Hydrogen peroxide induces apoptosis in human hepatoma cells and alters cell redox status. *Cell Biology International* 24, 9–23.
- Lindmark-Mansson H., Akesson B., 2000. Antioxidative factors in milk. *British Journal of Nutrition* 84, S103-S110
- Liu W., Kato, M., Akhand A.A., Hayakawa A., Suzuki H., Miyata T., Kurokawa K., Hotta Y., Ishikawa N., Nakashima I., 2000. 4-Hydroxynonenal induces a cellular redox status-related activation of the caspase cascade for apoptotic cell death. *Journal of Cell Science* 113, 635–641.
- Longstreth J., de Gruijl F.R., Kripke M.L., Abseck S., Arnold F., Slaper H.I., Velders, G., Takizawa Y., van der Leun J.C., 1998. Health risks. *Journal of Photochemistry and Photobiology B: Biology* 46, 20–39.
- Ma W., Wlaschek M., Tancheva-Poor I., Schneider L.A., Naderi L., Razi-Wolf Z., Schuller J., Scharffetter-Kochanek K., 2001. Chronological ageing and photoageing of the fibroblasts and the dermal connective tissue. *Clinical and Experimental Dermatology* 26, 592–599.
- Malecki A., Garrido R., Mattson M.P., Hennig B., Toborek M., 2000. 4-Hydroxynonenal induces oxidative stress and death of cultured spinal cord neurons. *Journal of Neurochemistry* 74, 2278–2287.
- Marrot L., Belaidi J.P., Chaubo C., Meunier J.R., Perez P., Agapakis-Causse C., 2001. Fluoroquinolones as chemical tools to define a strategy for photogenotoxicity in vitro assessment. *Toxicology In Vitro* 15, 131–142.
- Martindale J.L., Holbrook N.J., 2002. Cellular response to oxidative stress: signaling for suicide and survival. *Journal of Cellular Physiology* 192, 1–15.
- McKim J.M. Early life stage toxicity tests. In: Rand G.M., Petrocelli S.R. (eds.). *Fundamentals of Aquatic Toxicology*. pp. 58–95, Hemisphere Publishing, New York, 1985.
- Meisel H., 1997. Biochemical properties of bioactive peptides derived from milk proteins: potential nutraceuticals for food and pharmaceutical applications. *Livestock Production Science* 50, 125–138.
- Neely M.D., Boutte A., Milatovic D., Montine T.J., 2005. Mechanisms of 4-

- hydroxynonenal-induced neuronal microtubule dysfunction. *Brain Research* 1037, 90–98.
- Nosedá M.D., Tulio S., Duarte M.E.R., 1999. Polysaccharides from the red seaweed *Bostrychia montagnei*: chemical characterization. *Journal of Applied Phycology* 11, 35-40.
- O'Donoghue J.L., 2006. Hydroquinone and its analogues in dermatology—a risk-benefit viewpoint. *Journal of Cosmetic Dermatology* 5, 196–203.
- Pichler F.B., Laurenson S., Williams L.C., Dodd A., Copp B.R., Love D.R., 2003. Chemical discovery and global gene expression analysis in zebrafish. *Nat Biotechnology* 21, 879–883.
- Pietta P., Siimonetti P., Mauri P., 1998. Antioxidant activity of selected medicinal plants. *Journal of Agricultural Food and Chemistry* 46, 4487-4490.
- Poli G., Albano E., Dianzai M.U., 1987. The role of lipid peroxidation in liver damage. *Chemistry Physic Lipids* 45, 117–142.
- Rosenkranz A.R., Schmaldienst S., Stuhlmeier K.M., Chen W., Knapp W., Labinger G.J., 1992. A microplate assay for the detection of oxidative products using 20,70- dichlorofluorescein-diacetate. *Journal of Immunological Methods* 156, 39–45.
- Rubinstein A.L., 2003. Zebrafish: from disease modeling to drug discovery. *Current Opinion Drug Discovery Development* 6, 218-223.
- Rubinstein A.L., 2006. Zebrafish assays for drug toxicity screening. *Expert Opinion in Drug Metabolism and Toxicology* 2, 231-240.
- Satoh T., Enokido Y., Kubo K., Yamada M., Hatanaka, H., 1999. Oxygen toxicity induces apoptosis in neuronal cells, *Cellular Molecular Neurobiology* 18, 649–666.
- Satoh T., Lipton S.A., 2007. Redox regulation of neuronal survival mediated by electrophilic compounds, *Trends Neuroscience* 30, 37–45.
- Schirmer K., 2006. Proposal to improve vertebrate cell cultures to establish them as substitutes for the regulatory testing of chemicals and effluents using fish. *Toxicology* 224, 163–183.
- Seok S.H., Baek M.W., Lee H.Y., Kim D.J., Na Y.R., Noh K.J., Park S.H., Lee H.K., Lee B.H., Park J.H., 2008. *In vivo* alternative testing with zebrafish in ecotoxicology. *Journal of Veterinary Science* 9, 351-357.
- Shimizu K., Kondo R., Sakai K., Lee S.-H. Sato H., 1998. The Inhibitory Components from *Artocarpus incisus* on Melanin Biosynthesis. *Planta Medicines* 64, 408-412.
- Shimogaki, H., Tanaka, Y., Tamai, H., and Masuda, M., 2000. *In vitro* and *in vivo*

- evaluation of ellagic acid on melanogenesis inhibition. *International Journal of Cosmetic Science* 22, 291–303.
- Skandrani, I., Bouhlel, I., Limem, I., Boubaker, J., Bhourri, W., Neffati, A., Sghaier, M.B., Kilani, S., Ghedira, K., Ghedira-Chekir, L., 2009. *Moricandia arvensis* extracts protect against DNA damage, mutagenesis in bacteria system and scavenge the superoxide anion. *Toxicology In Vitro* 23, 166–175.
- Son S.M., Moon K.D., Lee C.Y., 2000. Rhubarb juice as a natural antibrowning agent. *Journal of Food Science* 65, 1288-1289.
- Spitsbergen, J.M., Kent, M.L., 2003. The state of the art of the zebrafish model for toxicology and toxicologic pathology research – Advantages and current limitations. *Toxicologic Pathology* 31, 62-87.
- Stern H.M., Zon L.I., 2003. Cancer genetics and drug discovery in the zebrafish, *Nature Reviews Cancer* 3, 533–539.
- Stern HM, Zon LI (2003) Cancer genetics and drug discovery in the zebrafish. *Nat Review Cancer* 3(7), 533-539..
- Stohs S.J., Bagchi D., 1995. Oxidative mechanisms in the toxicity of metal ions. *Free Radical Biology Medicine* 18, 321–336.
- Sturm, R.A., Teasdale, R.D., Box, N.F., 2001. Human pigmentation genes: identification, structure and consequences of polymorphic variation. *Gene* 277, 49–62.
- Sudheer, A.R., Muthukumaran, S., Devipriya, N., Menon, V.P., 2007. Ellagic acid, a natural polyphenol protects rat peripheral blood lymphocytes against nicotine-induced cellular and DNA damage in vitro: with the comparison of N-acetylcysteine. *Toxicology* 230, 11–21.
- Swanson A.K., Druehl L.D., 2002. Induction, exudation and the UV protective role of kelp phlorotannins. *Aquatic Bot* 73, 241–253.
- Takamatsu S., Hodges T.W., Rajbhandari I., Gerwick W.H., Hamann M.T., Nagle D.G., 2003. Marine natural products as novel antioxidant prototypes. *Journal of Natural Product* 66, 605–608.
- Tanaka K., Hasegawa J., Asamitsu K., Okamoto T., 2007. *Magnolia ovovata* extract and its active component magnolol prevent skin photoaging via inhibition of nuclear factor. *European Journal of Pharmacology* 565, 212–219.
- Tengamnuay P., Pengrungruangwong K., Pheansri I., Likhitwitayawuid K., 2006. *Artocarpus lakoocha* heartwood extract as a novel cosmetic ingredient: evaluation of the in vitro anti-tyrosinase and in vivo skin whitening activities. *International Journal of Cosmetic Science* 28, 269–276.

- Thiele J.J., Podda M., Packer L., 1997. Tropospheric ozone an emerging environmental stress to skin. *Biological Chemistry* 378, 1299–1305.
- Torres M.A., Barros M.P., Campos S.C., Pinto E., Rajamani S., Sayre R.T., Colepicolo P., 2008. Biochemical biomarkers in algae and marine pollution: a review. *Ecotoxicology and Environmental Safety* 71, 1–15.
- Usenko C.Y., Stacey L., Harper, Robert L., Tanguay., 2007. *In vivo* evaluation of carbon fullerene toxicity using embryonic zebrafish. *Carbon* 45, 1891–1898.
- Veerman E.C., Nazmi K., Hof, W.V., Bolscher J.G., Hertog A.L.D., Amerongen A.V.N., 2004. Reactive oxygen species play no role in the candidacidal activity of the salivary antimicrobial peptide histatin 5. *Biochemical Journal* 381, 447–452.
- Wang K.H., Lin R.D., Hsu F.L., Huang Y.H., Chang H.C., Huang C.Y., Lee M.H., 2006. Cosmetic applications of selected traditional Chinese herbal medicines. *Journal of Ethnopharmacology* 106, 353–359.
- Wang Y., Feinstein S.I., Fisher A.R., 2008. Peroxiredoxin 6 as an antioxidant enzyme: Protection of lung alveolar epithelial type 2 cells from H₂O₂-induced oxidative stress. *Journal of cellular biochemistry* 104, 1274–1285.
- Whittemore E.R., Loo D.T., Watt J.A., Cotman C.W., 1995. A detailed analysis of hydrogen peroxide-induced cell death in primary neuronal culture. *Neuroscience* 67, 921–932.
- Wixon J., 2000. *Danio rerio*, the zebrafish. *Yeast* 17, 225–231.
- www.ensembl.org, *D. rerio* genome release Zv7, April 2007.
- Xu J., Srinivas B.P., Tay S.Y., Mak A., Yu X., Lee S.G.P., Yang H., Govindarajan K.R., Leong B., Bourque G., Mathavan S., Roy, 2006. Genome-wide expression profiling in the zebrafish embryo identifies target genes regulated by hedgehog signaling during vertebrate development. *Genetics* 174, 735–752.
- Xu Q., Konta T., Nakayama K., Furusu A., Moreno-Manzano V., Lucio-Cazana J., Ishikawa Y., Fine L.G., Yao J., Kitamura M., 2004. Cellular defense against H₂O₂-induced apoptosis via MAP kinase-MKP-1 pathway. *Free Radical Biology and Medicine* 36, 985–993.
- Xu Y., Stokes A.H., Freeman W.M., Kumer S.C., Vogt B.A., Vrana K.E., 1997. Tyrosinase mRNA is expressed in human substantia nigra. *Molecule Brain Research* 45, 159–162.
- Yamakoshi Y., Umezawa N., Ryu A., Arakane K., Miyata N., Goda Y., Masumizu T., Nagano T., 2003. Active oxygen species generated from photoexcited fullerene (C₆₀) as potential medicines: O₂⁻ versus ¹O₂. *Journal of Am Chemistry Society*

125, 12803–12809.

Yasui H., Sakurai H., 2003. Age-dependent generation of reactive oxygen species in the skin of live hairless rats exposed to UVA light. *Experimental Dermatology* 12, 655–661.

Zon L.I., Peterson R.T., 2005. *In vivo* drug discovery in the zebrafish. *Natural Review Drug Discovery* 4, 35–44.



ACKNOWLEDGEMENT

